Synthesis and *In silico* Molecular Docking Studies of Tetrazole and Thiazole - Based Schiff Base Derivatives as Antibacterial and Antioxidant Agents

By

Fitsum Lemilemu Gessese

A Thesis Submitted to

The department of Applied Chemistry

School of Applied Natural Science

Presented in Partial Fulfillment of the Requirement for the Degree of Master's in Applied Chemistry (Specialization in Synthetic Organic Chemistry)

Office of Graduate Studies

Adama Science and Technology University

June, 2021

Adama, Ethiopia

Synthesis and *In silico* Molecular Docking Studies of Tetrazole and Thiazole-Based Schiff Base Derivatives as Antibacterial and Antioxidant Agents

By

Fitsum Lemilemu Gessese

Major Advisor: Milkyas Endale (PhD)

Co-Advisor: Venkatesha Perumal (PhD)

A Thesis Submitted to

The department of Applied Chemistry

School of Applied Natural Science

Presented in Partial Fulfillment of the Requirement for the Degree of Master's in Applied Chemistry (Specialization in Synthetic Organic Chemistry)

Office of Graduate Studies

Adama Science and Technology University

June, 2021

Adama, Ethiopia

DECLARATION

I hereby, declare that this Master Thesis entitled "**Synthesis and *In silico* Molecular Docking Studies of Tetrazole and Thiazole-Based Schiff Base Derivatives as Antibacterial and Antioxidant Agents**" is my original work. That is, it has not been submitted for the award of any academic degree, diploma or certificate in any other university. All sources of materials that are used for this thesis have been duly acknowledged through citation

_____	_____	_____
Name of the student	Signature	Date

RECOMMENDATION

I/we, the advisor(s) of this thesis, hereby certify that I/we have read the revised version of the thesis entitled "**Synthesis and *In silico* Molecular Docking Studies of Tetrazole and Thiazole-Based Schiff Base Derivatives as Antibacterial and Antioxidant Agents**" prepared under my/our guidance by Fitsum Lemilemu submitted in partial fulfillment of the requirements for the degree of Master's of Science in Applied Chemistry (Specialization in Synthetic Organic Chemistry).

Therefore, I/we recommend the submission of revised version of the thesis to the department following the applicable procedures.

_____	_____	_____
Major Advisor	Signature	Date
_____	_____	_____
Co-advisor	Signature	Date

APPROVAL OF BOARD OF EXAMINERS

We, the advisors of the thesis entitled "**Synthesis and *In silico* Molecular Docking Studies of Tetrazole and Thiazole-Based Schiff Base Derivatives as Antibacterial and Antioxidant Agents**" and developed by Fitsum Lemilemu, hereby certify that the recommendation and suggestions made by the board of examiners are appropriately incorporated into the final version of the thesis.

_____	_____	_____
Major Advisor	Signature	Date
_____	_____	_____
Co-advisor	Signature	Date

We, the undersigned, members of the Board of Examiners of the thesis by Fitsum Lemilemu have read and evaluated the thesis entitled "**Synthesis and *In silico* Molecular Docking Studies of Tetrazole and Thiazole-Based Schiff Base Derivatives as Antibacterial and Antioxidant Agents**" and examined the candidate during open defense. This is, therefore, to certify that the thesis is accepted for partial fulfillment of the requirement of the degree of Master of Science in Applied Chemistry (Specialization in Synthetic Organic Chemistry).

_____	_____	_____
Chairperson	Signature	Date
_____	_____	_____
Internal Examiner	Signature	Date
_____	_____	_____
External Examiner	Signature	Date

Final approval and acceptance of the thesis is contingent upon submission of its final copy to the Office of Postgraduate Studies (OPGS) through the Department Graduate Council (DGC) and School Graduate Committee (SGC).

_____	_____	_____
Department Head	Signature	Date
_____	_____	_____
School Dean	Signature	Date
_____	_____	_____
Office of Postgraduate Studies, Dean	Signature	Date

ACKNOWLEDGEMENTS

First and foremost, I would like to thank almighty God for giving me the strength, knowledge, ability and his mother St. Mary for their invaluable help to accomplish this work successfully.

Next, I would like to express my sincere gratitude to my advisor, Dr. Milkyas Endale (PhD) for his professional, technical, very invaluable and unreserved advice, guidance and constructive support during the whole period of the project and thesis write up. I also express my gratitude to co-advisor Dr. Venkatesha Perumal (PhD) for his kindness, unreserved help and guidance.

I am extremely thanks to Mr. Kebede Shenkute, Mr. Bayan Abdi, Mr. Yoseph Samuel, Mr. Demis Zelelew, Mr. Mona Fikadu, Miss. Merima Kufa, Miss. Embet Getahan, Mr. Mamaru Bitew, Mr. Tadewos Damena, Dr. Digafie Zeleke (PhD), Dr. Endale Mulugeta (PhD) and Dr. Yadessa Melaku (PhD) who gave me valuable comments, materials and chemicals needed during the research work. My heart-felt thanks also extend to all this year's ASTU graduating students from Department of Applied Chemistry. Especial acknowledgment goes to Dr. Rajalakshaanan Eswaramoorthy, Mr. Mamaru Bitew and Dr. Taye Beyene (University of Botswana) for their assistance during molecular docking, DFT and ADMET analysis studies.

My special thanks to my families particularly to my beloved mother and friends for their support, endless love and blessing that shape my life. Last but not least, I would like to acknowledge Adama Science and Technology University and Addis Ababa University for scholarship opportunity to pursue M.Sc. study and access to NMR Spectroscopy, respectively.

TABLE OF CONTENTS

LIST OF TABLES

LIST OF FIGURES

LIST OF SCHEMES

LIST OF ABBREVIATIONS AND ACRONMYS

Å	Angstrom
Nm	Nanometer
q	Quartet
R_f	Retention factor
s	Singlet
t	Triplet
d	Doublet
ADT	Auto Dock tool
$CDCl_3$	Deuterated Chloroform
DCM	Dichloro methane
DEPT	Distortionless Enhancement by Polarization Transfer
DMF	N,N-dimethylformamide
DMSO	Dimethyl sulfoxide
ED_{50}	Effective Dose which inhibit 50% of the test organism
HOMO	Highest Occupied Molecular Orbital
LUMO	Lowest Unoccupied Molecular Orbital
IC_{50}	50 % Inhibition Concentration
DNA	Deoxyribonucleic acid
MIC	Minimum inhibitory concentration
MIQ	Minimum inhibitory quantity
MHz	Megahertz
NMR	Nuclear Magnetic Resonance
LD_{50}	Lethal Dose
rt	Room temperature
Mp	Melting point
TLC	Thin Layer Chromatography
UV-Vis	Ultra Violet and Visible
DPPH	1,1-diphenyl-2-picrylhydrazyl
CFU	Colony forming unit
MABA	Microplate Alamar Blue assay

ROS	Reactive oxygen species
RGO	Reduced graphene oxide
EWG	Electron withdrawing group
EDG	Electron Donating Group
DPPA	Diphenylphosphorazidate
DBU	1,8-Diazabicyclo(5.4.0)undec-7-ene
SAR	Structure-activity relationships
THF	Tetrahydrofuran
RMSD	Root mean square deviation
LGA	Lamarckian genetic algorithm
PDB	Protein Data Bank
MRSA	Methicillin-resistant *Staphylococcus aureus*
IPT	Internal proton transfer

LIST OF APPENDIX

ABSTRACT

Nowadays, alarming and reemerging multidrug resistance bacteria are becoming a major public health concerns. Antibacterial activities of the synthesized compounds were examined using agar disk diffusion method against S. aureus, E. coli, S. pyogenes and P. aeruginosa strains. Compounds ***106****,* ***101****, and* ***105*** *showed good activities against E. coli with mean inhibition zone of* 14.4 ± 0.04, $12.5 \pm .04$ *and* 10.5 ± 0.02*mm diameter at 200 μg/mL compared to Amoxicillin (18* ± 0.01*, respectively. Of the synthesized compounds, compound* ***106*** *displayed the highest activity with zone of inhibition of* 14.4 ± 0.04, 15 ± 0.01, 13 ± 0.02, *and 14.45* ± 0.25 *at 200 μg/mL against E. coli, S. aureus, P. aeruginosa, and S. pyogenes, respectively. Compound* ***102****,* ***105*** *and* ***101*** *exhibited highest percent inhibition of the DPPH with* IC_{50} *value of 3.6, 3.65 and 4.91 in μg/mL, respectively. Molecular docking analysis of synthesized compounds against DNA gyrase B showed minimum binding energy ranging from -7.5 to -6 kcal/mol of which best binding affinity was achieved for compounds* ***106****,* ***101*** *and* ***105*** *(-7.5, -7.2 and -6.9 kcal/mol, respectively. Compounds* ***101*** *and* ***106*** *showed better binding affinity compared to standard drug, Amoxicillin. The docking analysis against human peroxiredoxin 5 revealed minimum binding energy ranging from - 5.3 to - 5.0 kcal/mol of which compounds* ***101, 102, 105*** *and* ***104*** *showed better binding affinity (-5.3, -5.3, -5.2 and -5.1 kcal/mol, respectively) compared to standard drug, Ascorbic acid. In vitro antibacterial activity of compounds* ***106****,* ***101****,* ***105*** *and antioxidant activity of compounds* ***102, 105*** *and****101*** *suggest the potential use of these compounds as potential drug lead candidates, supported by both experimental and computational analysis. Compounds* ***105*** *and* ***106*** *showed significant molecular interactions with topoisomerase II at active sites (- 5.8, - 5.9, kcal/mol, respectively) compared to Vosaroxin (- 6.2, kcal/mol). In silico cytoxicity predictions revealed* LD_{50} *value of class three* ($50 \leq LD_{50} \leq 300$) *inferring they are toxic if swallowed except compound* ***101*** *(class* 4, $300 \leq LD_{50} \leq 2000$). *The DFT and wave function analysis revealed that compound* ***102*** *showed the least HOMO-LUMO energy gap suggesting high chemical reactivity and considerable intramolecular charge transfer from electron donor (HOMO) to electron acceptor (LUMO) groups. However, except compound* ***101*** *all compounds showed small band gap energy ranging from 0.134-0.692 eV inferring good reactivity of molecules.*

Key words: Schiff base, tetrazole, thiazole, antibacterial, antioxidant, molecular docking.

1. INTRODUCTION

1.1 Background of the study

Heterocyclic systems are important building blocks for new materials possessing attractive electronic, mechanical or biological properties (Sharma *et al.,* 2020).The chemistry of heterocyclic compounds has attracted a great deal of interest in recent times due to the increasing importance of the heterocyclic scaffold in pharmaceuticals. A large number of heterocyclic compounds containing nitrogen and sulfur are used as medicine in different therapeutic targets (Elsadek *et al.,* 2021). Heterocyclic compounds are considered as the most promising molecules for the design of new drug, More than 60% of all known organic compounds are heterocyclic compounds (Heravi & Zadsirjan, 2020). However, the range of easily accessible and suitable functionalized heterocyclic building blocks for the synthesis of structurally diverse libraries of therapeutics is somehow limited. Therefore, the development of simple, elegant and facile methodologies towards focused libraries of such compounds is one of the most important aspects of drug discovery.

There are different numerous biologically active molecules that contain various heteroatoms, such as nitrogen, sulfur, and oxygen, which have drawn the attention of chemist's over the years (Shukla *et al.,* 2017).

Nitrogen and sulphur based heterocyclic compound is an important and unique class among the synthetic organic chemistry, with a significant amount of research dedicated to the development of novel molecules for drug discovery and development. These molecules have received increasing attention over the past two decades (Kerru *et al.,* 2020). They are a classified under synthetic organic heterocyclic compound, consisting of a 5-member ring of four nitrogen and one carbon atom (Nessim *et al.,* 2018). Tetrazole and its derivatives are an important class of heterocyclic compounds which possess wide spectrum of biological properties (Aziz *et al.,* 2018).

Tetrazole heterocyclic have attracted much attention because of their unique structure and applications as antihypertensive, anti-alergic, antibiotic and anticonvulsant agents *(*Myznikov *et al.,* 2007). Tetrazole heterocyclic was first discovered in 1985 by bladin in Uppsala

university upon formation of dicyan dimethyl hydrazine a product of reaction dicyan with phenyl hydrazine (Mohammadkhani & Heravi, 2020).

Tetrazoles are extensively applied in different areas of studies such as stabilizers in image industry, explosives in rocket propellants, herbicides, fungicides in agriculture (Karaghiosoff *et al.,* 2006).They do not exist in nature. Interestingly, they have the highest number of nitrogen atoms among the stable heterocycles because pentazoles are highly explosive compounds even at low temperature (Bhatt, 2011). The simplest tetrazole has the formula CN_4H_2, and is found in two tautomeric forms (Figure 1).Tetrazole has the highest ionization potential (11.3eV) and the dipole moment in dioxane is 5.15 D. Tetrazole is acidic in nature and its pKa of 4.89 is comparable to acetic acid (pKa 4.76).

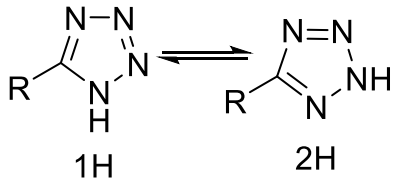

Figure 1: Tautomeric structures of tetrazole (R = H)

The introduction of the tetrazole moiety into a compound of an organic substrate quite often leads not only to an increase in the efficacy but also to an increase in the prolongation of drug action. These improvements are leaded to all based on the structural features of tetrazole ring. Tetrazoles are ionized at physiological pH (≈7.4), but are almost 10 times more lipophilic than the corresponding carboxylates which could facilitate further a drug molecule to pass through cell membranes. The high density of nitrogen's in tetrazoles could provide more opportunities to form hydrogen bonds with receptor recognition sites which explain the sometimes enhanced binding affinity. Last but not least, tetrazoles are resistant to many biological metabolic degradation pathways which are conjugation reactions to form *β*-N-glucuronides, a metabolic fate that often befalls aliphatic carboxylic acids to form *α*-*β*-glucuronic acid conjugates. Compounds containing azomethine group (–C=N–) in the structure are known as Schiff bases, which are usually synthesized by the condensation of primary amines and active carbonyl groups. Schiff bases are well known for their pharmacological properties as anti-bacterial, antifungal, anti-cancer and anti-viral agents (Wang *et al.,* 2001). The imine group present in such compounds has been exhibited to be essential to their biological activities such as antifungal,

antibacterial, antimalarial, anti-proliferative, anti-inflammatory, antiviral, and antipyretic properties (Hussain *et al.*, 2014).To improve the medicinal properties of Schiff bases, the incorporation of thiazole groups as moieties in molecules is considered as effective models for executing important biological reactions (Khandar *et al.*, 2005).

Several sulphur containing scaffolds exist in various natural compounds and drugs which serve as biologically active molecules in various physiological conditions. Molecules of thiazole moiety are one of the important pharmacophores in drug discovery and development processes (Pola, 2016). There are many substituted molecules with thiazole-containing heterocycles compound containing a wide range of therapeutic targets including antimicrobial, anti-cancer, anti-inflammatory and anti-HIV. Thiazoles also have emerged as a brand new elegance of robust antimicrobial marketers which might be reported to inhibit bacteria with the aid of blocking off the biosynthesis of positive bacterial lipids (Palanimurugan& Kulandaisamy, 2018).

Nowadays thiazole and its derivatives have been the structural motif of many natural compounds including vitamin B1 (thiamine), penicillin, and carboxylase. One of the most important bioactive thiazole moiety is 2-aminothiazole derivatives that possess an antitumor activity through the inhibition of the kinases (Gharamaleki *et al.*, 2016). They have also been employed in the preparation of different drugs required for treatment of allergies, hypertension, inflammation, schizophrenia, bacterial and HIV infections (Tsuji & Ishikawa, 1994).

The recent trend shows the applications of thiazole core structure in drug design and development of novel therapeutic agents. Thiazole ring is five membered heterocycles compound has been used for variety roles in the lead identification and optimization, including as pharmacophoric and bioisosteric elements, and as a spacer. Therefore the presence of thiazole ring as a part of drug structure can be determinant for its physicochemical and pharmacokinetic properties.

In classical way of synthesis to consider pharmacokinetics (i.e. the fate of a therapeutic compound within the organism) is to interrupt down the varied effects that impact the access to the target into individual parameters. In turn, these parameters such as Absorption, Distribution, Metabolism and Excretion (ADME) are often evaluated separately by dedicated methods. It has been demonstrated that early estimation of ADME within the discovery phase reduces drastically the fraction of pharmacokinetics-related failure within the clinical phases (Hazard, 2009). In

modern synthesis, *in silico* models have been fostered as a valid alternative to experimental procedures for prediction of ADME, especially at initial steps, when investigated chemical structures are numerous but the availability of compounds is scarce (Dahlin *et al.*, 2015).A large variety of *in silico* methods share the objective of predicting ADME parameters from molecular structure (Tian *et al.*, 2015). Noteworthy, the pioneer work of (Lipinski *et al.*, 2012) examined orally active compounds to define physicochemical ranges for top probability to be an oral drug (i.e. the drug-likeness). The Rule-of-five of Lipinski delineated the relationship between pharmacokinetic and physicochemical parameters in drug discoveries. Nowadays, research in the field of antimicrobial drug design is focused on the discovery of novel lead targets and chemical modification that possess high antibacterial activity in order to overcome the rapid development of drug resistance (Malik *et al.*, 2018).

1.2. Statement of the problem

The treatment of infectious diseases remains an imperative issue as a result of a number of factors including the rise of newer infectious diseases and, growing number of multi-drug resistant microbial pathogens (Buchy *et al.*, 2020);(Althagafi *et al.*, 2019). Nowadays, the alarming and reemerging multidrug resistance bacteria are becoming a major public health threat and concerns. To overcome these challenges searching of novel scaffold with improved therapeutic potential required in search for more effective, safer and affordable drugs. A couple of tetrazole and thiazole based heterocylic drugs were reported recently with a broad spectrum of biological activities. The synthesis of novel thiazole based Schiff base derivatives bearing different substituents were reported (Geronikaki *et al.*, 2004); (Amorim *et al.*, 2020). The authors reported that thiazole-based Schiff base derivatives showed promising results against bacterial strains (Petrou *et al.*, 2021). However, to the best of research knowledge hydroxyl- and nitro-substituted thiazole-based Schiff base derivatives have never been synthesized yet. Besides, the ADMET profile, molecular docking and DFT analysis of the synthesized compounds have never been explored.

1.3. Objectives of the study

1.3.1 General objective

The overall objective of this study is to synthesize, characterization, evaluate antibacterial, anti-oxidant activities of tetrazole and thiazole-based Schiff base derivatives and examines molecular docking, ADMET and DFT analysis.

1.3.2 Specific objectives

- To synthesize novel tetrazoles and Schiff base of thiazole derivatives.
- To characterize the synthesized compounds using melting point and NMR (^{1}H-NMR and ^{13}C NMR).
- To evaluate antibacterial activity of the synthesized compounds using agar disk diffusion method against Gram positive bacteria and Gram negative bacteria.
- To evaluate antioxidant activities of synthesized compounds using DPPH radical scavenging assay.
- To conduct *in silico* molecular docking analysis of synthesized tetrazole and thiazole based Schiff base derivatives against DNA gyrase B, human perorexidoxin 5 and human topoisomerase II α LasR binding domains using Autodoc vina version 4.2 software.

1.4. Significance of the study

The present study introduced new and green synthetic protocols resulting promising bioactive novel compounds. Hence, the output of the present study is highly significant to researchers in the same field and industries too. The research might also useful in search for drug lead candidates for treating various infectious diseases and in drug design and development. This study may provide documentary information about synthesis of some new tetrazole and Schiff base of thiazole derivatives from Schiff base via inorganic azide and condensation reaction under conventional and catalyzed reaction respectively. Moreover, the study provides quantum chemical description and, *in-silico* pharmacokinetic, drug likeness and toxicity profile of the synthesized compounds. Therefore, the study was significant in providing a combined wet laboratory and dry laboratory findings.

2. LITERATURE REVIEW

The development of simple and general synthetic routes for widely used organic compounds from readily available reagents is one of the major challenges in organic chemistry (Nicolaou, 2014). Therefore to meet the facile results of these tough challenges tetrazole and thiazole nucleus was being considered (Ruano *et al.*, 2016). Among the wide variety of heterocycles that have been explored for developed nitrogen contain and sulphur are fascinating class of molecules in pharmaceutically such as tetrazole and thiazole derivatives have played a vital role in the medicinal chemistry. Tetrazole and its derivatives play vital role in medicinal and pharmaceutical applications. The synthesis of tetrazole derivatives are often approached in ecofriendly approaches like the utilization of water as solvent, moderate conditions, nontoxic, easy extractions, easy setup, low cost, etc. with good to excellent yields (Varala & Babu, 2018). Thiazole ring moiety has promising many pharmacological activities including anticancer. This scaffold has been found alone or incorporated into the range of therapeutic active agents like tiazofurin, dasatinib, and bleomycin, which are well-known antineoplastic drugs. Nowadays, most of the compounds isolated from natural sources containing thiazole moiety exhibit notable cytotoxicities and present antitumor potentials (Ramos-Inza *et al.,* 2020).

2.1 Synthesis of tetrazole moiety

Several methods for the synthesis of tetrazoles are widely reported in the literature. They could be synthesized by the reaction of substituted amines **3** with triethylorthoformate and sodium azide in dimethyl sulfoxide (DMSO) (Palimkar *et al.,* 2003) (Scheme 1). The current progress in the design of new energetic materials is largely associated with synthesis studies of tetrazole and its derivatives (Dighe *et al.*, 2009).

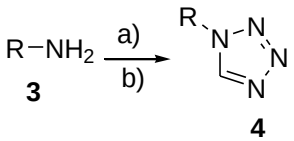

3 **4**

Reagent and condition a).CH $(OEt)_3$, b).NaN_3, AcOH

Scheme 1: Synthesis of tetrazoles and their derivatives

2.2. Synthesis of 1,5-disubstituted tetrazole derivatives by dipolar cycloaddition

Several methods have been described by researchers for the incorporation of tetrazole moiety. However, the most convenient and simple method for synthesis is [2 + 3] cycloaddition of nitriles with sodium azide (NaN_3) in the presence of an effective catalyst. In cyclization, catalyst plays an important role, and Lewis acid is the most widely used catalyst for tetrazole synthesis. It should be noted that if nitrile containing reactants used for the synthesis of tetrazoles then it is a [2 + 3] cycloaddition reaction in which catalyst plays an important role for cyclizationin (scheme 2). In general, required amount of catalyst is added to the reaction mixture of nitriles, sodium azide, and DMF and stirred vigorously at 120°C under reflux conditions. In the case of 5-substituted-1*H*- tetrazoles, acidification is required to free up the nitrogen (N_1) at first position in tetrazole ring (Tamoradi *et al.*, 2017).

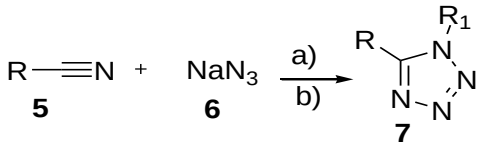

Reagent and conditions where R is Alkyl/aryl/phenyl, R_1: H/alkyl/aryl/phenyl a).NH_4Cl, DMF 120^{o}C, b) $ZnCl_2$ (1equiv) i-PrOH, 50^{o}C, 1-5hr

Scheme 2: Synthesis of tetrazoles via 2 + 3 cycloaddition

The greener synthesis reported by Demko and Sharpless in 2002, in which various organic nitriles **5** reacted with sodium azide and zinc bromide in water as a solvent under reflux to give compound **5** substituted-1*H*-tetrazoles in excellent yields (scheme 3) (Demko& Sharpless, 2002). The literature is replete with methods to perform this transformation; they fall into three main categories: those that make use of tin or silicon azides, those that use strong Lewis acids, and those that are run in acidic media. Each of these has one or more of the following drawbacks: expensive and toxic metals, severe water sensitivity, and the presence of hydrazoic acid, which is highly toxic and explosive as well as volatile. Zinc bromide was chosen as the best compromise between cost, selectivity, and reactivity. The process became even more attractive for large scale applications when we found that it could be run at higher concentration without sacrificing yield

and without the use of organic solvents in the workup or isolation phases. Recently, nanocrystalline ZnO was also shown to be an effective heterogeneous catalyst for the [2+3] cycloaddition of azides to nitriles to afford 5-substituted-1*H* -tetrazoles in good yields (Lakshmi Kantam *et al.*, 2005).

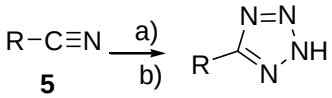

5 **8**

Reagent and conditions a).1.1 equiv NaN_3, b).1 equiv $ZnBr_2$, water, reflux

Scheme 3: Greener method of synthesis of tetrazole via [2 + 3] cycloaddition.

The [3+2] cycloaddition between hydrazoic acid and cyanide derivatives was well known as an efficient route (Scheme 4). The reaction of compound 5 and azidotrimethylsilane (1.5 equiv.) was conducted in MeOH (0.5M) within the presence of a catalytic amount of HCl (2 mol %, 1.0 M in Et_2O solution) at 60°C (Tienan *et al.*, 2004)(Medda & Hulme, 2012). Compound **9** was also obtained in a sealed pressure vessel reaction where NaN_3 dissolved in H_2O, compound 5, ammonium chloride, ammonium fluoride and propane-1,2-diol (DPOL) were stirred and heated for 48 hr (Xiang *et al.*, 2013).

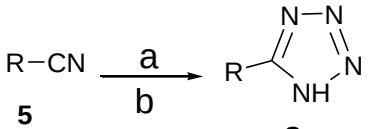

5 **9**

Reagents and Conditions: a) NaN_3, NH_4Cl, LiCl, DMF, 110°C; (b) NaN_3, NH_4Cl, NH_4F, DPOL, 48hr.

Scheme 4: Synthesis of tetrazoles via 3 + 2 cycloaddition

Tetrazoles have also been synthesized using fluorous chemistry (Scheme 5) (Curran *et al*., 1999). A fluorous tin azide reagent **10** is prepared and reacted with nitriles to produce the corresponding tetrazole compounds **11**. Subsequent cleavage by concentrated hydrochloric acid gives pure tetrazole products **12** and the fluorous tin chloride, which could be reconverted into tin azide. In

most cases, a 2–5-fold excess of the fluorous tin reagent is used and good yields of the tetrazole products are obtained.

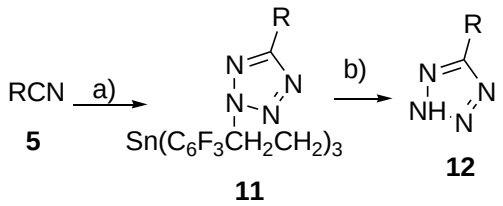

Reagent and conditions a) $(C_6F_3CH_2CH_2)_3SnN_3$ (**10**), b) HCl, R=aryl, alkyl, yield 60-99%
Scheme 5:Synthesis of tetrazoles under fluorous conditions.

2.2.1 Synthesis of tetrazole derivatives via Ugi-type multicomponent reactions

Multicomponent reactions (MCRs) are chemical reactions where quite two compounds react to make one product during a sequence with several descriptive features, like atom economy, efficiency and convergence. Ugi and co-worker firstly reported the use of HN_3 replacing carboxylic acid in the Passerini and Ugi reactions to form tetrazole derivatives in 1960s. Due to, numerous advancements were published on the synthesis of tetrazoles via multicomponent reaction nowadays. Aldhoun and co-workers (2008) described a short route based on [2+3]-dipolar cycloadditions using TMSCN and several azides as starting materials to access a series of 1,5-disubstituted-1*H*-tetrazoles with good to excellent overall yields(Aldhoun *et al.,* 2008). MCR have also been exploited to obtain compounds with a tetrazole ring system in short reactions time with good overall yields (Borah *et al.,* 2012). Among multicomponent reactions, the Ugi-type MCR combined with subsequent post condensation processes present several advantages over other methodologies for the 1,5-disubstituted-1*H*-tetrazoles synthesis (Laurent *et al.,* 2012). Also, Marcos *et al* 2008 also reported the synthesis of a series of tetrazoylisoindolinones via a tandem Ugi-4CR/amidation with moderate to good overall yields (Marcos *et al.,* 2008).In 20th century, Gunawan and coworkers (2012) published an elegant synthesis of a novel 1,5-disubstituted-1*H*-tetrazoles series with moderate yields based on the Ugi-azide process (Gunawan *et al.,* 2012).

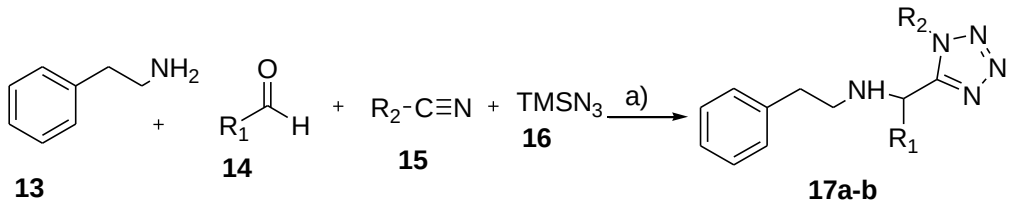

Reagent and conditions a).MeOH, rt, 6hr, 17a) $R_{1\,=}$ alkyl and17b) R_2 = aryl

Scheme 6: Synthesis of 1,5-disubstituted-1*H*-tetrazoles by an Ugi-azide process

2.3 Synthesis of 1,5-disubstituted tetrazoles from ketoximes via a Beckmann rearrangement

Pioneering studies for the synthesis of 1,5-disubstituted tetrazoles from oxime esters or ketones via the Beckmann or Schmidt rearrangement have also been reported (Motiwala *et al.,* 2016). In such way of those methods, both the starting materials and end products must be carefully handled due to their inherent toxicities and explosiveness. DPPA is a less explosive azidation reagent than sodium azide or trifluoromethanesulfonylazide due to the stabilization of the azide via conjugation with the phosphorus atom. Recently, we have reported the synthesis of 5-substituted1*H*-tetrazoles from aldoximes using DPPA (Ishihara *et al.,* 2018). This method improved the security of this azidation operation and utilized DPPA as both the activator and azide source. Therefore, 1,5-disubstituted tetrazoles could be obtained safely from ketoximes if a Beckmann type rearrangement proceeded by activation and azidation with DPPA (Scheme 7).

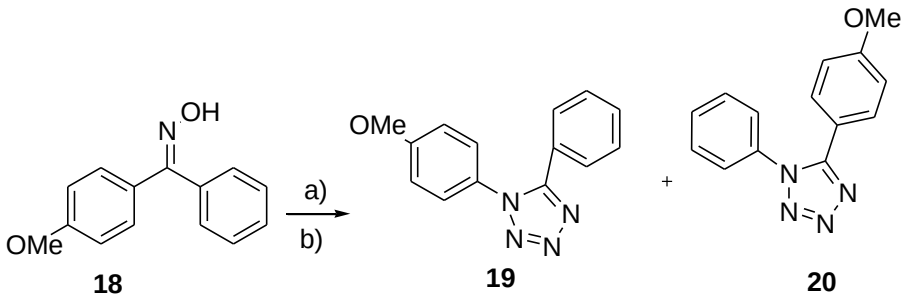

Reagent and conditions a)DPPA(1.2 equiv),DBU(1.2 equiv),b)MeCN,reflux,16hr

Scheme 7: Tetrazole synthesis using an isomeric mixture of ketoximes via a Beckmann rearrangement.

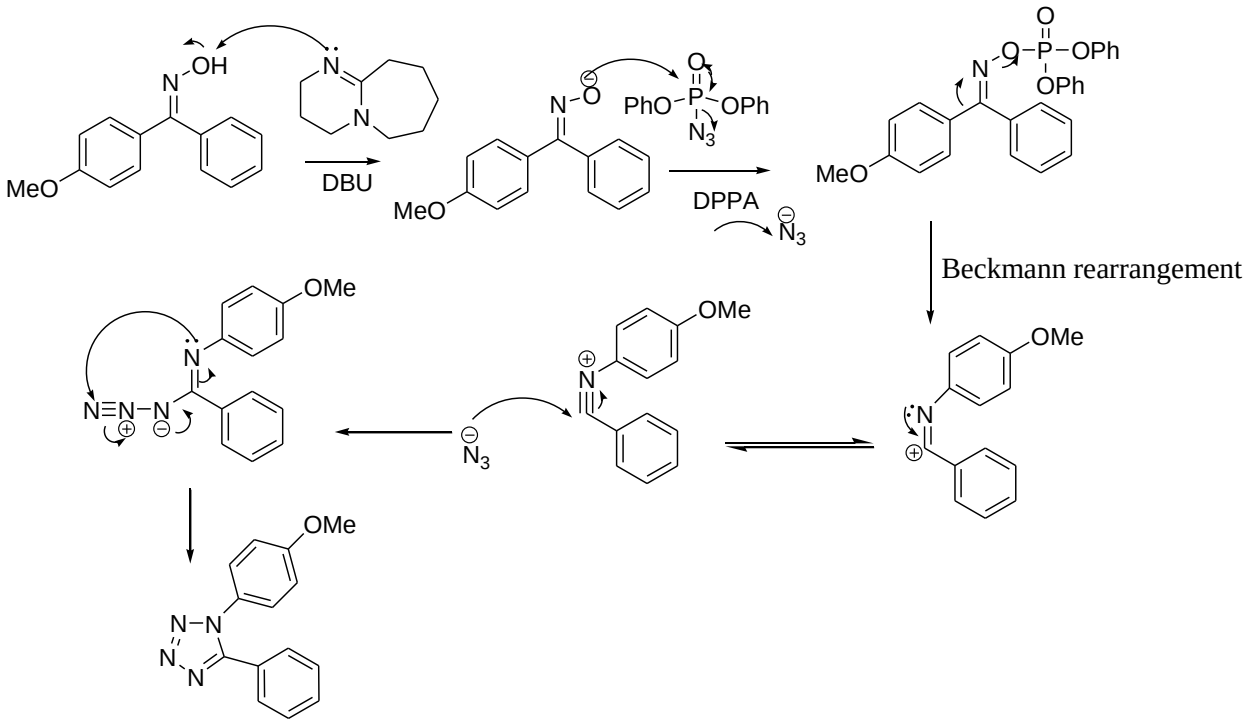

Scheme 8: The plausible reaction mechanism of tetrazole through Beckmann rearrangement.

Initially, the ketoxime is deprotonated by DBU and attacks DPPA to make a phosphate intermediate. Subsequently, the phosphate intermediate undergoes a Beckmann rearrangement to get a nitrilium ion, followed by attack by the free azide anion and cyclization yields the specified tetrazole. In summary, they developed a novel method for the synthesis of 1,5-tetrazole from ketoximes via a Beckmann rearrangement utilizing DPPA as both the activator and azide source (Ishihara *et al.,* 2019). Various ketoximes were easily converted into the corresponding tetrazoles (Scheme 8). No ketoxime isomerization occurred during the reaction and the rearrangement occurred stereo-specifically with only the migration of trans-group. The advantages of this method include operational simplicity and increased safety as toxic or explosive azide reagents are often avoided.

Synthesis of 5-substituted 1*H*-tetrazole from oximes was also reported by (Patil *et al.,* 2012*)* using copper acetate ($Cu(OAc)_2$) catalyst. The reaction was simply performed by stirring under reflux conditions followed by acidification and method affords the advantage of maximum yield of desired product (98%) which distinguishes it from the previous. The maximum yield was obtained by aromatic oximes bearing ERG at ortho and Para position whereas ERG at Meta position and aliphatic oximes resulted in poor yield (Patil *et al.,* 2012).

Another method for the synthesis of 5-substituted 1*H*-tetrazoles from aldoximes was reported by (Philippa *et al.*, 2016) using DPPA. This method offers a plus that DPPA is a smaller amount explosive compared to azides thanks to the phosphite group stabilization and therefore the reaction was further catalyzed by DBU which also eliminates toxic metal catalytic burden. On the other hand, reaction was suitable for aromatic or heteroaromatic aldoximes and the desired product was obtained in good yield but the yield from aliphatic or EWGs substituted aldoximes decreased through a long reaction time (Scheme 8) (Philippa and Andrew, 2016).

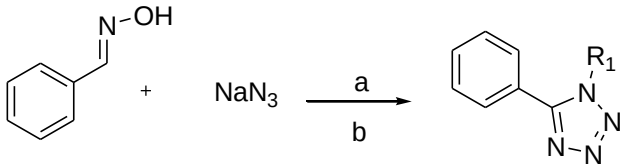

21 **22**

Reagent and conditions compounds 22 R_1: H/alkyl/aryl/phenyl a) $Cu(OAc)_2$ (25mol%), DMF 120^oC, b) DPPA(1.5 equiv) DBU (3 equiv) toluene, reflux, 16hr, 110^oC

Scheme 9:Tetrazole derivatives synthesis from oximes and their derivatives.

2.4 Synthesis tetrazoles derivatives from oximes and nitrile using nanoparticles

In this context, nickel as a transition metal catalyst, creates a promising center of attraction toward the researchers. Nanoparticles (NPs), having unusually huge surface area and large number of active sites, can efficiently catalyze several organic reactions providing the advantages of high atom economy, mild reaction conditions, simplified isolation of product, easy recovery, and recyclability of the catalysts (Shahbazali *et al.*, 2013). A novel and efficient synthetic strategy of designing recyclable heterogeneous nickel hydroxide NPs to surmount several aforementioned obstructions in the synthesis of 5-substituted 1*H*-tetrazoles starting from aldoximes and sodium azide in water under mild reaction conditions (Scheme 9) (Halder *et al.*, 2018).

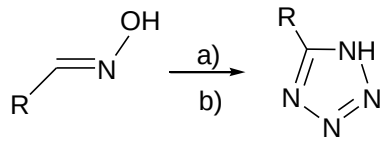

21 **23a-b**

Reagent and conditions a) $Ni(OH)_2$NPs b)NaN_3,H_2O

23a) R =Aromatic and 23b) R=Aliphatic

Scheme 10: Synthesis of 5-substituted 1*H*-tetrazoles from aldoxime

Considering the ongoing attempts and increasing awareness to develop simple, environment-friendly, economic, and profit-able synthetic methods, nickel-based NPs can serve as a powerful alternative. The conversion of benzaldoxime to benzonitrile in the absence of sodium azide was checked in the presence of the nickel hydroxide nanocatalyst, which did not take place under refluxing conditions in water. After 24hr, they get back to the corresponded aldoxime without formation of benzonitrile. This observation clearly indicates that nitrile formation is not necessary in our methodology. Initially, the $Ni(OH)_2$NPs bind with the oxygen atom of the aldoxime to activate the C=N bond. Then, azide ion undergoes cycloaddition with the activated imine bond. The cycloaddition between the C=N bond of aldoxime and azide takes place readily and form an intermediate. After removing the catalyst followed by acidic work-up, the desired product 5-substituted-1*H*-tetrazole was obtained. The common way of route for the synthesis of tetrazoles through [3 +2] cycloaddition of azide ions with organic nitriles or cyanamides in presence of acid or base catalysts has numerous drawbacks like uses of expensive toxic metal organic azide complexes, high moisture-sensitive reaction conditions, use of strong Lewis acids, and *in situ*-generated hydrazoic acid, which is extremely poisonous, water sensitive, explosive, and volatile (Halder *et al.*, 2018).

Heterogeneous catalysis in green solvents such as water reduces the environmental factor (E-factor) and also enhances the rate and selectivity of organic reactions (Mallesham *et al.*, 2020). To improve the long-term durability and activity of the catalyst, graphene-based graphitic structure is used as supporting materials. In ZnO–RGO nanocomposite, the surface polarity of ZnO is hydrophilic in nature and RGO is hydrophobic in nature. Hence, they used as nanocomposite to behave as amphiphilic heterogeneous reusable catalysts in a green solvent (Wang *et al.*, 2014). Thus, ZnO–RGO nanocomposite may overcome the mass transfer limitation

in water by enlarging the accessibility of organic molecules near the RGO surface. In continuation of our endeavors to develop heterogeneous catalysis in aqueous media, this reported method was a simple, practical, and efficient ZnO–RGO nanocomposite as a reusable heterogeneous amphiphilic catalyst for the synthesis of various 5-substituted 1*H*-tetrazoles in water. Compound **5** Substituted 1*H*-tetrazoles are synthesized conventionally via [2+3]-cycloaddition between an azide and a nitrile. ZnO anchored on RGO shows the best catalytic performance for the [3 +2] cycloaddition reactions of nitriles with sodium azide in high yield at a lower temperature and quick reaction time compared with previously reported solid-supported ZnO(Scheme 10) (Clarina & Rama, 2018).

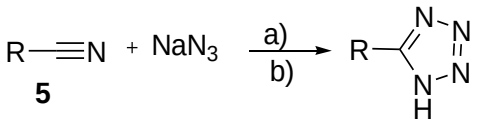

Reagent and conditions a) ZnO RGO, b) H_2O, 100°C, 2hr, yield 72-96%

Scheme 11: Synthesis of 5-substituted-1*H*-tetrazoles catalyzed by ZnO–RGO

2.4.1 Ultrasound assisted synthesis of tetrazole

Ultrasound irradiation has increasingly been utilized in organic synthesis within the past three decades. Compared with traditional methods, this method is more convenient and simply controlled. A large number of organic reactions have been carried out in higher yields, shorter reaction times, and milder conditions under ultrasound irradiation (Prukała, 2006). It is a technique to promote chemical reactions under the influence of ultrasound irradiation which is a part of the sonic spectrum that ranges from 20 kHz to 100 kHz. MCRs with ultrasonic irradiation techniques play an important role that provides an efficient access to highly complex products in a single step, green, and an innocuous technique (Gohil *et al.*, 2016). Unfortunately, all of those methods have some drawbacks like long reaction times, use of pricy and toxic reagents and high boiling solvents, harsh reaction conditions, low yield, tedious work-up, and even the need for excess amounts of highly toxic and explosive hydrazoic acid (Naeimi & Kiani, 2015). Therefore, so as to beat these drawbacks, it's necessary to develop an easy, convenient and more efficient method for the synthesis of tetrazoles. (Naeimi *et al* 2015) synthesized three-component, one-pot condensation reaction of various primary amines(**24**), sodium azide and triethylorthoformate in the presence of zinc sulphide nanoparticles as a catalyst at room temperature under ultrasonic

irradiation to afford 1-substituted tetrazoles(**25**) (Naeimi & Kiani, 2015). This novel method offers high yields shorter reaction time and catalyst can be recyclable (Scheme 12).

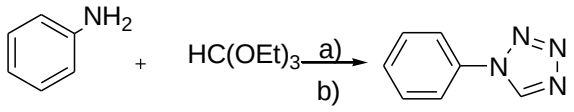

24 **25**

Reagent and conditions a) NaN_3,ZnS nanoparticles b) ultrasound, DMF, rt, yield 70-92%

Scheme 12: Synthesis of tetrazole derivatives via ultrasound assisted

2.4.2 Synthesis tetrazole catalyzed by ionic liquids

Ionic liquids (ILs) represent one point of 'green chemistry', since they are non-flammable, non-volatile, can be regenerated and reused repeatedly (Villa *et al.*, 2019).In recent times, ionic liquids have attracted increasing interest within the context of green synthesis. Although ILS were initially introduced as alternative green reaction media due to their unique chemical and physical properties of non-volatility, non-flammability, thermal stability, and controlled miscibility, today they have marched far beyond this border, showing their significant role in controlling reaction as catalysts (Potewar *et al.*, 2007). Many tetrazole derivatives have been synthesized using ILS as part of green synthesis report a new synthesis of 1-substituted-1*H*-1,2,3,4-tetrazoles by one-pot condensation of sodium azide, substituted thiazolylamine or oxazolylamine and triethylorthoformate in the presence of tributylmethyl ammonium chloride (TBMAC) as a catalyst in DMSO (Scheme 13) (Nagaraju *et al.*, 2017).

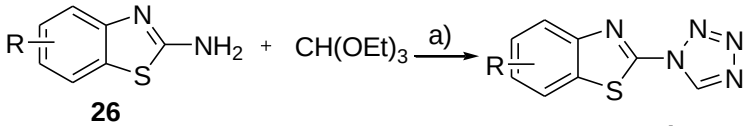

26 **27a-d**

Reagent and conditions a).NaN_3, TBMAC (2mol %), DMSO, 1-2 hr.80^{o}C,

27a) R =4-Cl, 27b) R= 5-NO_2, 27c) R=5-Me and 27d) R=H yield 76-96%.

Scheme 13: Synthesis of tetrazole via ILS

2.5 Synthesis of 1,5-disubstituted tetrazoles via Suzuki and his group

Suzuki and his group have found that treatment of both aliphatic and aromatic ketones with an excess of sodium azide in the presence of titanium(IV) chloride in boiling acetonitrile are converted to 1,5-disubstituted 1*H*-tetrazoles (Wittenberger *et al*., 2009). Unsymmetrical ketones afforded either one or both isomeric tetrazole products. The ratio of the isomers depended on the relative migratory aptitude of the substituent groups (Scheme 14).

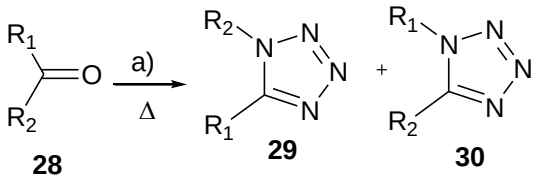

28 **29** **30**

Reagent and conditions a).NaN_3, $TiCl_4$, CH_3CN, yield 70 -95%,

Scheme 14: Synthesis of 1,5-disubstituted tetrazoles via Suzuki reaction.

Other Lewis acids like aluminiumtrichloride, tin (II) chloride, tin (IV) chloride, titanium tetrachloride, tetrachlorosilane, zinc (II) chloride and trimethylsilylazide were also used with success. Typically, an excess of the azide is used in the presence of a Lewis acid and the ketone in this reaction. Mixtures of 1,5-disubstituted 1*H*-tetrazoles **31** and **32** are obtained when aliphatic or aromatic ketones are treated with excess sodium azide in the presence of titanium chloride in refluxing acetonitrile (Scheme 15). The use of a large excess of sodium azide relative to the amounts of ketone and titanium (IV) chloride (i.e., 8:1:2) provides the most satisfactory results. Performing the reactions in other solvents like benzene, THF, ether or methylene chloride led to lower yield of the tetrazole products in the reported study.

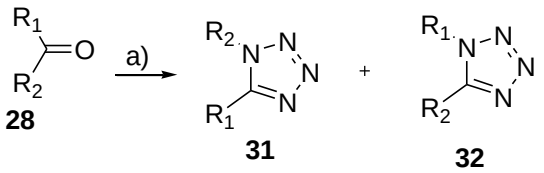

Reagent and conditions a).NaN_3, $TiCl_4$, acetonitrile, reflux 50-90%R_1=Ph, 4-ClPh, 4-OMePh, 4 -NO_2Ph, $PhCH_2CH_2$ and R_2=Ph,4-MeOPh

Scheme 15: Synthesis of tetrazoles from ketone and its derivatives.

2.5.1 Synthesis of 1,5- disubstitutedtetrazoles via Schmidt reaction

The Schmidt reaction (Wittenberger *et al*., 2009) is another general and useful method for the synthesis of 1,5- disubstitutedtetrazoles. Amides are common side-products due to hydrolysis of the nitrilium inter- mediate **33** (Scheme 16).

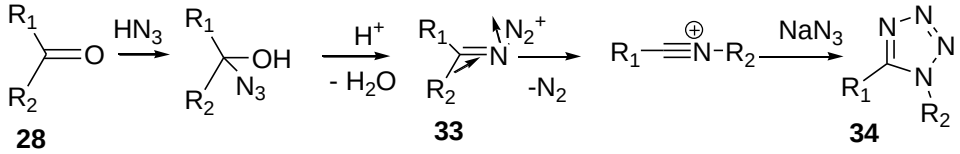

Scheme 16: Synthesis of 1,5-disubstituted tetrazoles via Schmidt reaction

2.6. Synthesis of tetrazole and its derivatives via microwave

Microwave assisted organic synthesis (MW) has emerged as a replacement "lead" in organic synthesis. The technique offers simple, clean, fast, efficient, and economic for the synthesis of an outsized number of organic molecules. Microwave-assisted organic synthesis is an invaluable technology for medicinal chemistry and drug discovery since it greatly reduces reaction time, typically from days or hours to minutes or even second (Sahu *et al.*, 2016) and (Zhou *et al.*, 2010). Acriflavin (ACF) inhibits the growth of both chloroquine (CQ) asexual aspects. Mixtures 0.01 mole of Schiff bases compounds and sodium azide dissolved in 20 ml of tetrahydrofuran(THF) and 2 mL of distilled water and refluxed the mixture by microwave oven for 6 minutes 200Watt(Scheme 17). On completion of the reaction as observed by TLC eluting with a mixture of n-hexane and ethyl acetate (3:2) and left to stand for 24 hr (Dana *et al.*, 2014).

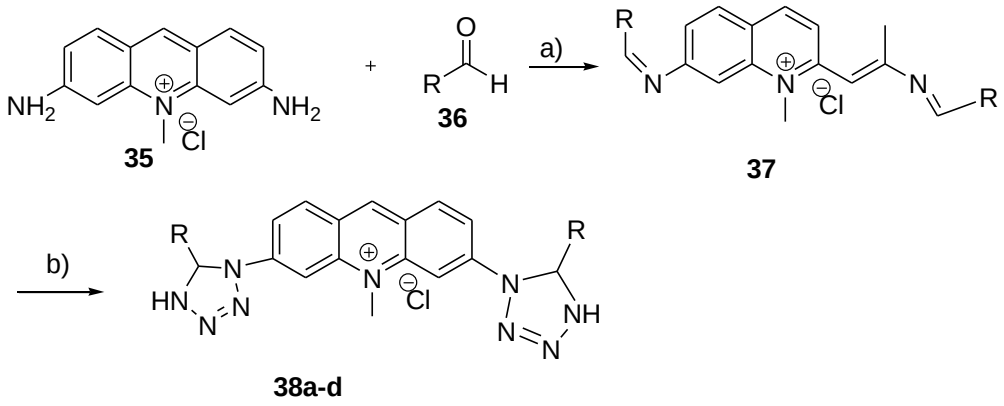

Reagent and conditions a).EtOH,refluxMW,200 watt,4-10 min b).2NaN_3,THF

38a) R= Br-C_6H_4,

38b) R=*P* -OH-C_6H_4,

38c) R=*P* -Cl-C_6H_4 and 38d) R=Glucose

Scheme 17: Synthesis of tetrazole derivatives via microwave method.

2.6.1 Synthesis of thiazole derivatives via microwave

To facilitate the synthesis of hybrid phenyl thiazolyl-triazine derivatives and also to minimize the impurities owing to high temperature, long-term open vessel reactions reported to successful microwave-assisted replacement of second and third chlorine atoms of this class of compounds (Sahu *et al.*, 2016). To reveal their possible antimalarial activity, synthesized compounds were screened against 3D7 strain of *P. falciparum*. The yields of varied phenyl thiazolyl-triazine derivatives were improved using microwave heating under solvent-free conditions. Besides, the technique has the advantage of being simple and allows the synthesis of this hybrid class of compounds during a minimum response time since the reactions were carried out struggling in closed vessels, it minimizes the chances of fabric loss then the occurrence of impurities too. Sahu and coworkers (2019) synthesized hybrid thiazole-1,3,5-triazines via microwave and examined their antimalarial activities against choroquine sensitive 3D7 and chloroquine resistant Dd2 strain of *P. falciparum*. The result suggested that compounds (43a) and (43b) (Scheme 18) as most potent derivatives among the tested compounds with significant *in vitro* antimalarial activities and may serve as leads for identifying new class of Pf-DHFR inhibitor.

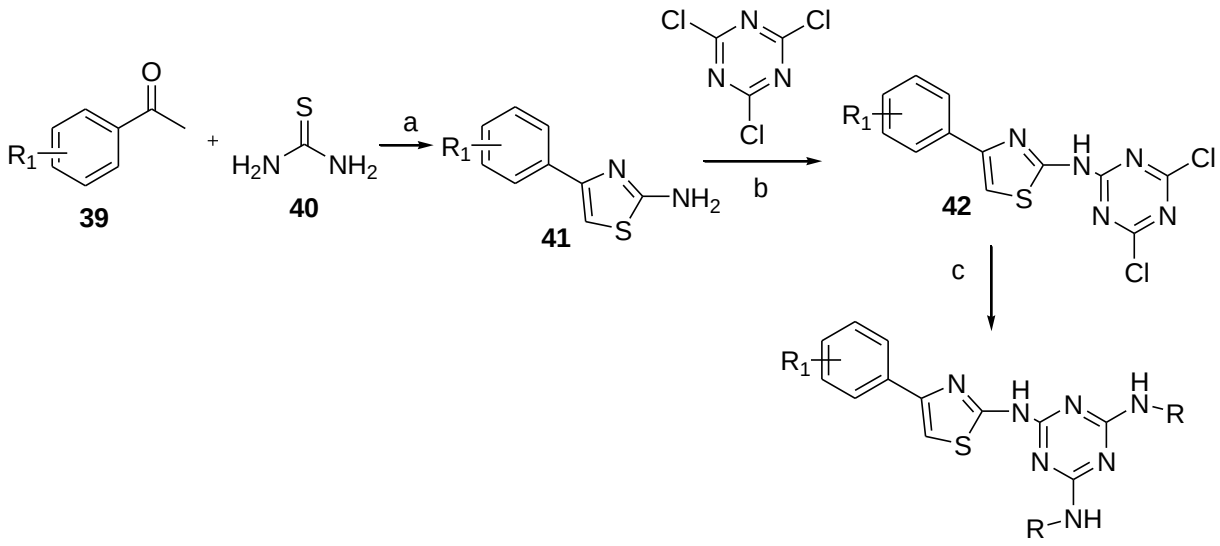

Reagent and conditions a) Bromine, neat, MW130^{o}C,10 min, 50W, b) acetone 0-5°C and c) RNH_2, MW, neat, 120^{o}C, 100W, 9 min, 10 Bar

43a) R_1=2,4-Cl and 3-NO_2

43b) R_1=CH_3NHCH_3 and R= phenylamine

Scheme 18: Synthesis of thiazole derivatives via microwave

2.7 Synthesis of thiazole from acetophenone derivatives

The4-fluoro-N-[4-(2-hydroxy-4-methoxyphenyl)thiazol-2-yl]benzenesulfonamide (**47d**)(Scheme 18) was the second potent compound, showing IC_{50} values of 7.2, 11.2 and 13.8μM to AGS, HT-29 and HeLa cells, respectively. These compounds are superior to 5-fluorouracil (5-FU) for relatively higher potencyagainst AGS and HT-29 human cancer cell lines along with lower cytotoxicity to fibroblasts. Novelaminothiazole-paeonol derivatives these might be a series of promising lead compounds to develop anticancer agents for treating gastrointestinal adenocarcinoma (Elsadek *et al*., 2021) (Scheme 19).

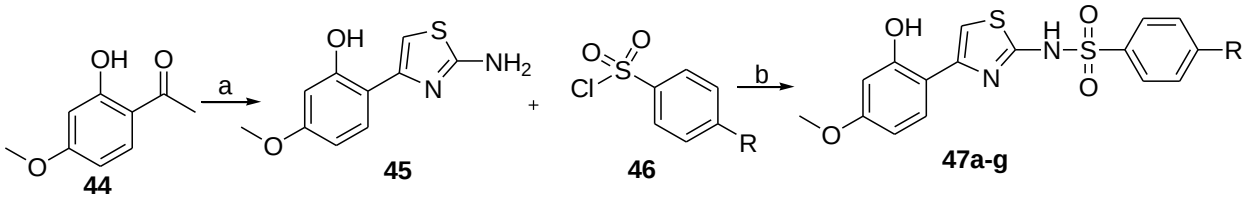

Reagent and conditions a).thiourea,I_2,EtOH,reflux12-16hr,b).K_2CO_3,THF,Cpd47a).R=H, b).R=Me, c)R=OMe, d)R=F, e)R=Cl, f)R=Br, and g) R=NO_2 respectively

Scheme 19: Synthesis of aminothiazole from acetophenone and its derivatives

2.7.1 Synthesis of some novel thiazole hydrazine derivatives from thiosemicarbazones

Synthesis of some novel thiazole hydrazine derivatives from thiosemicarbazones of salicylaldehyde and 5-chlorosalicylaldehyde with phenacyl bromide in ethanol under reflux condition is reported (Gore *et al.,* 2020). Thiazolyl-hydrazine derivatives are a crucial class of heterocyclic compounds obtained by incorporating the hydrazino-thiazolyl group and therefore the phenothiazine structures during a single molecule. Thus, thiazoles containing hydrazone functionality are of accelerating interest thanks to their significant role in medicinal chemistry. For instances compounds (**52b**) and (**52h**) (Scheme 20) showed promising antibacterial activities against *E. coli* as they had lower MIC values in comparison with the standard ampicillin. Thiazolehydrazines (**52a**), (**52b**), (**52c**), (**52d**), (**52e**), and (**52f**) (Scheme 20) exhibited better antibacterial activity than the standard drug Ampicillin. Compounds (**52b**), (**52e**), and (**52g**)

(Scheme 20) were better in terms of antifungal activity against *C. albicans* having lower MIC values than the standard Griseofulvin, thus due to SAR.

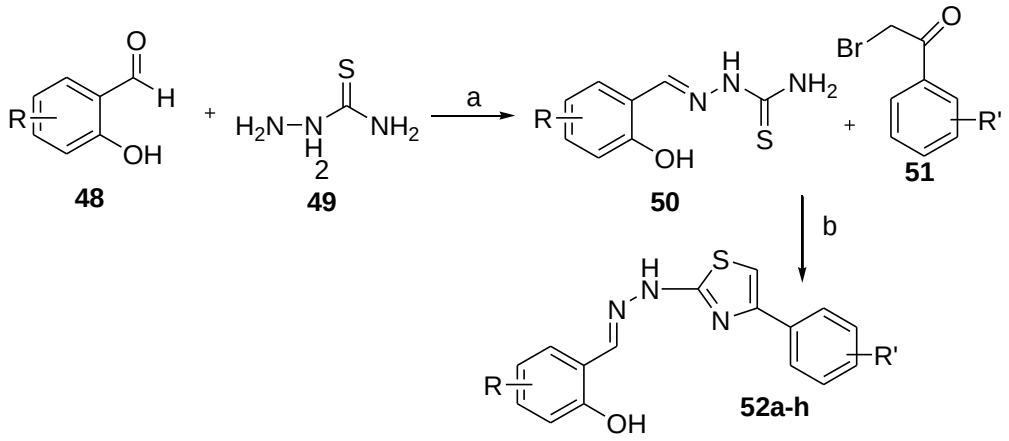

Reagent and conditions: a).Conc. HCl, EtOH, reflux 3hr, b)α-halocarbonyl compound, EtOH, reflux 4hr,cpd 52a).Rand R' =H,52b).R=H &R' =4-OMe,52c)=R=H&R' =4-F 52d)R=H&R' =4-NO_2, 52e)R= 5-Cl &R' =H, 52f) R= 5-Cl &R'= 4-NO_2 52g) R= 5 –Cl & R'= 4-Cl 52h) R= 5-Cl &R' = 4-OMe

Scheme 20: Synthesis of thiazoles derivatives from thiosemicarbazones

2.7.2 Synthesis of Schiff base of thiazole via condensation reaction

The antimicrobial activity of the two methoxyimio thiazole derived Schiff bases (**55a** and **55b)** were tested against selected species of bacterial (*E. coli* and *R. solanacearum*) and fungi (*F. oxysporum* and *A. niger*) (Vinusha *et al.*, 2015). Both the compounds were found to be moderately potent towards the microbial growth inhibition. Particularly, compound (**55a**) was significantly active against the tested microbes than compound (**55b**) (Scheme 21). The possible reason for this potency of compound (**55a**) may be due to the presence of electron withdrawing nitro group which can alter the tertiary structure of membrane proteins and thus growth (Karthikeyan, 2009).

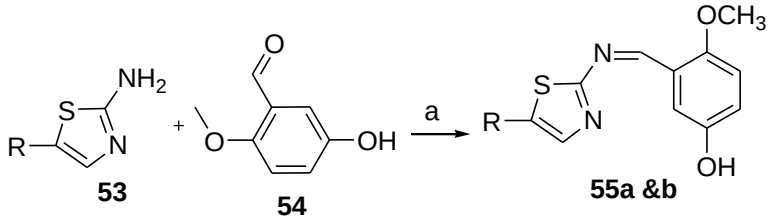

Reagent and conditions a).CH_3OH,80°C,reflux 6hr 55a) R=NO_2 and55b) R=ethyl

Scheme 21: Synthesis of thiazole Schiff base via condensation reaction

2.8 Biological activities of tetrazole and Schiff base of thiazole moiety

Compounds derived from tetrazole and thiazoles have received particular attention due to their pharmacological properties. Numerous studies have been published on the antibacterial(Bush, 2004) and antifungal (Łączkowski *et al.*, 2018) properties of these derivatives. Furthermore, these compounds also showed anti-inflammatory (Karthikeyan, 2009), analgesic, anticancer (Sharma *et al.*, 2012), anticonvulsant, antihypertensive, hypoglycemic, anti-parasitic, and antiviral activities. The aforementioned properties and the possibility to attach several structurally distinct substituents to the heterocycle ring to modify either the biological or physico-chemical properties of these compounds have prompted the use of this heterocycle as a template in many research programs aimed at the development of new bioactive compounds.

2.8.1 Antibacterial activity

In spite of the introduction of a variety of antibacterial agents in multiple unrelated drug classes, resistance continues to emerge. The pharmaceutical field must respond to these clinical challenges by bringing forward a stream of new agents with promising antibacterial activity against bacteria (Bush, 2004). Advantages of these agents include their higher predictability for success, well-defined biomarkers, shorter clinical trials, and shorter duration of therapy leading to fewer long-term safety concerns. The newly synthesized tetrazole derivatives were investigated for their growth inhibition against *S. aureus, E. coli*, *P. aeruginosa* and *K. pneumoniae* (recultured) bacterial strains by the disc diffusion method (Broekema *et al*., 2009). Compound **56, 57a, 57b, 57c, 57d** and **57e** (Figure 3) showed good growth inhibition towards four bacterial strains, and **57b**and **57d** showed the pronounced growth inhibition for *P. aeruginosa* and *K. pneumoniae*. In 2015, a nontoxic and nonhemolytic compound **59**, which have the same active previous moieties, was prepared and assayed for its biological properties. It displayed inhibition activity against Gentamicin-resistant and Methicillin-resistant *S. aureus* (Arora *et al*., 2016). Tetrazole-containing derivatives possess potential antibacterial activity, and some tetrazole hybrids such as tetrazole-oxazolidinone Tedizolid **60** and Tedizolid phosphate **61** have already been marketed for the treatment of skin and skin structure infections caused by various bacteria, demonstrating the possible utility of the tetrazole scaffolds in the development of new antibacterial agents (Figure 3).

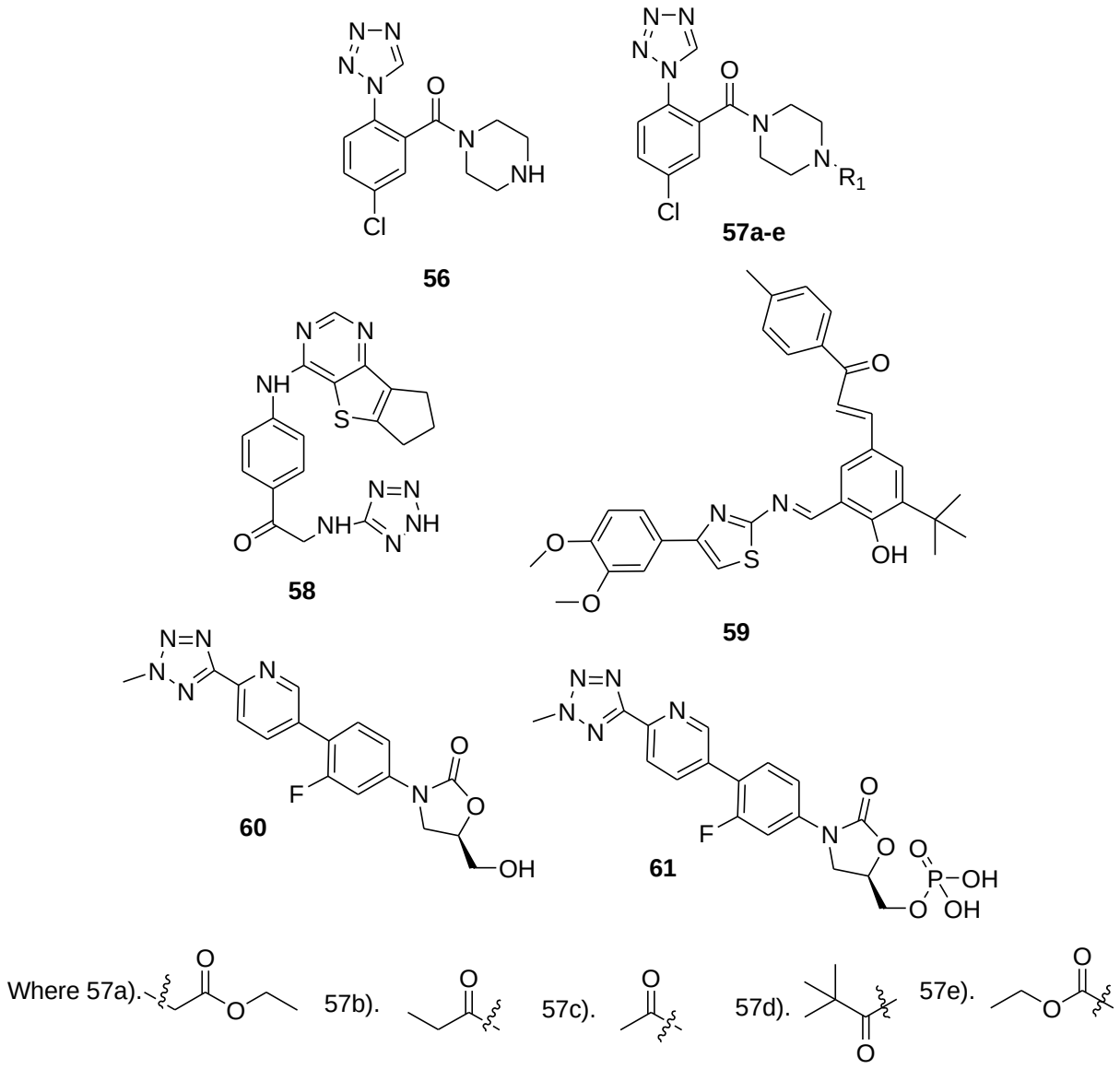

Figure 2: Potential tetrazole and thiazole contains compounds with antibacterial activities.

2.8.2 Anti-oxidant activities of tetrazole and its derivatives

Antioxidant therapies are gaining importance due to their ability to retard disease progression by reducing the damage caused by free radical or reactive oxygen species (Koppireddi *et al*., 2013) . Physiological levels of (ROS) play vital role as signaling molecules to mediate numerous biological functions causing alterations in cell growth, gene expression and host defense. Tetrazoles act as free radical scavengers. For a certain extent, their antioxidant potential depends on substituted terminal groups and structure conjugation (Chand *et al.,* 2018). Bacterial

responses to tetrazoles oxidative stress are expressed as the generation of (ROS) leading to the oxidative damage to cellular proteins. Compound **63**(Figure 4) had been found to have antioxidant properties offering potential efficacy against oxidative stress induced by acrylamide administration (Mohareb *et al*., 2011). Adibi *et al.,* (2011) also reported the synthesized a novel series of 3-substituted-5-(1-phenyl-1*H*-tetrazole-5-yl) methyl)benzene-1,2-diol. The antioxidant activity was performed by (DPPH) radical scavenging and reducing power assay method. Among the synthesized compounds, compound **62**(Figure 4)was exhibited more potent antioxidant activity (Adibi& Nematollahi, 2011).

The antioxidant activity of 2,4-dioxo-1,3-thiazolidine thiazoles have been studied using DPPH method. Based on perilously reported, para-bromo derivative **64**(Figure 4) showed the highest antioxidant potency (EC_{50} = 49.71 µg/mL), comparable to ascorbic acid and luteolin as reference compounds (Koppireddi *et al.,* 2013). Several series of thiazole-modified compound **103** and **66** (Figure 4) containing hydrazineimidazolyl moiety were evaluated for their antioxidant ability using DPPH method. Among the synthesized compounds, 4-fluorobenzylidene-thiazolidin-4-one derivative (Ar= 4-F-Ph) was found to be the most potent compound (Ayati *et al*., 2015).

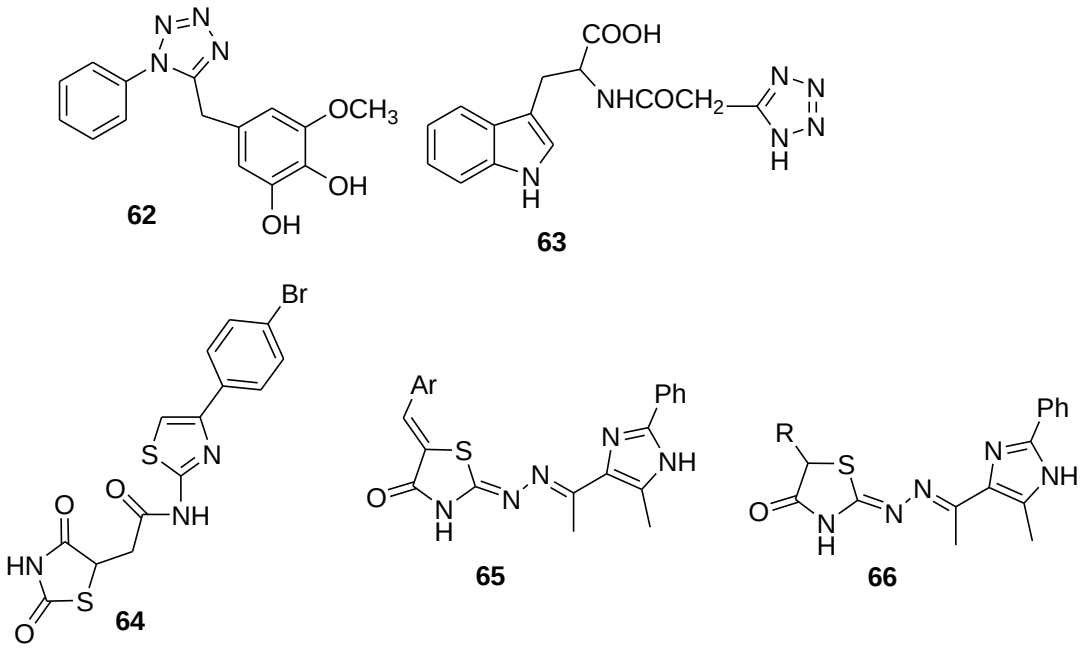

Figure 3: Compounds (**62-66**) with tetrazole and thiazole moieties with potential anti-oxidant activities

2.8.3 Anti-diabetic activity

Shaikh and coworkers (2017) reported synthesized of tetrazoles having N-glycosides as SGLT2 inhibitors and evaluated for their hypoglycemic effects *in vivo* by mice oral glucose tolerance test (OGTT). Compound **67 (**Figure 5**)** was found to be most active against standard drug Dapagliflozin (Shaikh *et al*., 2017). These thiazolidinedione derivatives were synthesized by the reaction of 5-(4-chlorosulfonyl benzylidene)-2,4-thiazolidenedione and aromatic amines (Kaushik *et al*., 2018) and evaluated for anti-diabetic activity by alloxan induced tail tipping method in albino rats by using glibenclamide as a standard drug. Among the synthesized derivatives, compound **68** exhibited significant anti-diabetic activity (Pattan *et al*., 2009). Sharon *et al*., (2005) synthesized a series of 5-[(5-aryl-1*H*-pyrazol-3-yl) methyl]-1*H*-tetrazoles derivatives and evaluate for their *in vivo* anti-hyperglycemic activity by sucrose loaded model of which compound **69** (Figure 5) showed significant anti-hyperglycemic activity (Sharon *et al*., 2005)

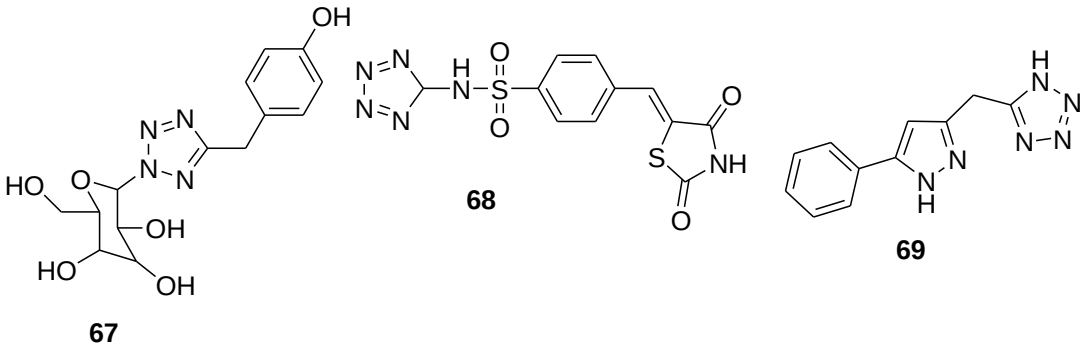

Figure 4: Compounds with potent anti-diabetic activity

2.8.4 Anticancer activity of tetrazole and thiazole moieties

Cancer is basically a group of dreadful diseases recognized by uncontrolled cell growth. Cancer is considered to be one of the most intractable diseases because of the innate characteristics of cancer cells to proliferate uncontrollably, avoid apoptosis, invade and metastasize. The low-toxicity broad-spectrum therapeutic approaches has been explored by various research organizations (Roberts *et al.,* 2014).Ali *et al*., (2017) synthesized a series of steroidal tetrazole derivatives from convenient method in a two-step process. The anti-proliferative activities of the synthesized compounds were tested *in vitro* against cervical cancer (HeLa), myeloid leukemia (KCL-22), breast cancer (MDA-MBA-231) and normal cell lines by MTT assay method. The synthesized compound **70** exhibited significant activity (IC_{50}>60μM) against the three human cancer cell lines and were also found to be nontoxic to the normal cell lines (Ali *et al.,* 2017). Arshad *et al*. (2014) were synthesized a series of novel substituted tetrazole derivatives and evaluated on MCF-7, MDA-MB-231 and ZR-75 breast cancer cell lines. Compounds **72**, **73** and **74** (Figure 6)exhibited 10^{-30} percent negative growth on MCF-7 cells, whereas the compound **48** exhibited a higher inhibition effect on MDA-MB-231 cells and ZR-75 cells at a concentration of 10^{-5}M (Arshad *et al*., 2014).

A series of 1,5-disubstituted tetrazole derivatives were reported by Jedhe *et al*., (2013) and evaluated them for their antitubulin and antiproliferative activity. Compound **71** was found to be tough inhibitors of tubulin polymerization and anti-proliferative agent having IC_{50} value in micro molar concentration level (Jedhe *et al*., 2013). Many thiazoles were found to be associated with various biological activities, that anticancer property is known as the most important ones. Series of substituted 2-phenylthiazole-4-carboxamide derivatives **49c** (Figure 6) were synthesized as potential anticancer agents of which compound **76** was evaluated against three

human cancer cell lines including T47D (Breast cancer), Caco-2 (Colorectal cancer) and HT-29 (Colon cancer). Based on the results, compound with 4-methoxy substituent, showed the highest activity against Caco-2 cells while compound with 2-methoxy substituent showed high activity against HT-29 and T47D cell lines. Moreover, 3-fluoro analog showed good cytotoxic activity against all tested cell lines (IC_{50} values <10mg/ml) (Aliabadi *et al*., 2010).

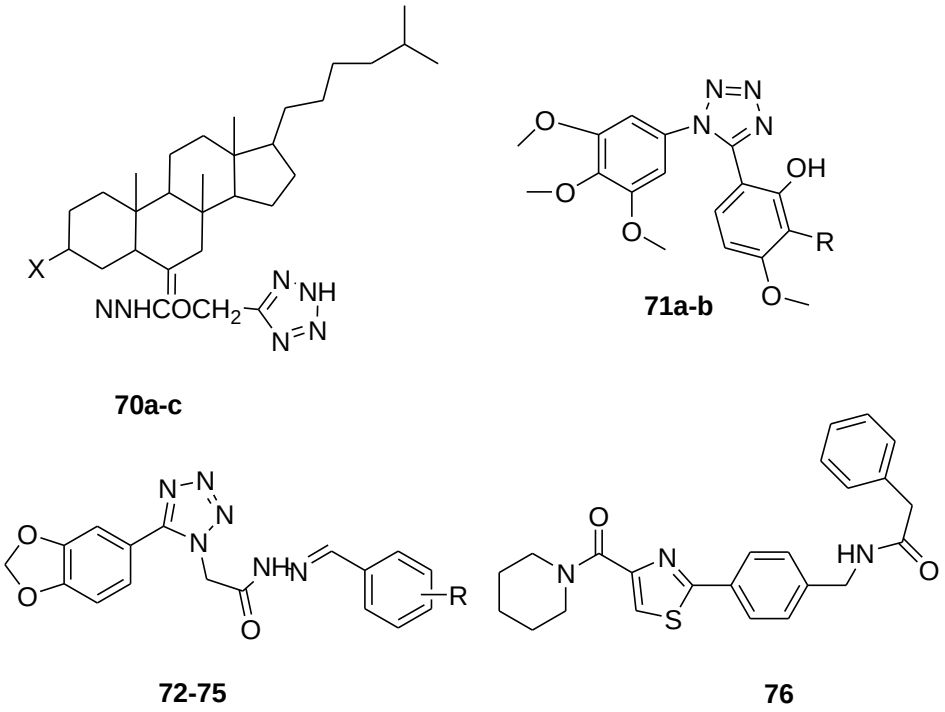

Where X is Compounds 70a) X=OAc, 70b) X= Cl, 70c) X=H, 72) R=2-NO_2, 73) R=3-NO_2, 74) R= 4 -NO_2, 75) R= 2,3-di -OCH_3,71a) R=OH 71b) R=NH_2

Figure 5: Structures of some tetrazole and thiazole derivatives with possessing anticancer activity.

2.8.5 Anti-inflammatory and analgesic activities

Murumkar and coworkers (2018) synthesized a series of 1,5-diaryl-substituted tetrazole derivatives and evaluated for their anti-inflammatory activity. All the synthesized compounds were found to exhibit IC_{50} values for COX-1 ranging from 0.42 to 8.1 μM and 2.0 to 200 μM for COX-2 of which compound **78**, showed most significant activity (IC_{50}= 2.0 μM) (Murumkar & Chikhale, 2018). Rajasekaran *et al,*. (2004) synthesized a series of 5-[β-(phenothiazinyl-10-

yl)ethyl]-1-(acyl)-1,2,3,4-tetrazole derivatives. The synthesized derivatives were evaluated for analgesic and anti-inflammatory activity. Compounds **79** and **80** (Figure 7) showed remarkable analgesic activity, while compounds with chloro group **81** and nitro group **82** show potential anti-inflammatory activity (Rajasekaran& Thampi, 2004). Kalkhambkar and coworkers (2007) reported thiazoles **83** (Figure 7) containing coumarin and carbostyril as anti-inflammatory agents. The compounds have been obtained by the reaction of 4-thioureidomethyl carbostyril (1-azacoumarin) and 3-bromoacetyl coumarin derivatives and tested for their *in vivo* analgesic and anti-inflammatory activities and were compared to phenyl butazone (standard drug). The tested compounds were slow acting anti-inflammatory agents and showed significant activity after 4-8hr. The anti-inflammatory, analgesic and ulcerogenic activities of several 3-thiazolyl quinazolin-4-ones **84** (Figure 7) were evaluated by (Kumar *et al.*, 2007) They reported that 2-chloro phenyl derivative (R = 2-Cl) had anti-inflammatory activity equal to phenylbutazone at the dose of 25 and 50 mg/kg, while at 100 mg/kg had better anti-inflammatory activity than the standard drug.

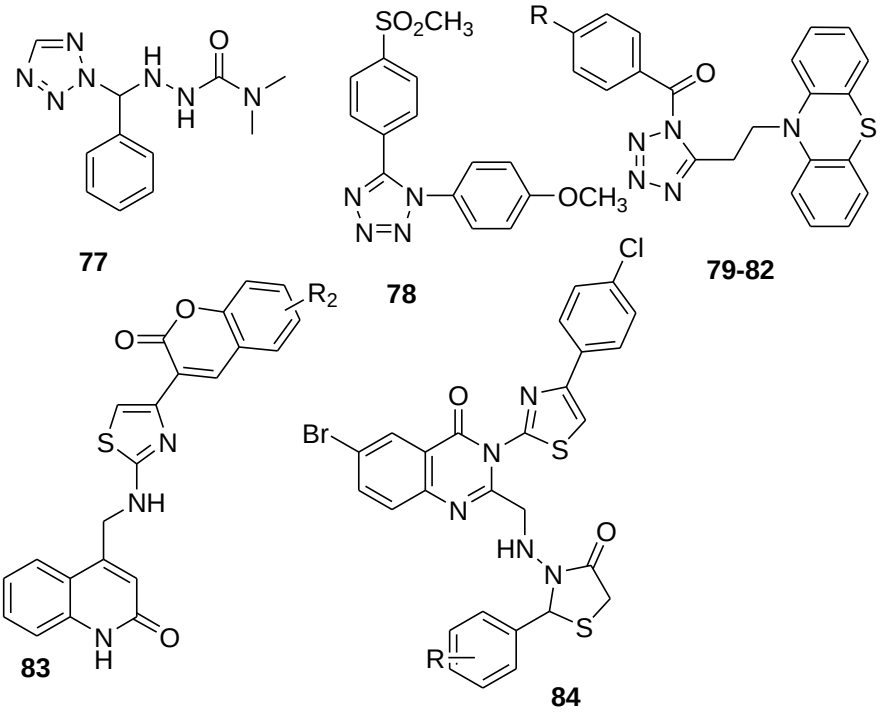

79) R= H, 80) R= CH_3, 81) R=Cl and 82) R=NO_2

Figure 6: Compounds of tetrazole and thiazole moiety with potential anti-inflammatory activity

2.8.6 Anti-tuberculer activity

Tuberculosis is a significant medical problem worldwide, particularly in the developing world, where up to 80% of the populations are thought to be infected by the bacterium *M. tuberculosis* in either latent or active form. Kaushik *et al.* (2018) synthesized several derivatives of 5-chloro-2-(5-(substituted phenyl)-1*H*-tetrazol-1-yl) pyridines from the reaction of 2- amino pyridine derivative with substituted aromatic acid chlorides and sodium azide. All the synthesized analogues were evaluated for antitubercular activity by Microplate Alamar Blue assay (MABA) method. Compound **85** (Figure 8) exhibited potential activity against *M. tuberculosis* H37Rv (Kaushik *et al*., 2018). Roh *et al.* (2017) synthesized a series of tertiary amine-containing 3,5-dinitrophenyl tetrazole derivatives and evaluated there *in vitro* antimycobacterial activities against *M. tuberculosis.* The MIC values of 1,4-dimethylpiperazine substituted **57**, 4-methylmorpholine substituted **87** and 1-benzyl-4-methylpiperazine substituted **88** compounds against *M. tuberculosis* of which compound **88** was found to be comparable to those of first-line

anti-TB drugs INH and RIF, ranging from 0.125 to2 µM (Roh,& Karabanovich, 2017) (Figure 8).

(Abhale *et al.*, 2017) the preliminary (SAR) study it is noteworthy to mention that thiosemicarbazide of unsubstituted 2-phenylthiazole-4-carbaldehyde **89**, showed excellent activity against *M. bovis*, whereas replacement of hydrogen atom of phenyl ring by substituent groups like 4-Cl, 4-F, or 4-CH_3 significantly decrease the anti-tubercular activity.

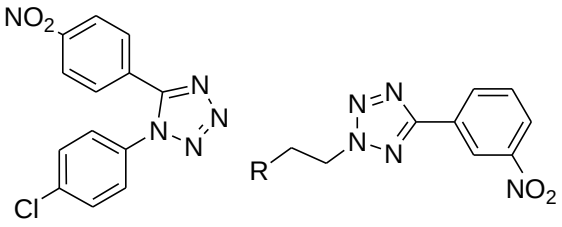

85

86-88

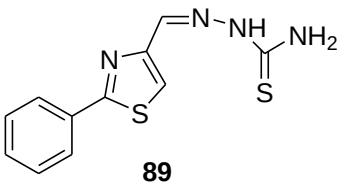

89

Cpd86) R=1,4-dimethylpiperazine,

Cpd87) 4-methylmorpholine,

Cpd88) 1-benzyl-4methylpiperazine

Figure 7: Compound with exhibited potential activity against *M. tuberculosis.*

2.8.7 Anti HIV activity

Zhan and coworkers (2012) synthesized a series of aryltetrazolylacetanilides and screened them as HIV-1 non-nucleoside reverse transcriptase inhibitor on the clinically relevant K-103N mutant strain of which compound **90** exhibited remarkable activity (Zhan *et al.*, 2012). The results showed that compounds **91d** (IC_{50}=0.50µM), and **91c** (IC_{50}=0.45µM) (Figure 8) were the most active analogs of the series against HIV-1, while compounds **91a** and **91b (**Figure 9**)** displayed activity against HIV-1 (IC_{50}>0.45 and>0.47µM) but no selectivity can be witnessed (Madni *et al.*, 2017). Due to the cytotoxicity of the latter compounds, they have been selected for

evaluation of their anti-proliferative activity with IC_{50}=2.4 μM against solid tumor-derived cell lines (Irfan *et al.*, 2020).

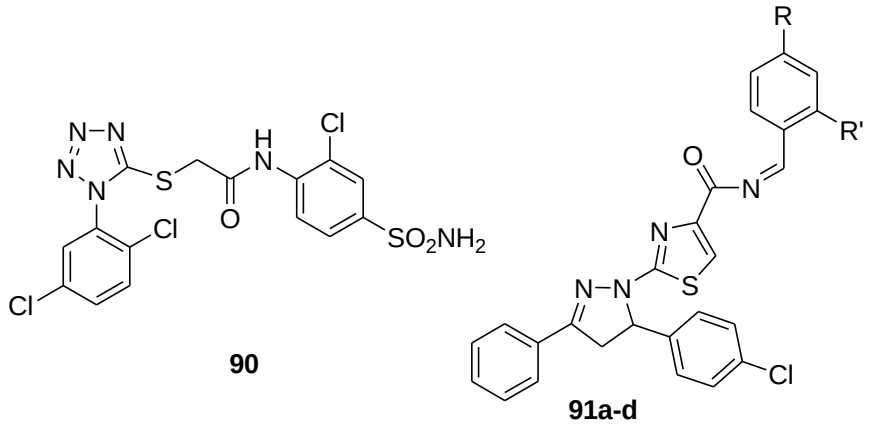

91a) R&R'=H
91b) R=3-NO_2&R'=H
91c) R=Cl and R'=OH
91d) R=F and R'=H

Figure 8: Compound with anti HIV activity.

2.8.8 Antimalarial activity

Malaria is the most serious parasitic disease in the world with mortality and morbidity rates only exceeded by those of tuberculosis (Salas *et al.*, 2004). About 90% of all malaria deaths in the world today occur in Africa south of the Sahara. This is because the majority of infections in Africa are caused by *P. falciparum*, the most dangerous of the four human malaria parasites (Conn *et al.*, 2018). Marella *et al*. (2014) reported the synthesis of a new series of tetrazole derivatives containing aminoquinoline moiety and evaluated their antimalarial activities against chloroquine-senstive (3D7) and chloroquine- resistant (K1) strains of *P. falciparum*. The synthesized compounds showed potent antimalarial activity as compared to chloroquine against K1-strain. Those compounds which showed potent *in vitro* antimalarial activities were then screened for their *in vivo* activity in Swiss mice against *P. yoelii.* Compounds **92** and **93 (**Figure 10**)** showed *in vivo* suppression of 99.99% parasitaemia (Marella *et al*., 2014).

Compounds **94**a &**b (**Figure 9**)** was evaluated for their inhibitory potential against *P. falciparum*. The inhibition activities are calculated by *in vitro* blood stage assay starting from 10 lμM concentration to the lowest concentrations possible and are represented in values. Chloroquine

and artemisinin, the drugs in clinical practice are used in this study as standards for comparison. It is interesting to note that among the six membered 2- or 3- or 4-pyridyl systems (**95**–**96**) (Figure 10), 2-pyridylhydrazinyl group at 2-position of thiazole ring containing molecules found to be the potent molecules. 2-Pyridyl hydrazinyl group at 2-position of the thiazole ring with $COOC_2H_5$ at the 5- position (**95**) showed significant activity with IC_{50} value of 0.725 µM in (Figure 10). Similarly, replacement of $COOC_2H_5$ with $COCH_3$ at the 5-position increases the activity to a very small extent and exhibited significant activity with IC_{50} value of 0.648 µM. This suggests that the keto group at 5-position enhance the activity and this could be due to the possibility of keto-enol tautomerism which influences activity (Katritzky *et al*., 2010).

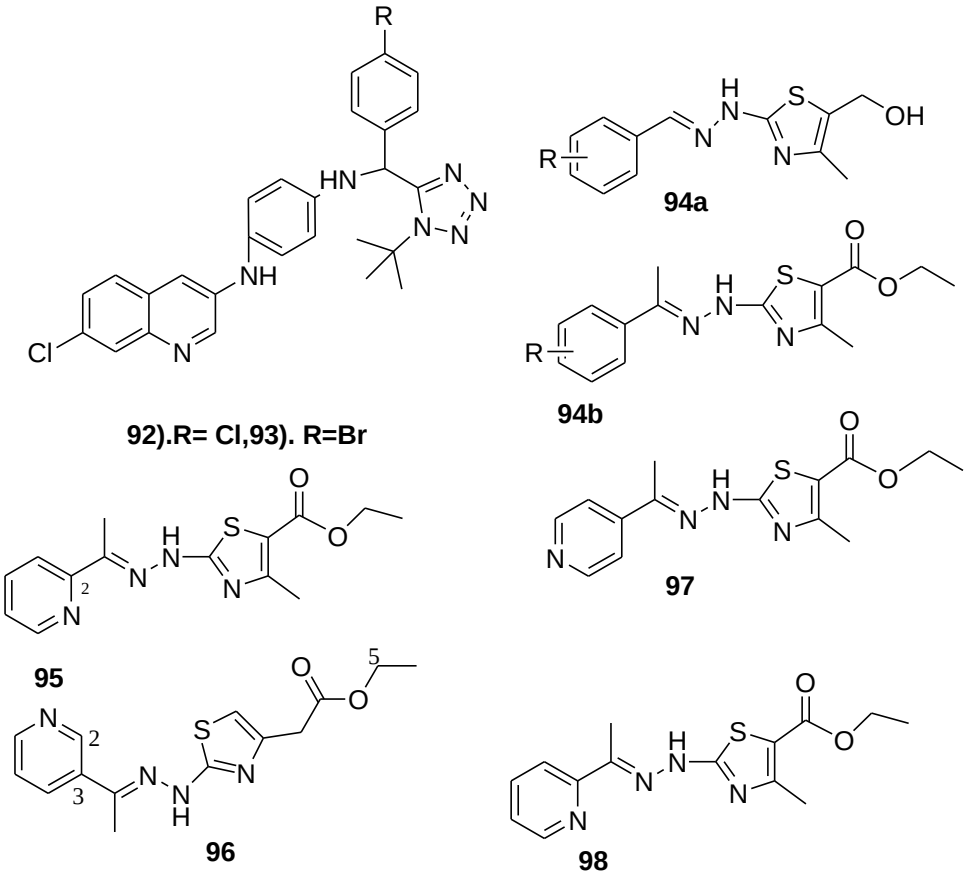

Figure 9: Tetrazole and thiazole bridged molecular scaffold with potent antimalarial activity.

3. MATERIALS AND METHODS

3.1 General

All chemicals were purchased from Loba Chemie PVT, Ltd. All chemicals were used without further purification. Melting points were determined using open capillary tubes (Thiele tube) filled in oil and were uncorrected.

3.2 Chemicals and reagents

Distilled water, *n*-hexane, ethyl acetate, chloroform, methanol, absolute ethanol, dichloromethane, silica gel (60-120 mesh) benzaldehyde, *p*-nitrobenzaldehyde *p*-hydroxybenzaldehyde, *p*-nitroacetophenone, acetophenone *o*-hydroxyacetophenone, *m*-chloroaniline, iodine, thiourea, diethyl ether, petroleum ether, glacial acetic acid, dimethyl sulfoxide, N,N-dimethylformamide, sodium thiosulfate penta hydrate, sodium bicarbonate anhydrous, sodium sulfate anhydrous and ZnO NPs (received from Applied Physics Department, ASTU) were chemicals used in this work.

3.2.1 Instruments and apparatus

The progress of reaction were controlled by thin layer chromatography (TLC) plates were percoated 0.2mm silica gel 60 F254 on aluminum foil and compounds on TLC spot were detected under UV lamp at 254 and 346nm . The synthesized compounds were characterized on the basis of physical and spectral analyse. The UV-Vis spectra of some compounds were recorded on Double-beam UV-Vis spectrophotometer using DMSO and MeOH as blank solvents. IR spectra were recorded on KBr disk on the 'PerkinElmer IR' instrument and are reported in cm^{-1}, NMR spectra were recorded by Bruker avance 400 MHz spectrometer using tetramethylsilane (TMS) as the internal standard and DMSO-d_6 and $CDCl_3$ as a solvents. Chemical shifts δ are quoted in ppm.

3.3 Synthesis method 1

3.3.1 The Synthesis of these compounds were synthesized by employing Koppireddi *et al.*, 2013) protocol with modifications

Thiourea (40 mmol, 2 molar equiv.) was mixed with iodine beads (20 mmol, 1 molar equiv.) in a mortar and the mixture was homogenised with a pestle. The solids were scratched off into a 250 mL round-bottom flask with a magnetic stirring bar and mixed with the corresponding acetophenone or 2-hydroxy acetophenone and 4-nitro acetophenone (20 mmol, 1 molar equiv.). The mixture in flask was heated in an oil bath under air-cooled condenser at 100°C with stirring refluxed for 3hr. Upon heating, the mixture liquefied. After 3 hr, the mixture was cooled and it solidified again. Saturated aqueous solution of sodium thiosulfate ($Na_2S_2O_3.5H_2O$ 5%) was added (with concomitant mechanical disruption of the solid matrix) in sufficient amount to reduce the remaining iodine (until brown colour disappeared). The product as a suspension was filtered off and carefully washed with approx. 20 mL of diethyl ether (caution: product partially soluble) to remove the residues of unreacted acetophenone and its derivatives. The crude product was dissolved in hot water, filtered, and the hot filtrate was adjusted to pH = 9 by aqueous Na_2CO_3 anhydrous. The products was collected by suction filtration to yield 3.49 g (99.2%), 4.22 g (55 %) and 4.36 g (98.64 %), respectively, and were recrystallized from hot EtOH, white crystal, Mp 144-146°C, 85%, red crystal, Mp 92-94°C,30% and yellow crystal, Mp 226-228°C,75%, respectively in (scheme 22).

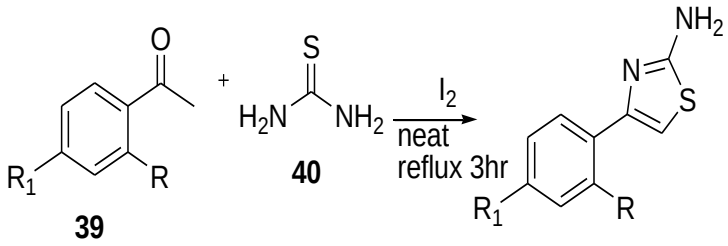

Where Cpd**41a**) R is H, R_1=H

41b) R=OH, R_1=H

41c) R_1 is NO_2, R=H

Scheme 22:Synthesis of thiazole derivatives from acetophenone and derivatives.

3.3.2 Synthesis of Schiff base of thiazoles using Sakarya *et al.*,(2012) modified synthesis protocol

A solution of phenylthiazole (25 mmol) and benzaldehyde/ its derivatives (25 mmol) were mixed in methanol (40 ml) within 150 mL of round bottom flask while magnetic stirring and refluxed for 4 hr at 65°C. The mixture was left to stand at room temperature overnight to and concentrated using rotary evaporator. The residue was washed with *n*-hexane (2·50 mL) and filtered off. The residue was hydrolyzed in water and extracted with EtOAc (4·20 mL). After drying with Na_2SO_4, 0.53g (68.83%), 0.53 g (77.3%) and 0.55g (69.3%) of crystals were obtained, respectively. Recrystallized from CH_2Cl_2 and washed with cold ethanol and diethyl ether to remove unreacted amine, aldehyde and its derivatives. Compounds **102**, **103 and 105** were prepared using the same method described above (Scheme 23).

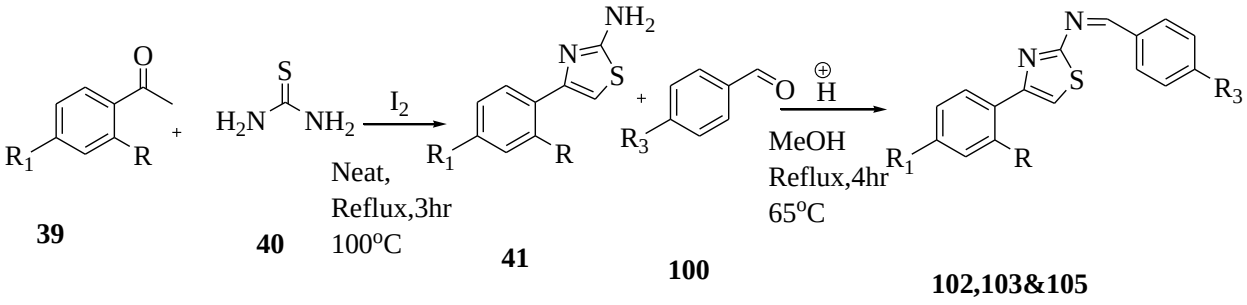

102 R_1= H, R=OH, R_3 = OH

103 R = H, R_1=H, R_3= H

105 R= NO_2, R_1=H, R_3=OH

Scheme 23: Synthesis of Schiff base via condensation reaction

3.3.3 Green synthesis of Schiff base via ZnO nanoparticle using Sakarya *et al.*,(2012) modified synthesis protocol

A solution of *p*-nitro acetophenonethiazole (0.3g, 13.5 mmol) and *p*-nitro benzaldehyde (0.205 g, 13.5 mmol) were mixed in absolute ethanol (30 mL) and refluxed for 4 hr in presence of 15% ZnO nanoparticles load at 78°C. The mixture was poured in to 150 mL of crushed ice, while being stirred with glass road to yield 0.507 g (84.6 %) and 0.48 g (83.3%) crystals after recrystallization in CH_2Cl_2 and the crystals were washed with cold ethanol and diethyl ether to remove unreacted amine, aldehyde and its derivatives (Scheme 24).

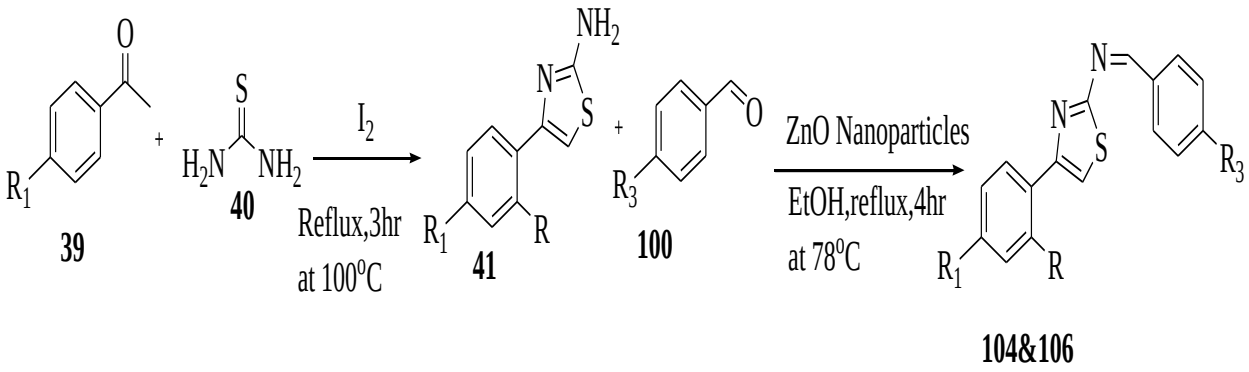

104 R_1 = H, R_3 = NO_2

106 R_1=NO_2, R_3 = NO_2

Scheme 24: Green synthesis of Schiff base from thiazole derivatives via ZnO nanoparticles.

3.4 Synthesis method 2

3.4.1 General procedure for synthesis of Schiff base via conventional method

A solution of 7.5 mL of benzaldehyde (73.75mmole) in 30 mL of ethanol, and 9.5 mL of 3-chloro aniline (73.75mmole) in 30mL ethanol were added in 150 ml of round bottom flask. Two to three drops of glacial acetic acid was added to adjust the pH of the solution(Ommenya *et al*., 2020). The reaction mixture was refluxed for 6 hr. Progress of the reaction was monitored by TLC. After 6 hr reflux, the mixture was cooled to room temperature and poured into 150 mL

crushed ice water, while stirring with glass rod. The brown solid product was collected after suction filtration which was washed continuously with cold water. The final product was obtained by recrystallization in ethanol to afford 14 g (91.1%) yield (Scheme 25).

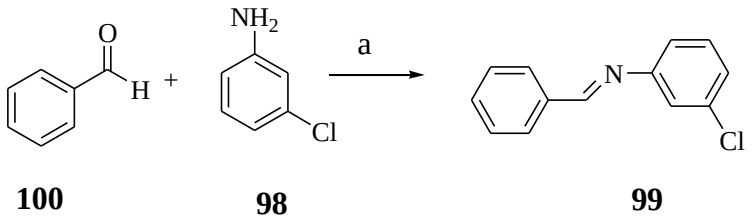

100 **98** **99**

Reagent and conditions a) absolute EtOH, AcOH, reflux 6 hr

Scheme 25: Synthesis of imine intermediate via condensation reaction.

3.4.2 Synthesis of tetrazole from Schiff base via cycloaddition reaction.

To a stirring solution of Schiff bases **99** (2.16 g, 0.01mol) in 150 mL round bottom flask, sodium azide (0.65 g,0.01mol) in 10 mL of dry N,N-dimethylformamide was added(Hoti *et al.*, 2017). The mixture was refluxed for 5 hr while stirring with magnetic hotplate at temperature of 89-92^{o}C, cooled to room temperature and poured to 100mL of crushed ice water while stirring with glass rod. The brown solid product was collected by suction filtration and washed with cold water. The final product was obtained by recrystallization in petroleum ether to afford 1.27 g (81.4%) yield (Scheme 26).

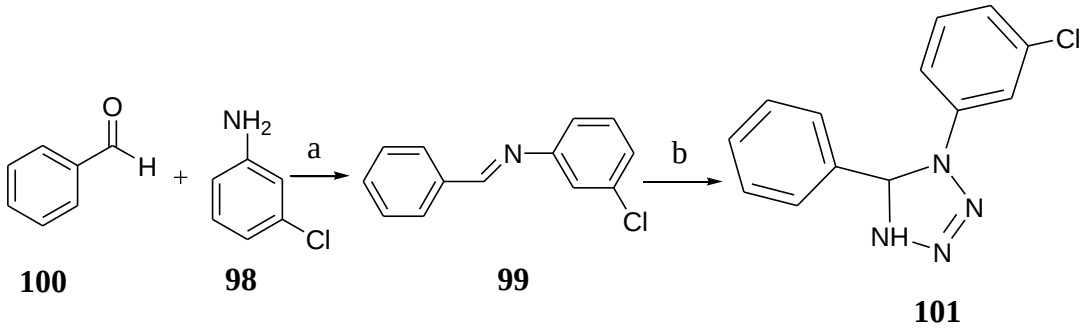

100 **98** **99** **101**

Reagent and conditions a) Absolute EtOH, AcOH, reflux 6 hr, b) NaN_3, dry DMF, reflux 5 hr

Scheme 26: Synthesis of tetrazole derivatives from Schiff base via sodium azide.

3.5. Antibacterial activity

The antibacterial activities of the synthesized compounds were done in collaboration with the Department of Applied Biology (microbiology stream), Adama Science and Technology University.

3.5.1. Preparation of discs containing synthesized compounds

Different concentrations were prepared from each synthetic compound by dissolving 5mg of each synthetic compound in 5mL of DMSO to make 1mg/mL of standard solution. The standard solution was serially diluted to furnish100μg/mL and 200μg/mL sample for each synthesized compound for the analysis. The concentrations of each were incorporated into sterile blank paper discs and were dried at 37°C (Piotto *et al.,* 2017). The paper discs were weighed carefully for confirming exact amount of the synthesized compounds being incorporated.

3.5.2 Bacterial culture

Four strains of bacterial species, two Gram-positive bacteria (*Staphylococcus aureus* (ATCC25923), *Streptococcus pyogenes* (ATCC19615)) and two Gram-negative bacteria (*Escherichia coli* (ATCC25922), *Pseudomonas aeruginosa* (ATCC27853)) which were provided by Adama Public Health Research & Referral Laboratory Center, Ethiopia were used to evaluate antibacterial activity of the synthesized compounds.

3.5.3. Determination of antibacterial activity by agar disk diffusion method.

In vitro antibacterial activity of the prepared synthetic compounds were done against two selected Gram-negative of strain *P. aeuroginosa* (ATCC27853) and *E. coli* (ATCC25922) and two strain the Gram-positive *S. aureus* (ATCC25923)and *S. pyogenes* (ATCC19615) bacterial strains was examined by disk diffusion assay (Ommenya *et al.,* 2020). The medium was prepared by dissolving 38 g of Mueller Hinton agar (MHA) medium in 1000 mL of distilled water and the autoclaved at 121°C for 15 min. The autoclaved medium was poured into sterile plates (20-25 mL/plate) and the plates were allowed to solidify under sterile condition at room temperature. The bacterial cultures were inoculated into the nutrient broth (inoculation medium) and

incubated overnight at 37°C. Inoculated medium containing 24 hr grown culture were added aseptically to the nutrient medium and mixed thoroughly to get a uniform distribution. The solution was poured approximately 20 mL of sterile MHA in sterile culture plates and allowed to attain room temperature. Sterile agar-disc diffusion previously soaked in a known concentration (100 µg/mL and 200 µg/mL per disc) synthetic compound and standard drugs was prepared in DMSO using nutrient agar tubes and carefully placed at the center of the labeled seeded plate. Mueller–Hinton sterile agar plates were seeded with indicator bacterial strains (1.3 *10^8cfu/mL) and allowed to stay at 37°C for 3 hr. Sterile filter paper disks with a diameter of 6 mm were placed over these plates. Finally, the plates were incubated at 37°C for 24 hr. The inhibition zones were measured with a ruler and compared with the positive control disk (disk containing Amoxicillin) of the same concentration in millimeter. DMSO used as negative control during the whole test on bacteria. The result was expressed as mean value ± standard deviation.

3.6 Evaluation of antioxidant activity

In vitro antioxidant activity of the synthesized compounds were assessed according reported procedure (Basyirah *et al.,* 2018) by the DPPH radical scavenging method. The nitrogen centered stable free radical (DPPH) has often been used to characterize antioxidants. It is reversibly reduced and therefore the odd electron within the DPPH radical gives a robust absorption maximum at 517 nm using spectrophotometer, which is purple in color. The radical scavenging activity of the synthesized target compounds was evaluated with (DPPH). In the process, 0.04 mg/mL(0.004% (w/v)) solution of DPPH in methanol was prepared; 1 mL of this solution was poured into 4 mL of the synthesized samples in methanol to furnish four different concentrations (1.25, 2.5, 5, 10µg/mL); and control was made by adding 1 mL of the DPPH solution to 5mL of methanol or 5mL DMSO, while 5 mL methanol or 5mL DMSO was used as a blank. After a 30 min incubation period at room temperature, the absorbance was measured against blank at λ 517 nm (Mukhia *et al.,* 2018). Ascorbic acid was used as the standard. The activity was expressed as IC_{50}, which is the concentration of the test compound required to give a 50% decrease of the absorbance from that of the control solution. The inhibition curves was plotted to obtain IC_{50}

values synthetic compound. The percent of inhibition (I %) of free radical production from DPPH was calculated by the following equation:

$$\% \text{ of } I = [(A_{control} - A_{sample}) / A_{control}] \times 100$$

Where $A_{control}$ is the absorbance of the control reaction, A_{sample} is the absorbance of the test compounds.

3.7 *In silico* molecular docking

Synthesized tetrazole and Schiff base of thiazole derivatives were subjected to molecular docking studies using the ADT version 1.5.2 and Auto Dock version 4.2 docking program to investigate the potential binding mode. The crystal structure of the enzyme (PDB ID: 3S7S) with resolution 2.3 Å was chosen as the protein model. The structures of ligands were optimized using the Chem Office software. Auto Dock version 4.2 was used to prepare the molecules and parameters before submitting it for docking analysis with Auto Dock. Polar hydrogen atoms were added while non-polar hydrogen atoms were merged and then, Gasteiger partial atomic charges were assigned to the ligands. All rotatable bonds of ligands, defined by default of the program, was allowed to rotate during the automated docking process and then prepared protein and ligand structures was saved in the PDBQT format suitable for calculating energy grid maps. A grid box size of 46×46×46 Å points with a grid spacing of 0.375 Å was considered. Lamarckian genetic algorithm (LGA) program with an adaptive whole method search in the Auto Dock was chosen to calculate the different ligand conformers. After 200 independent docking runs for each ligand, a cluster analysis was done. In according to the root mean square deviation (RMSD) tolerance of 2.0 Å conformations were clustered and ranked by energy of which the conformation with the best scored pose with the lowest binding energy were selected for these ligands (Garofalo *et al.,* 2011).

3.7.1 *In silico* ADMET and drug likeness studies

The physicochemical properties (molar refractivity, topological polar surface area, number of hydrogen bond donors/acceptors), lipophilicity ($logP_{O/w}$), pharmacokinetics properties (GI absorption, BBB permeate, P-gp substrate, cytochrome-P enzymes inhibition, skin permeation

(log Kp)) and drug likeness (Lipinski's rule of five) were predicted via SwissADME (http://www.swissadme.ch. (Daina *et al*.**,** 2017). The percent absorption (%Abs) of the ligands were calculated using the formula %Abs = 109 - 0.345 TPSA(Remko, 2009).

The high cost and longtime request of a drug discovery process for ADMET and drug likeness studies in early stage of drug discovery process would be shorten by employing computer aided design and ADMET predictive models (Lin *et al.*, 2020);(Wang *et al.*, 2015). The organ toxicity (hepatotoxicity), toxicological endpoints (carcinogenicity, immunotoxicity and mutagenicity), and the level of acute toxicity (LD_{50} (mg/Kg)) of the synthesized tetrazole and thiazole based Schiff base derivatives (Cpd **101**- Cpd**106**) in (Table 9) were determined by using Pro Tox II web server (http://tox.charite.de/protox_II) (Banerjee *et al.*, 2018)(Drwal *et al.*, 2014).

3.7.2 Computational methods

Geometry optimizations and frequency calculations of the synthesized compounds (**101**-**106**) were performed using the Gaussian 09 package and the results were visualized using Gauss view 06 software. Density functional theory (DFT) calculations in which the DFT/B3LYP hybrid functional was used together with 6–311^{++}G(d,p) basis set. The optimized geometries were confirmed to be real minimum without any imaginary vibrational frequency by performing vibrational frequency calculations at the same level of theory. The frontier molecular orbitals (FMOs), energy gap ($\Delta E = E_{LUMO} - E_{HOMO}$), electronegativity ($\chi = -½ (E_{HOMO} + E_{LUMO})$), electronic chemical potential ($\mu = ½ (E_{HOMO} + E_{LUMO}) = -\chi$), global chemical hardness ($\eta = ½ (_{E}LUMO - E_{HOMO})$), global softness ($\sigma = 1/2\eta$), global electrophilicity index ($\omega = \mu^2/2\eta$), and nucleophilicity index ($Nu = 1/\omega$), dipole moment and molecular electrostatic potential (MEP) were also calculated and analyzed at the same level of theory (Ismael *et al.*, 2020).

4. RESULTS AND DISCUSSIONS

4.1. Synthesis of the target compounds

Schiff base (**99**) was prepared by condensation of benzaldehyde and meta-chloroaniline in absolute ethanol under reflux for 6 hr (Obadahun *et al.,* 2020) catalyzed by glacial acetic acid to afford 84.1 % yield (Scheme 27).

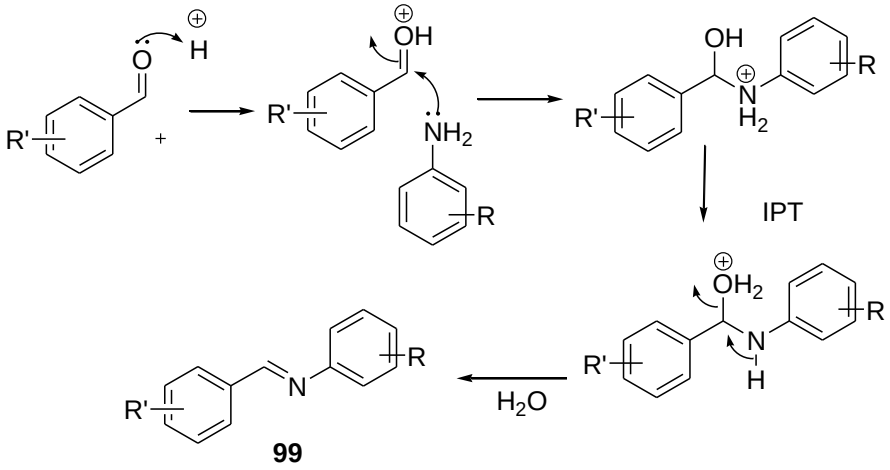

Scheme 27: Mechanism for the synthesis of a schiff base intermediate (**99**).

Reaction of compound **99** with sodium azide in [3+2] 1,3-dipolar cycloadditions reaction manner in dry DMF at 90°C under reflux for 5 hr afforded tetrazole **101** with 81.4 % yield (Scheme 28)(Hoti *et al.,* 2017).

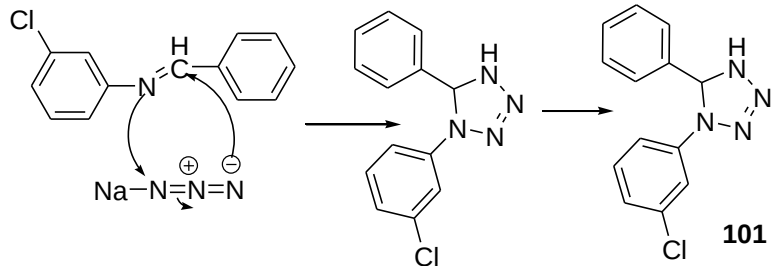

Scheme 28: Mechanism of synthesis of **101** via 1,3 -dipolar cyclo additions reaction.

Conventional and green syntheses of thiazole based Schiff base derivatives were done as per the experimental protocol outlined in (Schemes 27 and 28). Physical properties and percent yield of the synthesized compounds are presented in Table 1. Progress of the reactions was monitored using TLC by visualizing with UV lamp at 254 nm and 346 nm. The R_f values for synthesized compounds were also calculated (Table 1).

Table 1: Physical characterization and percentage yield of the synthesized compounds.

Compound	Percentage yield (%)	Color	R_f (*n*-hexane/ EtOAC)	Melting point (°C)
101	81.4	Gray brown crystal	0.67 (hex:Et 3:1)	72-74
102	68.83	Red crystal	0.8(hex:Et 1:1)	152-154
103	77.33	White crystal	0.77(hex:Et1:2)	170-172
104	79.3	Green powered	0.67(hex:Et1:4)	148-150
105	69.3	Pale orange powered	0.86(hex:Et 7:3)	190-192
106	83.3	Yellow crystal	0.4(hex:Et2:1)	188-190

Note: Rf is retention factor

4.2 Characterization of the synthesized compounds

4.2.1 Characterization of 1-(3-chlorophenyl)-4,5-dihydro-5-phenyl-1*H*-tetrazole (101)

Compound **101** was obtained as gray brown crystal melting point 72-74°C with yield of 81.4%. Its ^{1}H NMR spectrum (DMSO-d_6, 400 MHz, Appendix 1) showed a singlet peak at δ 6.72 (s,1H,H-1) attributed to N-H (on tetrazole ring) and 3.48 were for deuterated water. A peak at δ 8.61 (s, 1H, H-1) belong to methine proton of tetrazole ring. The presence of a disubstituted phenyl ring having ABX spin pattern was evident from peaks at δ 7.42 (m, 1H, H-14), 7.40 (d, 1H, *J*= 8Hz, H-15), 7.03 (d, 1H, H-13) and 7.53 (s, 1H, H-17). The presence of monosubstituted phenyl ring having was clearly evident from peaks at δ 7.95(m, 1H, H-9), 7.28 (dd, 1H, H-8, 10, *J*=8Hz), 7.26 (dd, 1H, H-7, 11, *J*=8Hz) (Appendix 1).

Its ^{13}C NMR spectrum (100 MHz, DMSO-d_6) revealed a total of eleven peaks at δ 161.1 (C-1), 151.9(C-12),136.5(C-16),131.9(C-6),129.7(C14),129.3(C-9),129.1(C-8,10,),128.6(C-7,11)127.8 (C-15),126.4 (C-17), 121.5 (C-13) (Appendix 2). Its DEPT-135 spectrum (Appendix 3) showed eight peaks pointing up in agreement with the proposed structure. Thus, based on the above spectral data the following structure is proposed, in agreement with the target compounds as per the theoretical framework of the reaction.

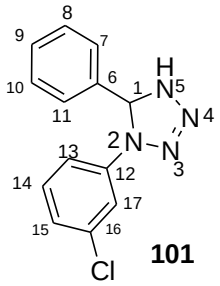

101

4.2.2 Characterization of compound 102

Compound **102** was obtained as red crystal a melting point 152-154^{o}C and the percent yield was 68.83%. Its ^{1}H NMR spectrum (DMSO-d_6 and $CDCl_3$, 400 MHz, Appendix 4) showed a broad peak at δ 3.40 attributed to deuterated water, 2.5 was solvent peak of DMSO, 4.02 were peak of hydroxyl proton of ethanol and 5.7-5.7 was peak of methylene proton in solvent diethyl ether. A singlet peaks at δ 9.79 (s, 1H, H-13) δ 7.86 (s, 1H, H-8) belong to Schiff base imine protons and protons of thiazole ring (Litr 9.22, s, 1H, H-13 & 6.93, s, 1H, H-8 (Prakash *et al.*, 2014), respectively. The presence of AA'XX' spin system para substituted phenyl ring was clearly evident from peaks at δ 7.76 (d, 1H,H-18,J=8Hz), 7.78(d,1H-16,J=8Hz), 8.15(dd,1H,H-15, J=8Hz,12Hz), 8.19(dd,1H,H-19,J=16,8Hz) and singlet aromatic hydroxyl proton at 9.49 (s, 1H, H-21). A disubstituted phenyl ring was evident from peaks at δ 7.48 (d, 1H, H-6, J=8Hz), 6.94(dd, H-2, J=8Hz, 24Hz) 6.86(m, 1H, H-1), 7.46(d, 1H, H-3, J=8Hz) and singlet aromatic hydroxyl proton at δ 9.62 (s, 1H, H-20). Its ^{13}C NMR (100 MHz, DMSO-d_6 and $CDCl_3$) spectrum showed fourteen peaks at δ 169.4 (C-13), 162.4 (C-17), 158.4(C-4) 156.4(C-10) ,152.8 (C-14), 141.8 (C-5), 135.9(C-15, 19), 132.2 (C-4,6), 131.3 (C-7), 129.2(C-2), 122.8 (C-1), 121.8 (C-3), 120.5 (C-16,18) and 115.8 (C-8) (Appendix 5). The differences in C-17 & C-4 were due to imine functional groups through anisotropic effects. Its DEPT-135 spectrum (Appendix 6) showed ten peaks pointing up in agreement with the proposed structure. Thus, based on the

above spectral data the following structure (**102**) is proposed, in agreement with the target compound as per the theoretical framework of the reaction.

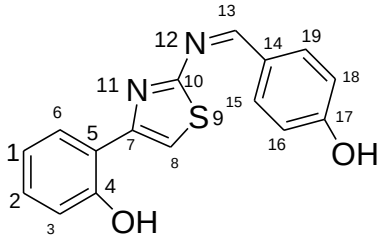

102

4.2.3 Characterization of (Z)-N-benzylidene-4-phenylthiazol-2-amine (103)

Compound **103** was obtained as white crystal, melting point 170-172^{o}C and yield of 77.3%. Its ^{1}H NMR spectrum (DMSO-d_6, 400 MHz, Appendix 7) showed spectra at two singlet peaks attributed to imine proton and thiazole ring proton at 7.64 (s,H-13) and 7.30 (s,1H, H-8), respectively. The presence of two mono substituted phenyl rings are evident at δ ,7.39 (dd,1H, H-4,6, *J*=8Hz,16Hz),7.37 (dd,1H,H-1,3, *J*=8Hz,28Hz), 7.35 (m, 1H, H-2) and 7.28 (dd, H-15, *J*=8Hz,24Hz), 7.24 (dd, H-19, *J*=8Hz,16Hz),7.22(dd, H-16, *J*=8Hz,24Hz), 7.20 (dd,1H, H-18, *J*=8Hz,16Hz) and 7.18 (m, H-17) were due to anisotropic effect. Its ^{13}C NMR (100 MHz, DMSO-d_6) shows twelve peaks at δ 167.3 (C-13), 149.7(C-10), 144.4 (C-7),136.6 (C-5),133.6 (C-14),129.3 (C-17), 128.7 (C-15, 19), 128.5 (C-16, 18), 128.4 (C-1, 3), 127.8 (C-2), 125.8 (C-4,6), and 122.8 (C-8) were less deshielding relative to C-7 (Appendix 8). Thus, based on the above spectral data the following structure (**103**) is proposed, which match with the target compound as per the theoretical framework of the reaction.

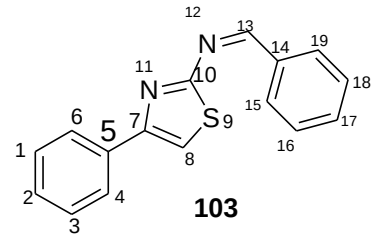

103

4.2.4 Characterization of compound 104

Compound **104** was obtained as green powder with melting point of 148-150^{o}C and yield of 79.3%. Its ^{1}H NMR spectrum (DMSO-d_6 and $CDCl_3$ 400 MHz, (Appendix 10) showed a singlet

peak at δ 7.39(H-13) and 7.18(H-8) attribute to imine proton and thiazole ring proton respectively. The presence of AA'XX' spin system phenyl ring is clearly evident from peaks at δ 8.24 (d, 1H, H-16, 18, *J*=8Hz) and 8.22 (d, 1H, H-15, 19, *J*=8Hz). The presence of monsubstituted phenyl ring is evident having from peaks at δ 7.57 (m, 1H, H-2), 7.47 (d, 1H, H-4, 6, *J*=8Hz) and 7.45 (dd, 1H, H-1, 3, *J*=8Hz). Its ^{13}C NMR (100 MHz, DMSO-d_6 & $CDCl_3$ (Appendix 11) showed twelve peaks at δ 168.1 (C-13), 149.5 (C-10), 147.3 (C-17), 135. (C-7), 128.9 (C-14),128.7(C-5),128.4(C-15,19),127.9(C-1,3),128.7(C-2),128.3(C-4,6),124.2(C16,18) and 120 (C-8). In agreement with the ^{1}H and ^{13}C NMR spectra, its DEPT-135 spectrum (Appendix 12) showed seven peaks pointing up in agreement with the proposed structure. Thus, based on the above spectral data the following structure (**104**) is proposed, which match with the target compound as per the theoretical framework of the reaction.

.

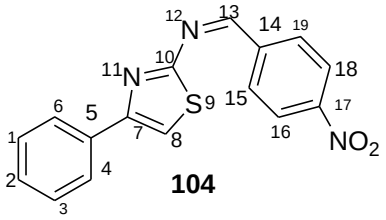

104

4.2.5 Characterization of compound 105

Compound **105** was obtained as pale orange powered with melting point 190-192^{o}C and the percent yield was 69.3%. It's ^{1}H NMR spectrum (DMSO-d_6 and $CDCl_3$ 400 MHz, (Appendix 13) showed singlet peaks at δ 8.86(H-13) and 8.3(H-8) attributed to imine protons and proton of thiazole ring. The presence of two AA'XX' spin system para-substituted phenyl rings were observed at δ 8.17 (dd, H-1,3,*J*=8Hz,12Hz), 8.12(dd,1H, H-4,6, *J*=8Hz,12Hz) and 7.96 (d,1H,H-15,*J*=8Hz), 7.9 (d, 1H, H-19, *J*=8Hz), 7.69 (d, 1H, H-16, *J*=8Hz), 7.67 (d, 1H, H-18, *J*=8Hz) and the presence of aromatic hydroxyl group at δ 9.80 (s, 1H, H-20). Its ^{13}C NMR (100 MHz, DMSO-d_6 & $CDCl_3$ (Appendix 14) showed twelve carbons at δ 169.1(C-13), 167.2(C-17), 148.3(C-10), 146.51(C-2,C-NO_2), 144.9 (C-7), 143 (C-5), 141.7 (C-14), 129.52 (C-15, 19), 128.03 (C-4,6), 126(C-1,3) ,124.31(C-16,18) and 107.04 (C-8). In agreement with the ^{1}H and ^{13}C NMR spectra, its DEPT-135 spectrum (Appendix 15) showed six peaks pointing up in agreement with the proposed structure. Thus, based on the above spectral data the following structure (**105**)

is proposed, which match with the target compound as per the theoretical framework of the reaction.

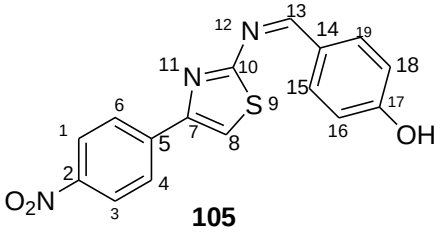

105

4.2.6 Characterization of compound 106

Compound **106** was obtained as yellow crystal with melting point 188-190°C with yield of 83.3%. Its ^{1}H NMR spectrums (DMSO-d_6, 400 MHz Appendix 16) showed a singlet peaks at δ in ppm 8.88(H-13) and 8.21(H-8) that belong to imine protons and thiazole proton respectively. 5.6 is methylene proton, 1.98 were methyl proton,3.38 hydroxyl proton of recrystallized solvent, 3.53 of proton deuterated water and 2.5 were DMSO. The presence of two AA'XX' spin system phenyl ring was observed at δ 8.04 (m,1H,H-1,3) ,7.85 (m, 1H, H-16,18) , 7.66(dd, 1H, H-4,6,J=8Hz and 7.64 (dd,1H, H-15,19,J=8Hz,24Hz). Its ^{13}C NMR (100 MHz, DMSO-d_6) twelve δ 169.1 (C-13), 150.8 (C-10),148.3 (C-17, C-NO_2), 147.2 (C-2, C-NO_2), 146.3 (C-7), 143.8(C-14),141.3(C-5),128.2 (C-15,19), 126.7 (C-4,6), 124.4 (C-16, 18), 123.8 (C-1, 3) and107.0 (C-8), (Appendix 17). In agreement with the ^{1}H and ^{13}C NMR spectra, its DEPT-135 spectrum (Appendix 18) showed seven peaks pointing up in agreement with the proposed structure. Thus, based on the above spectral data the following structure (**106**) is proposed, which match with the target compound as per the theoretical framework of the reaction.

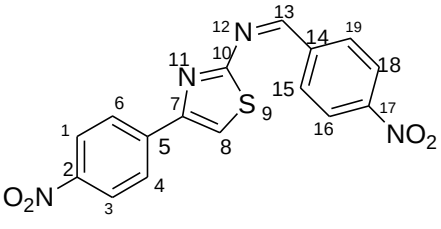

106

4.3. Biological activity of synthetic compounds

4.3.1. Antibacterial activity

Thiazole contain compounds has exhibit potent antimicrobial activity against multidrug-resistant strains of *S. aureus,* including methicillin resistant *S. aureus*(MRSA) (Mohammad *et al.,* 2015). Synthesized compounds were examined for their antibacterial activities against selected bacterial strains. The mean inhibition zones ranged from the lowest (7 mm at 100μg/mL) to the highest (15 mm at 200 μg/mL). Compounds **106**,**101 and 105** showed good activities against *E. coli* with mean inhibition zone of 14.4 ± 0.04, $12.5 \pm .04$ and 10.5 ± 0.02 mm diameter compared to standard 18 ± 0.01 at 200μg/mL, respectively. Likewise, compounds **105, 106**, **102** and **101** (Table 2) showed promising antibacterial activity against *S. aureus* of which the maximum inhibition zone was observed at 15.4 ± 0.01 displayed by compound **106** against the Amoxicillin standard 17 ± 0.04 at 200 μg/mL. All of the synthetic compounds **101-106** displayed moderate to higher activity against *P. aeruginosa* of which maximum inhibition zone observed was at 13 ± 0.02 mm displayed by compound **106** compared to Amoxicillin (18.5 ± 0.45 mm for at the same concentration 200 μg/mL). Activity displayed by six synthetic compounds in descending order looks **106**>**101**>**105**>**104**>**102**>**103** compared to Amoxicillin (Table 2, Figure 10 and 11). Compounds with nitro group are considered to be a versatile and unique functional group in medicinal chemistry. Compounds with nitro group are considered to be a versatile and unique functional group in medicinal chemistry. Compound **106** possesses a strong electron attracting ability that creates localized electron deficient sites within molecules and interacts with biological nucleophiles present in living systems, such as proteins, amino acids, nucleic acids, and enzymes (Nepali *et al.,* 2019). As result Gram positive bacteria strains exhibit resistance to the effect of *β*-lactam antibiotics, such as Amoxicillin rather than Gram negative bacteria due to the outer membrane of Gram-negative bacteria is the main reason for resistance to a wide range of antibiotics including *β*-lactams and other antibiotics. *β*-lactams having antibiotics must pass the outer membrane to access their targets, for instance , hydrophobic drugs can undergo by a diffusion pathway, on the opposite hand, hydrophilic antibiotics like *β*-lactams pass through porins can't cross the outer membrane due to its structure that hinder it from using any of these passages. Any alteration within the outer membrane by Gram-negative bacteria like changing the hydrophobic properties or mutations in porins and other factors can create resistance. Gram-

positive bacteria lack this important layer, which makes Gram-negative bacteria more resistant to antibiotics than Gram-positive ones (Breijyeh *et al.,* 2020).

Table 2: The inhibition zone of the synthesized compound in mm (mean ±SD)

Samples name	Conc. in $\mu g / mL$	Zone of inhibition (mm) Mean ± SD			
		E. coli	*S.aureus*	*P. aeruginosa*	*S. pyogenes*
Compound **101**	100	9.57 ± 0.3	9 ± 0.01	10.98 ± 0.35	7.8 ± 0.01
Compound **102**		7.31 ± 0.03	$8.6 \pm .02$	$8 \pm .025$	7.95 ± 0.25
Compound **103**		7.45 ± 0.02	7.2 ± 0.04	7.95 ± 0.3	7.25 ± 0.01
Compound **104**		8 ± 0.02	7	7 ± 0.01	7.9 ± 0.25
Compound **105**		9 ± 0.01	8 ± 0.04	10 ± 0.01	8.67 ± 0.3
Compound **106**		$12 \pm .01$	$11 \pm .004$	$12.43 \pm .02$	$13 \pm .01$
Amoxicillin		16 ± 00	15 ± 0.01	$16 \pm .45$	$16 \pm .55$
Compound **101**	200	12.5 ± 0.04	11 ± 0.02	12 ± 0.01	9.5 ± 0.03
Compound **102**		8.5 ± 0.01	$9.23 \pm .02$	9.8 ± 0.25	10.03 ± 0.04
Compound **103**		9.25 ± 0.04	9.8 ± 0.45	9 ± 0.01	$8.67 \pm .25$
Compound **104**		9.08 ± 0.01	$9.56 \pm .25$	9.43 ± 0.23	9.89 ± 0.05
Compound **105**		$10.5 \pm .02$	11.25 ± 0.15	12 ± 0.01	11.67 ± 0.3
Compound **106**		$14.4 \pm .04$	15 ± 0.01	13 ± 0.02	14.45 ± 0.25
Amoxicillin		18 ± 0.01	17 ± 0.04	18.5 ± 0.45	$18 \pm .02$

Notice SD: Standard deviation, Amoxicillin acts positive control and DMSO as negative control.

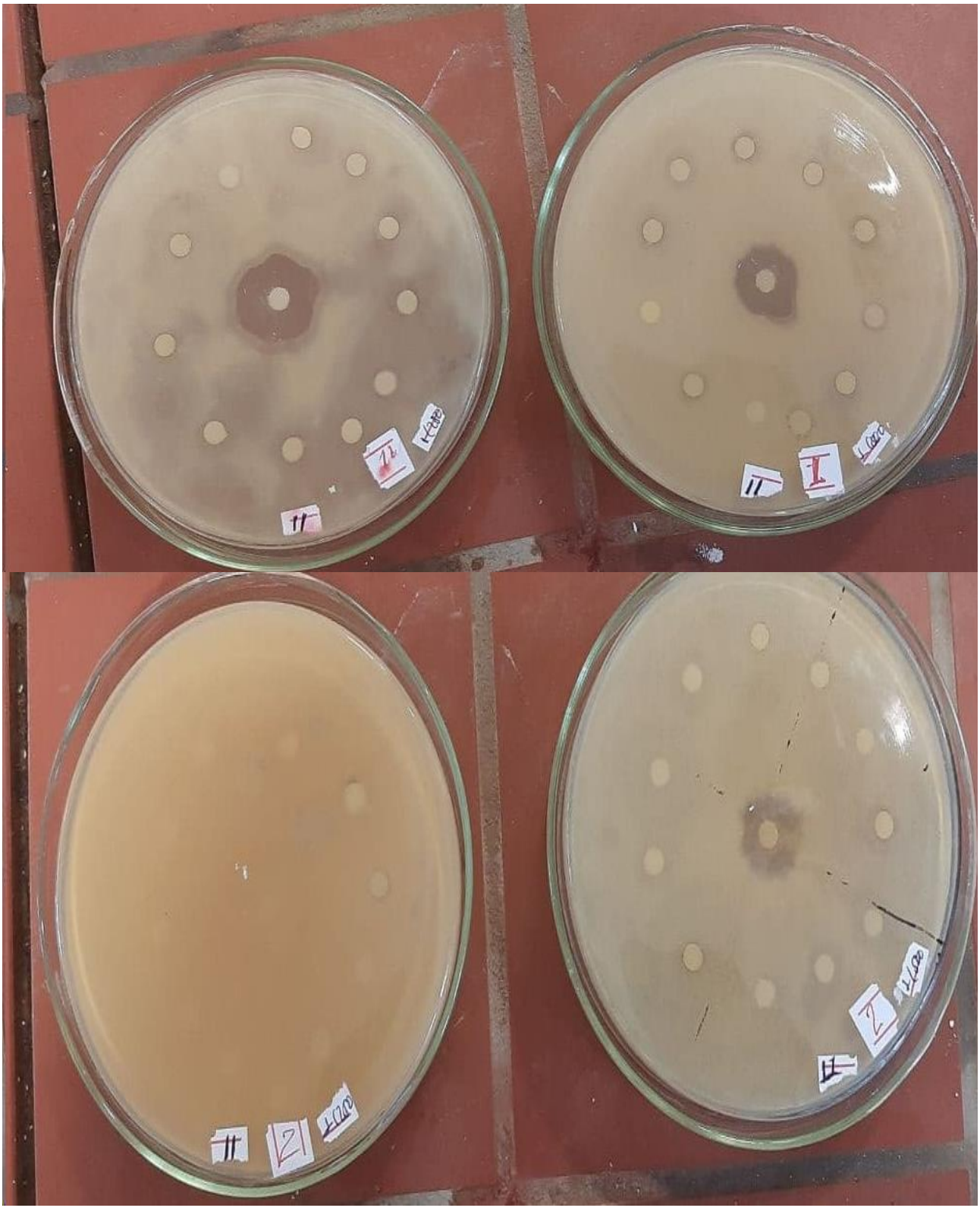

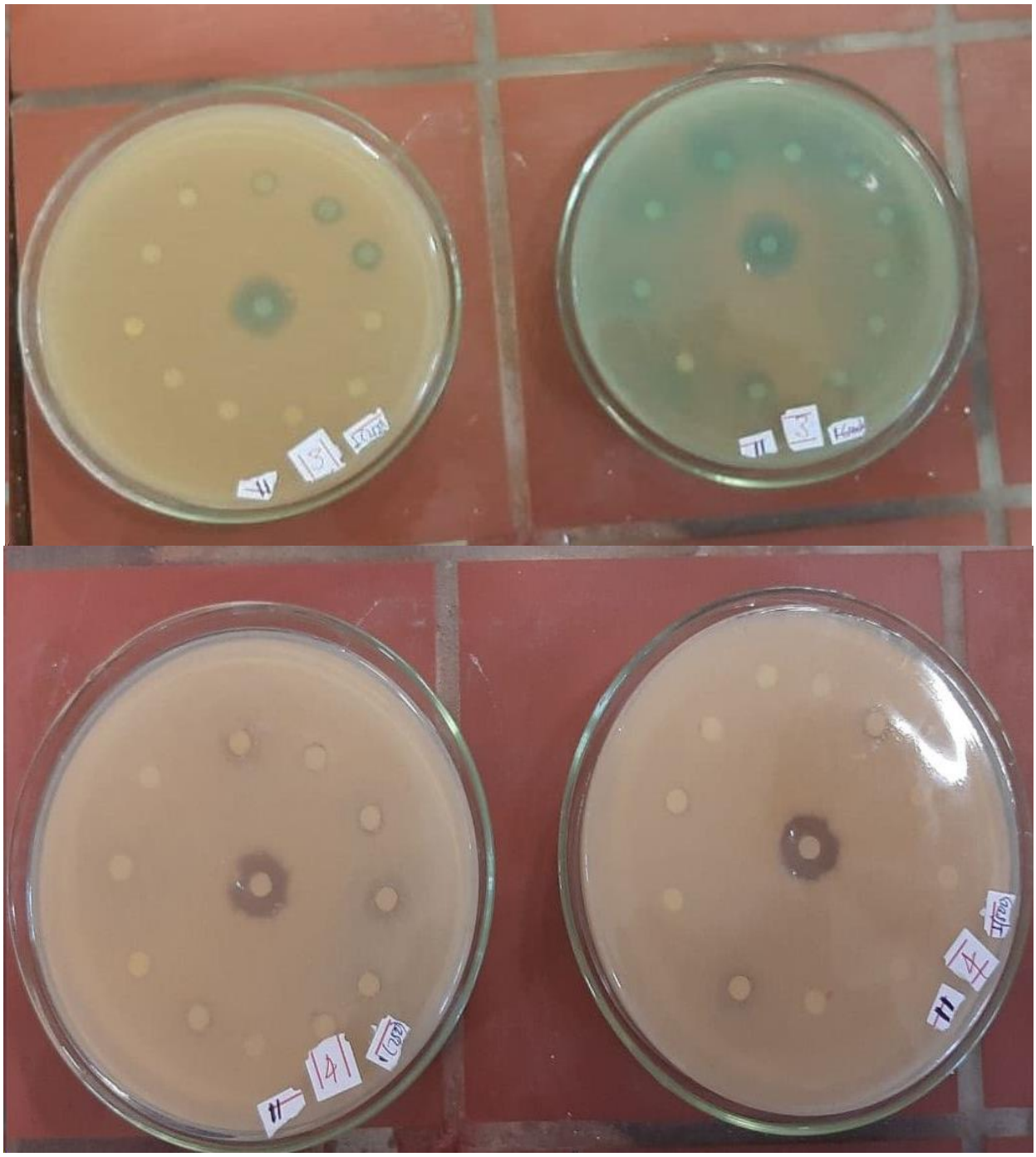

Figure 10: Antibacterial test results of synthesized compounds **101-106** against bacterial strains *E. coli*, *S.aureus*, *S. pyogenes*, *P. aeruginosa* at 100*µg/mL* and 200*µg/*mL respectively.

Note: (1) is stand for *E. coli* ATCC25922, (2) *S. aureus* ATCC25923, (3) *P. aeruginosa* ATCC27853 and (4) *S. pyogenes* ATCC19615

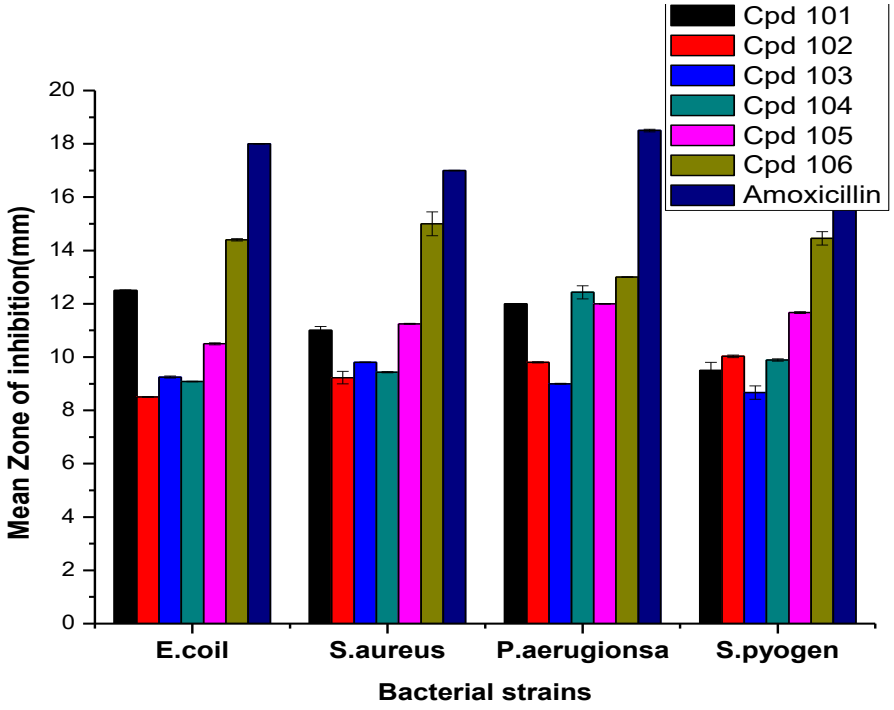

Figure 11: Inhibition zone of the synthesized compounds in mm (mean ± SD) at 200µg/mL

Note: the error indicates the standard deviation.

4.3.2. Antioxidant activity

The antioxidants have been shown to reduce the risk of cancer as well as neurological and cardiovascular pathologies among others (Mukhia *et al.*, 2018). In physiological conditions, the concentration of free radicals–including reactive oxygen, nitrogen, sulfur and carbon species (ROS, RNS and RSS) is regulated by antioxidant defense systems. Free radicals indiscriminately oxidize any substance within range, causing injury to endogenous also as exogenous substances, including all classes of biomolecules (proteins, lipids, DNA), disrupting normal cell signaling mechanisms, devastating cellular energy supplies, depleting reducing equivalents (reduced nicotinamide adenine dinucleotide and glutathione) and causing cell death by eventually inducing apoptosis (Phaniendra *et al.*, 2015). *In vitro* antioxidant activities of the synthetic compounds were determined by the DPPH radical scavenging method at four different concentrations (1.25, 2.5, 5 and 10µg/mL).

Compound **102,101** and **105** are promising shows antioxidant activity compared to the strand of abscorbic acid with IC_{50} of 3.98µg/mL. The synthesized compounds were investigated for their free radical scavenging activity via their reaction with the stable DPPH radicals. The reduction of the DPPH was followed via the decrease in absorbance at 517 nm. It was observed that the DPPH scavenging activity increased in a dose-dependent manner (Table 5, Figure 13). Compounds **102**,**105** and **101** (Table 5) exhibited better antioxidant activity (80.89, 77 &70% radical scavenging activity at concentration of10 µg/mL respectively with IC_{50} value of 3.6, 3.65 and 4.91 µg/mL respectively. The activity pattern of synthetic compounds follows **102** > **105** > **101 > 106** > **104** > **103** pattern compared to abscorbic acid. Overall, compound **102**, **105** and **101** showed promising antioxidant activity among the six synthetic compounds (Table 3, Figure 12 and 13).

Table 3:Percent radical scavenging activity of the synthesized compounds.

Concentration	**Abscorbic acid**	**101**	**102**	**103**	**104**	**105**	**106**
1.25	22.69	20.76	15.73	17.13	21.6	17.13	15.4
2.5	35	32.31	58.15	42.7	27.2	64.5	22
5	73.1	64.2	71.35	43.8	59.83	66	58.15
10	91.2	77	80.89	75.8	74.5	70	88.8
IC_{50}	3.98	4.91	3.6	5.56	5.36	3.65	5.14

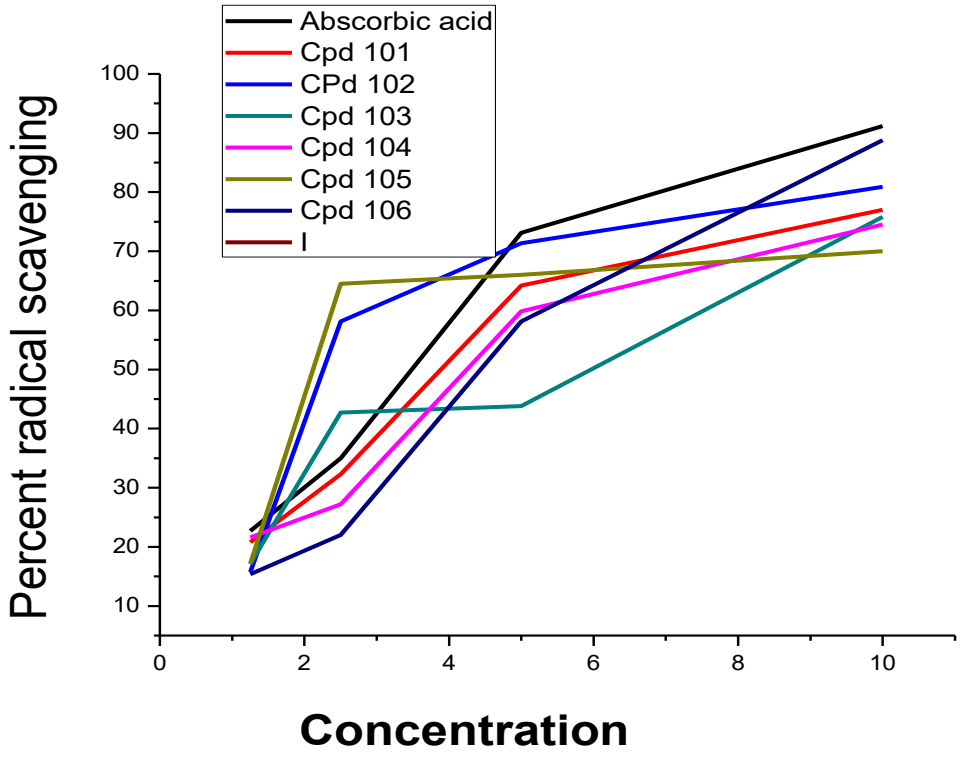

Figure 12: DPPH scavenging activity (%) of synthetized compounds with positive reference (L-Ascorbic acid.

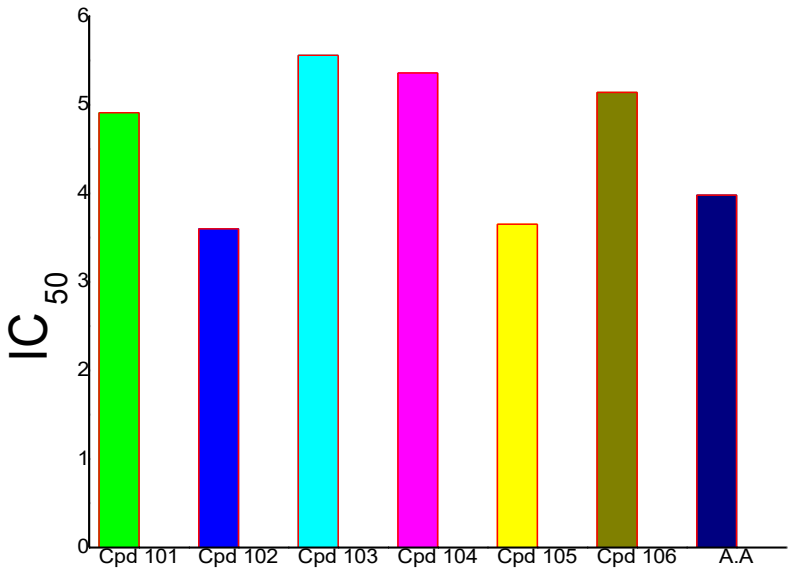

Note: IC_{50} is half maximal inhibitory concentration and A.A is Ascorbic acid

Figure 13: half maximal inhibitory concentration of synthetized compound (**101**-**106**) with IC_{50} via L-Ascorbic acid standard.

4.4 *In silico* molecular docking

In silico molecular modeling approaches, driven by rapidly improving computational platforms, have allowed many success stories for the use of computer-assisted drug design in the discovery of new mechanism- or structure-based drugs (Ruyck *et al.*, 2016). Molecular docking studies were performed for six synthetic compounds in order to predict the interaction of ligand molecules with the binding sites of *E.coli* DNA gyraseB (PDB ID: 6F86). Most antibacterial agents act by targeting key components of bacterial metabolism including cell-walls, DNA-directed RNA polymerase, protein synthesis, enzymes and DNA gyrase (Lade & Kim, 2021).In this regard, bacterial DNA gyrase is important for bacterial survival and thus necessary to be exploited as an antibacterial target (Collin *et al.*, 2011). By this manner DNA gyrase effects many various supercoiling-dependent process like DNA replication, regulation of organic phenomenon and chromosome condensation. Thus, this enzyme plays an essential role in

bacterial life, and hence makes it is very important target for drug discovery (Emmerich *et al.*, 2021). Therefore, in the present study, the molecular docking analysis of the synthesized compounds (**101**-**106**) was carried out to investigate their binding pattern with DNA gyrase B and compare them with standard inhibitor (Amoxicillin). The six synthesized compounds were found to have minimum binding energy values ranging from -7.5 to -6 kcal/mol (Table 4), with the best binding affinity was achieved for compounds **106**, **101** and **105** (-7.5, -7.2 and -6.9 kcal/mol, respectively, Table 4) of which compounds **106** and **101** showed better binding affinity compared to standard drug, Amoxicillin. The binding affinity, hydrogen bond, and residual interaction of six synthesized compound compounds and amoxicillin were summarized in (Table 4). All synthesized compound showed binding affinity within the binding sites of co-crystallized ligand (Figures 14-19). Among the synthesized compound **106** having lower score value formed via hydrogen bond interaction with Ser-121, Asn-46, Val-120, Arg- 76, Asp-73 and residual hydrophobic interaction with Glu-50, Ile-78 (Figures 19) are active against standard these due strong ability of electron attracting groups of nitro group (Nepali *et al.,* 2019). Similarly, compound **101** and **105** forms hydrogen bond via (Asp-73, Thr-165), (Ile-94, Asn-46, Arg-76, Glu-50) and residual hydrophobic interactions with amino acids Asn-46, Ala-47, Ile-78 and Glu-50, Ile-94 (Figure 14&18) respectively. *In silico* docking results revealed that compounds **106**,**101** and **105** showed low docking scores docked score (−7.5,7.2 and −6.9 kcal/mol, respectively) compared with other compounds and comparable residual interactions with that of Amoxicillin with(-6.1 kcal/mol) within the binding pocket (Table 4), suggesting that these compounds are promising antibacterial agents against *E. coli* (Abu-Melha, 2018). Except, compound **103** the entire five active against *E. coli* and they are promising antibacterial activity. Compared to amoxicillin, the synthesized compounds (**106** and**105**) showed similar residual interactions profile with amino acid residues Glu-50, Ile-78 and compound **101**,**102**,**103** having similar residual amino acid Ala-47 and Thr-165 and Hydrogen bond with Asp-73, Arg-76, and Asn-46.

Table 4: Molecular docking value of synthetic compounds against *E. coli* DNA gyraseB

Ligands	**Affinity (kcal/mol)**	**H-bond**	**Residual Amino acid Interactions**	
			Hydrophobic/Pi-Cation/Pi-Anion/ Pi-Alkyl interactions	**Van-der Walls interactions**
101	-7.2	Asp-73, Thr-165, Asn-46	Ala-47, Ile-78,Asn-46	Asp-49, Val-43, Val-167, Ile-94, Gly-77
102	-6.2	Glu-50, Asn-46, Ile-78	Asn-46, Glu-50, Asp-73, Ile-78, Ala-47, Thr-165, Val-167	Val-43,
103	-6.0	Asp-73, Glu-50	Asp-73, Glu-50, Ile-94, Ile-78, Ala-47, Thr-165	Val-43, Val-167
104	-6.6	Asn-46,	Asp-73, Thr-165, Ala-47, Ile-78	Val-43, Val-167, Ile-94
105	-6.9	Arg-76, Asn-46 Ile-94	Arg-76, Ile-78 Glu-50,	Gly-77, Gly-75, Thr-165, Val-97, Val-120, Ser-121
106	-7.5	Asp-73, Val-120, Asn-46, Ser-121	Glu-50, Ile-78	Asp-49, Gly-77, Gly-75, Thr-165, Val-97, Leu-98, Gly-119
Amoxicillin	-6.1	Asp-73, Arg-76, ,	Glu-50, Ile-78,Thr-165	Gly-77, Gly-75

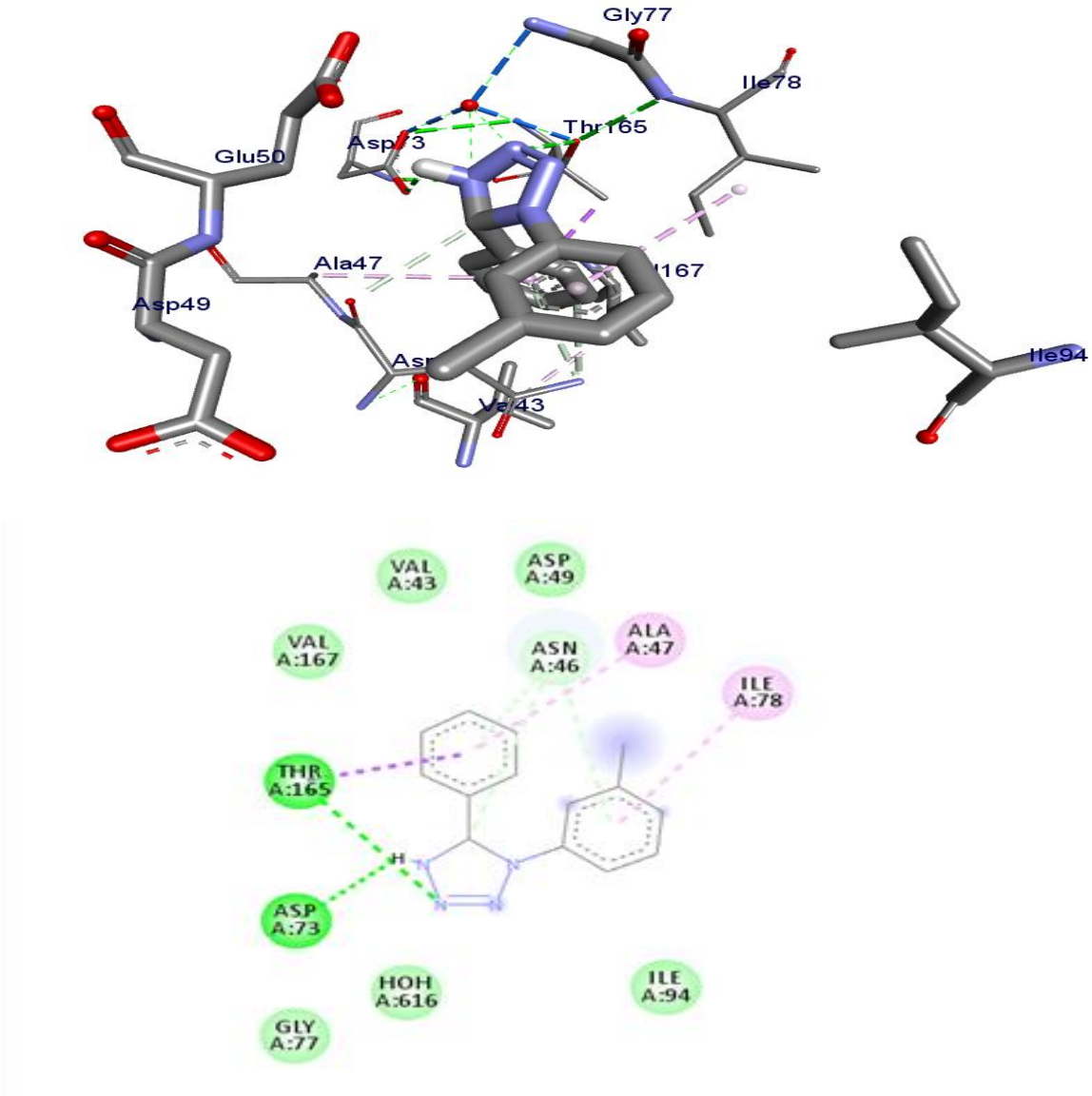

Figure 14: 3D & 2D binding interaction of compounds **101** against *E. coli* DNA gyraseB.

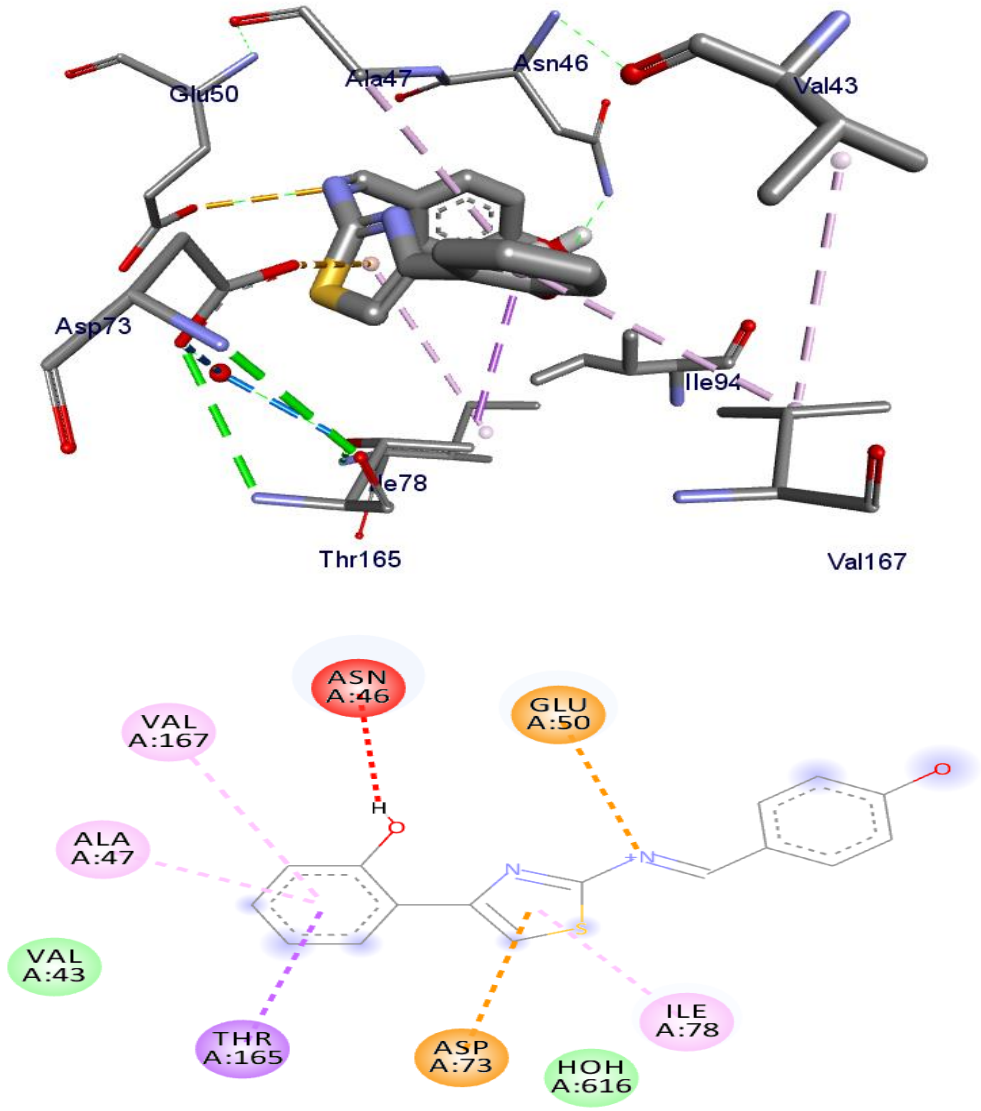

Figure 15:3D & 2D binding interaction of compound**102** against *E.coli* DNA gyraseB.

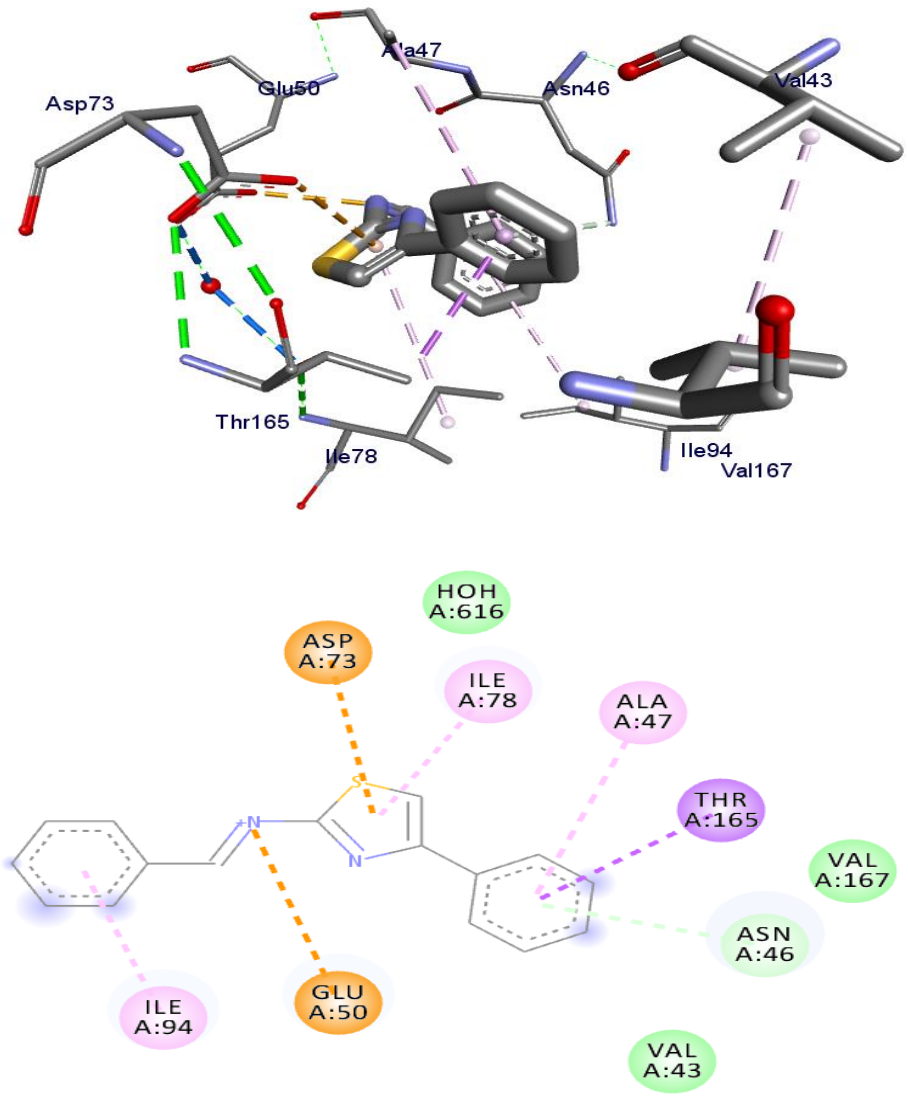

Figure 16: 3D&2D binding interaction of compound **103** against *E.coli* DNA gyraseB

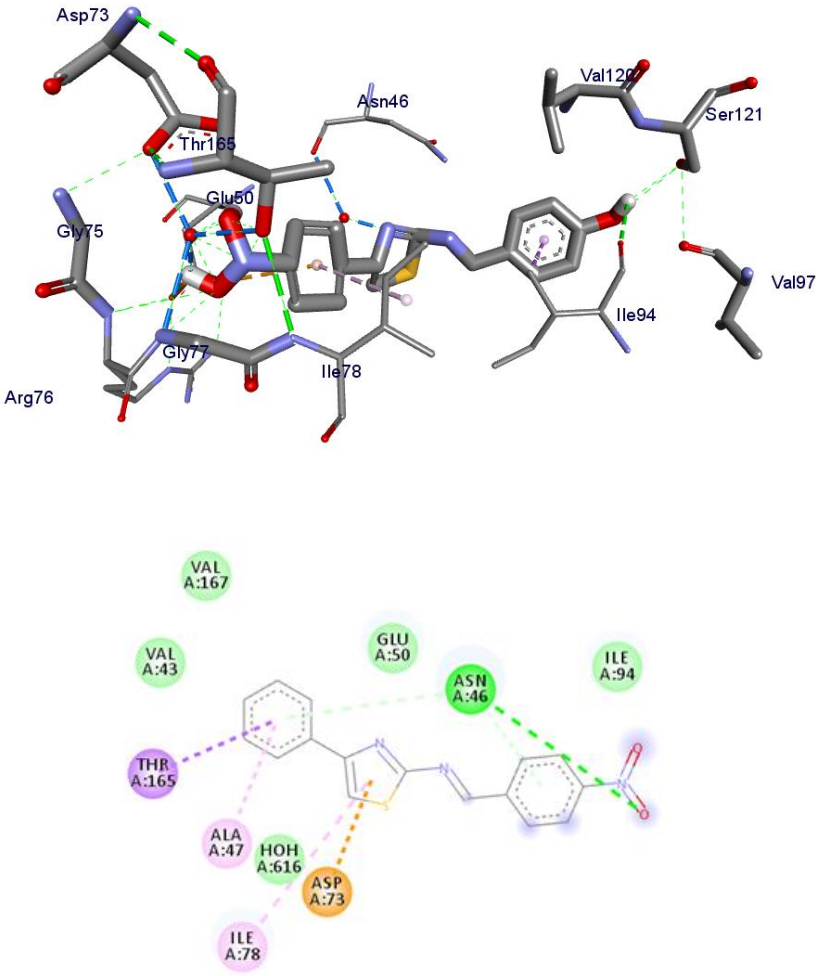

Figure 17: 3D& 2D binding interaction of compound **105** against *E.coli* DNA gyraseB.

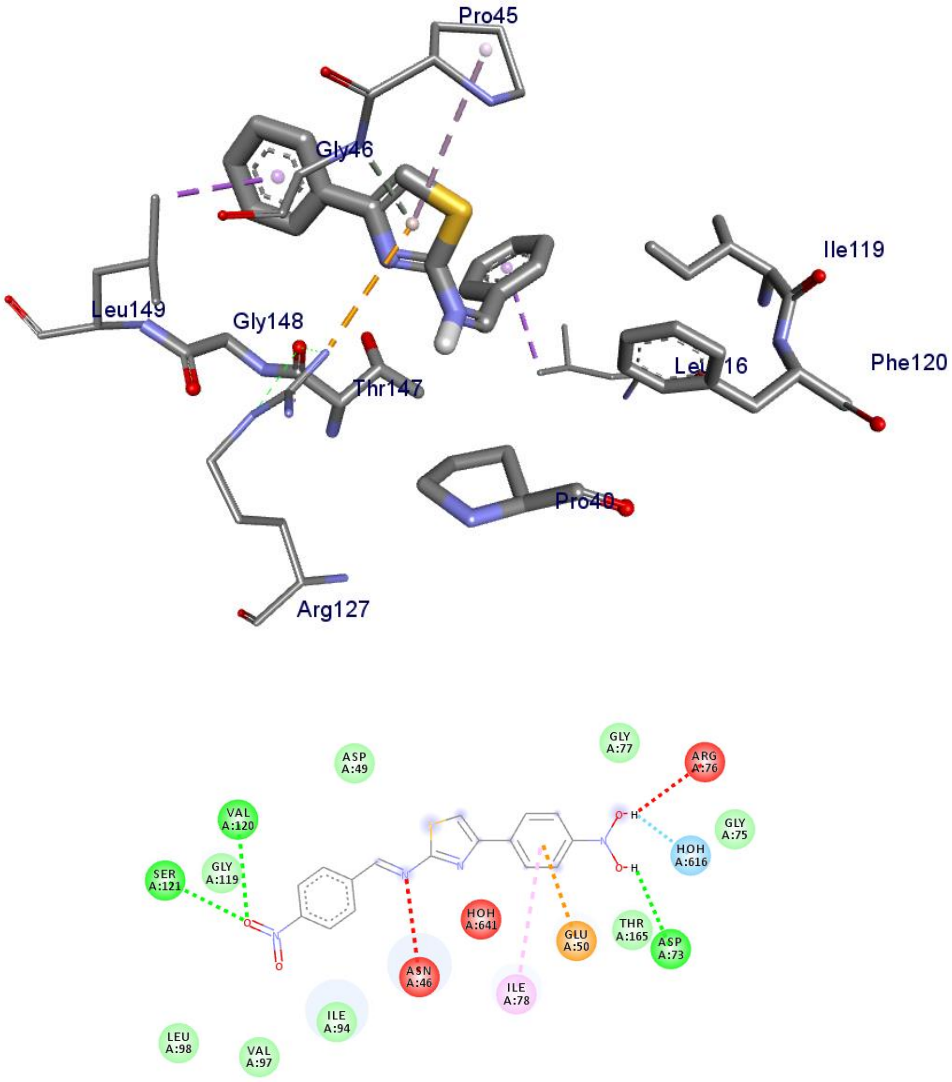

Figure 18:3D & 2D binding interaction of compound **106** against *E.coli* DNA gyraseB

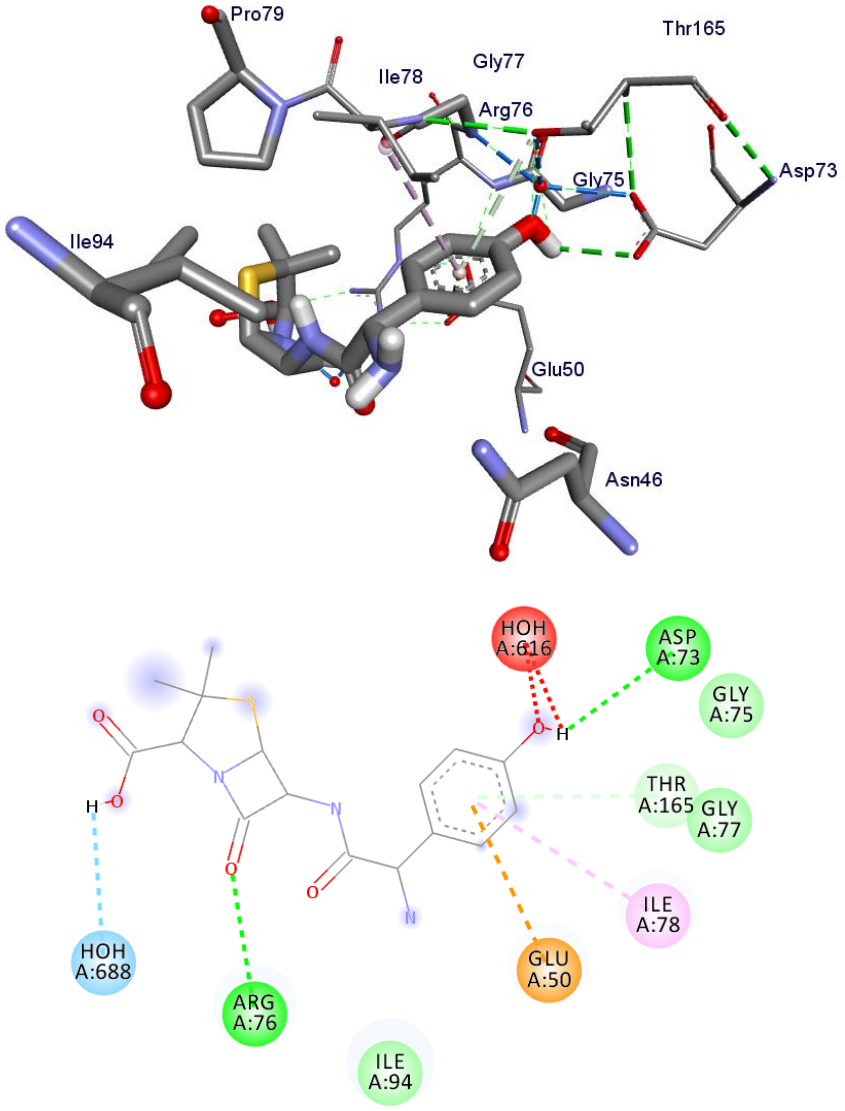

Figure 19:3D & 2D binding interaction of Amoxicillin against *E.coli* DNA gyraseB.

4.4.1 Molecular docking against human peroxiredoxin

The human body protects itself from oxidative stress through either of enzymatic and non-enzymatic defense mechanisms (Lobo *et al.*, 2010). The enzymatic part of this antioxidant defense system includes superoxide dismutase, catalase, and peroxidases, which play crucial roles for the metabolization of superoxide, hydrogen peroxide, and lipid peroxides and in this way prevent the formation of hydroxyl radical (Kurutas, 2016). The molecular docking analysis of the synthesized compounds was carried out to investigate their binding pattern with human peroxiredoxin (PDB ID: 1HD2) and compared with the natural antioxidant Ascorbic acid. The analysis of the compounds (**101**-**106)** revealed minimum binding energy values ranging from -5.3 to - 5.0 kcal/mol (Table 5) within the binding pocket of human peroxiredoxin 5. The binding affinity, H-bond and Hydrophobic/Pi-Cation/Pi-Anion/ Pi-Alkyl interactions and Van der Waals interactions of ligands (**101**-**106**) were summarized (Table 5). The entire synthesized compound shows higher binding affinity than ascorbic acid. Compound **102** and **105** having lower score value formed via hydrogen bond interaction with Thr-44, Cys-47 and residual hydrophobic interactions with amino acids Pro-40 in (Figure 21&26). Similarly compound **101** &**102** having same value of binding score with -5.3 kcal/mol formed via hydrogen bond of Cyst-47 (Figure 20&21). Compound **105** having lower binding score than Abscorbic acid similar hydrogen bond with Thr-147, Thr-44, Cyst-47 and Gly-46 and residual interaction via Pro-40 (Figure25 & 27).The key amino acid residues within the active sites of peroxreidoxin 5 are Cys 47, Pro45, Phen120, Leu116, Arg127, Thr-44, Gly-46 and Tr-147. The molecular docking study of these compounds displayed comparable docking score of synthesized compounds within binding pocket toward peroxiredoxin 5. Overall, *in silico* docking analysis of the compounds **101**-**106** binding affinity are match experimental antioxidant activity displayed. The results show that compounds **101**, **102**, **104** and **105** can act as potential antioxidants.

Table 5: Molecular docking value of synthetic compounds against human peroxiredoxin.

Ligands	Affinity (kcal/mol)	H-bond	Residual Amino acid Interactions	
			Hydrophobic/Pi-Cation/Pi-Anion/ Pi-Alkyl interactions	Van-der Walls interactions
101	-5.3	Cys-47, Gly-46	Pro-45, Thr-147	Thr-44, Leu-116
102	-5.3	Cys-47, Thr-44, Gly-46 Pro-45	Pro-40, , Leu-149, Arg-127	Phe-120, Gly-148, Thr-147
103	-5.0	Gly-46, Arg-127, Pro-45	Leu-116, Leu-149	Pro-40, Thr-147, Gly-148, Phe-120
104	-5.1	Cys-47, Thr-44, Arg-127, Thr-147	Phe-120, Leu-116, Leu-149	Gly-148, Gly-41, Pro-40
105	-5.2	Cys-47, Thr-44, Arg-127, Thr-147, Gly46	Pro-40	Phe-120, Ile-119, Leu-149
106	-5.1	Cys-47, Gly-46, Arg-127,	Thr-147	Thr-44, Gly-148, Leu-149
Ascorbic Acid	-4.9	Cys-47, Thr-44, Gly-46, Thr-147	Pro-40, Pro-45, Phe-120, Arg-127, Leu-149	--

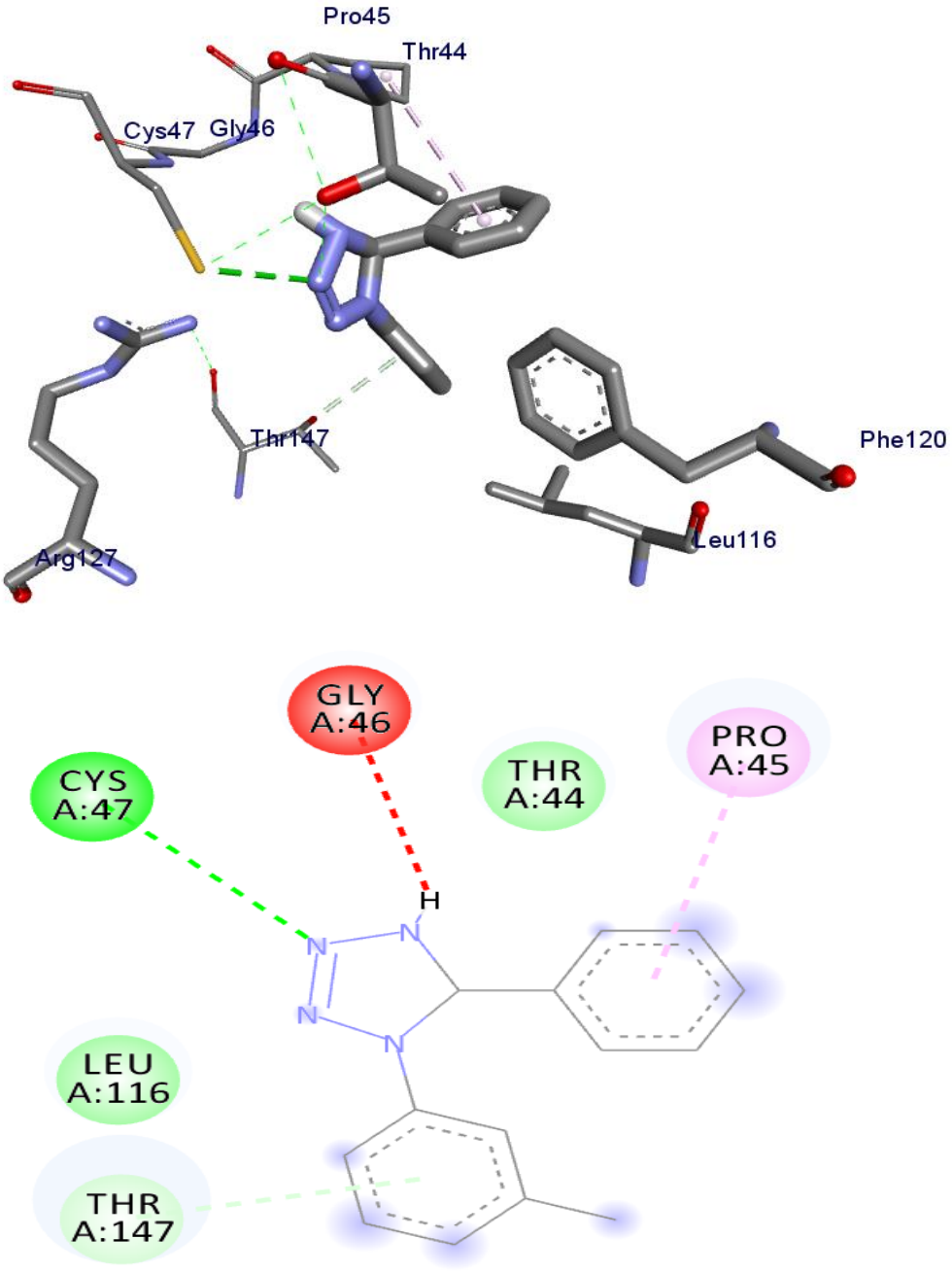

Figure 20: 3D & 2D binding interaction of compound **101** against human perorexidoxin.

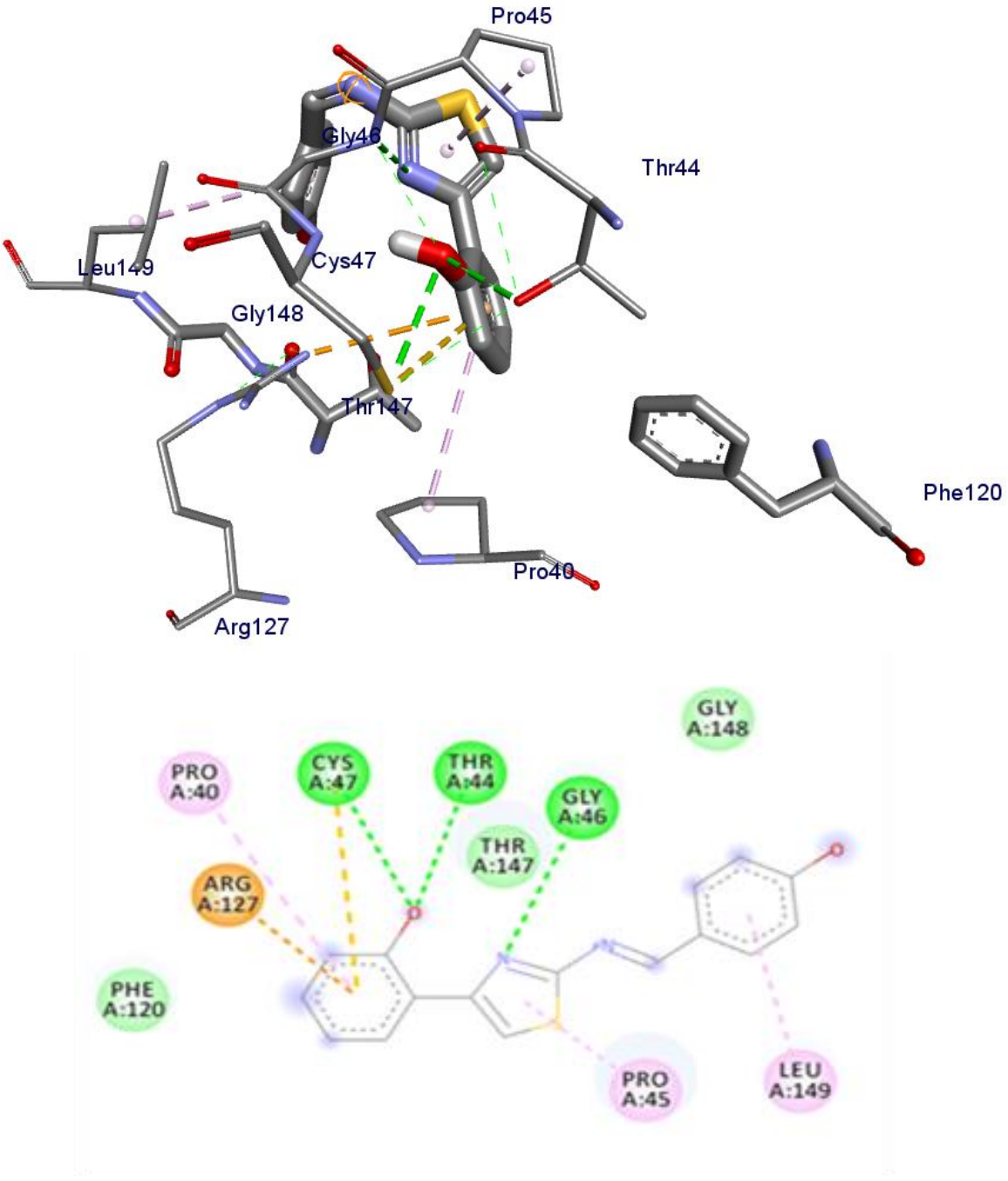

Figure 21:3D& 2D binding interaction of compound **102** against human peroxiredoxin.

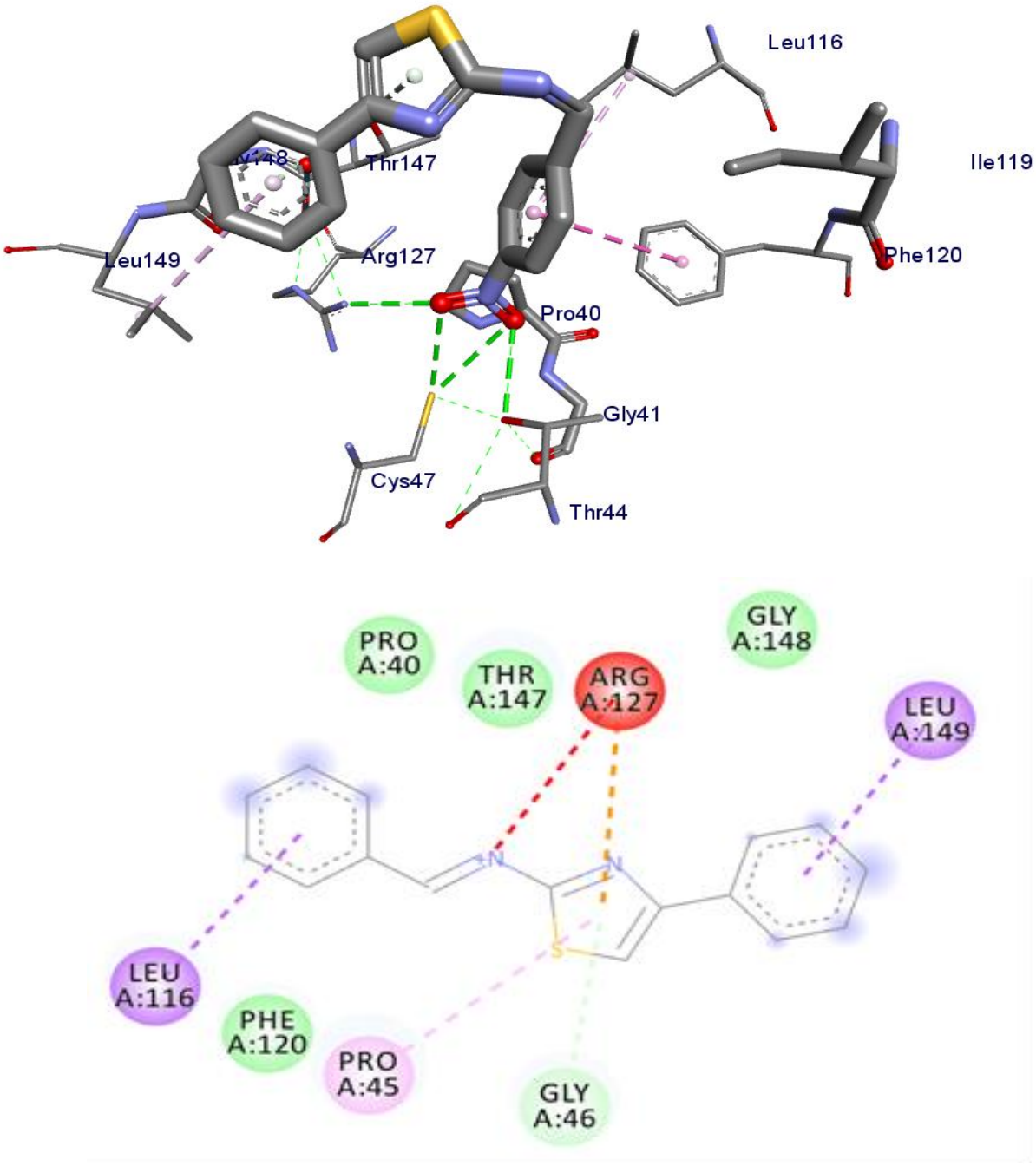

Figure 22: 3D & 2D binding interaction of compound **103** against human peroxiredoxin.

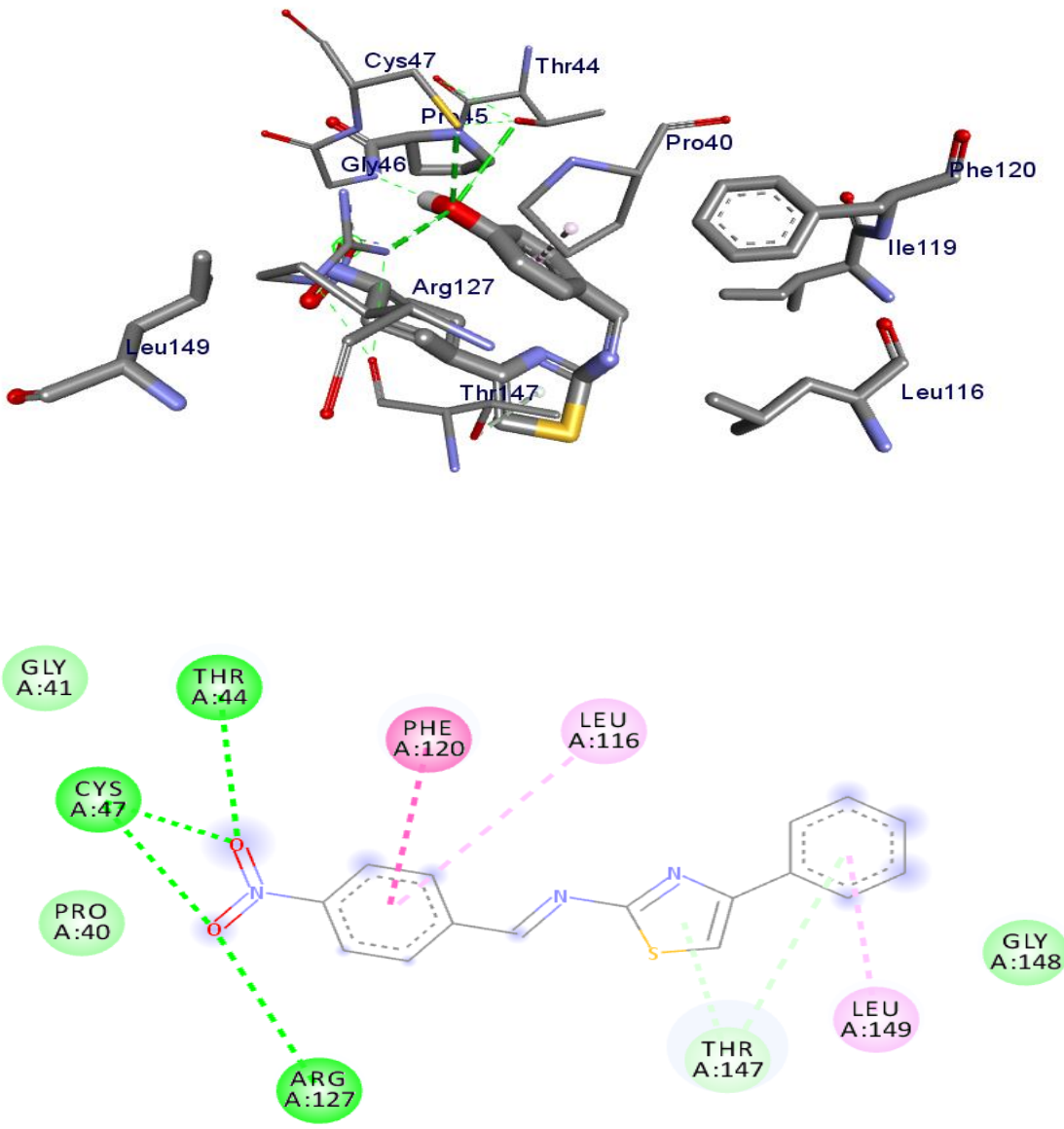

Figure 23:3D & 2D binding interaction of compound **104** against human peroxiredoxin.

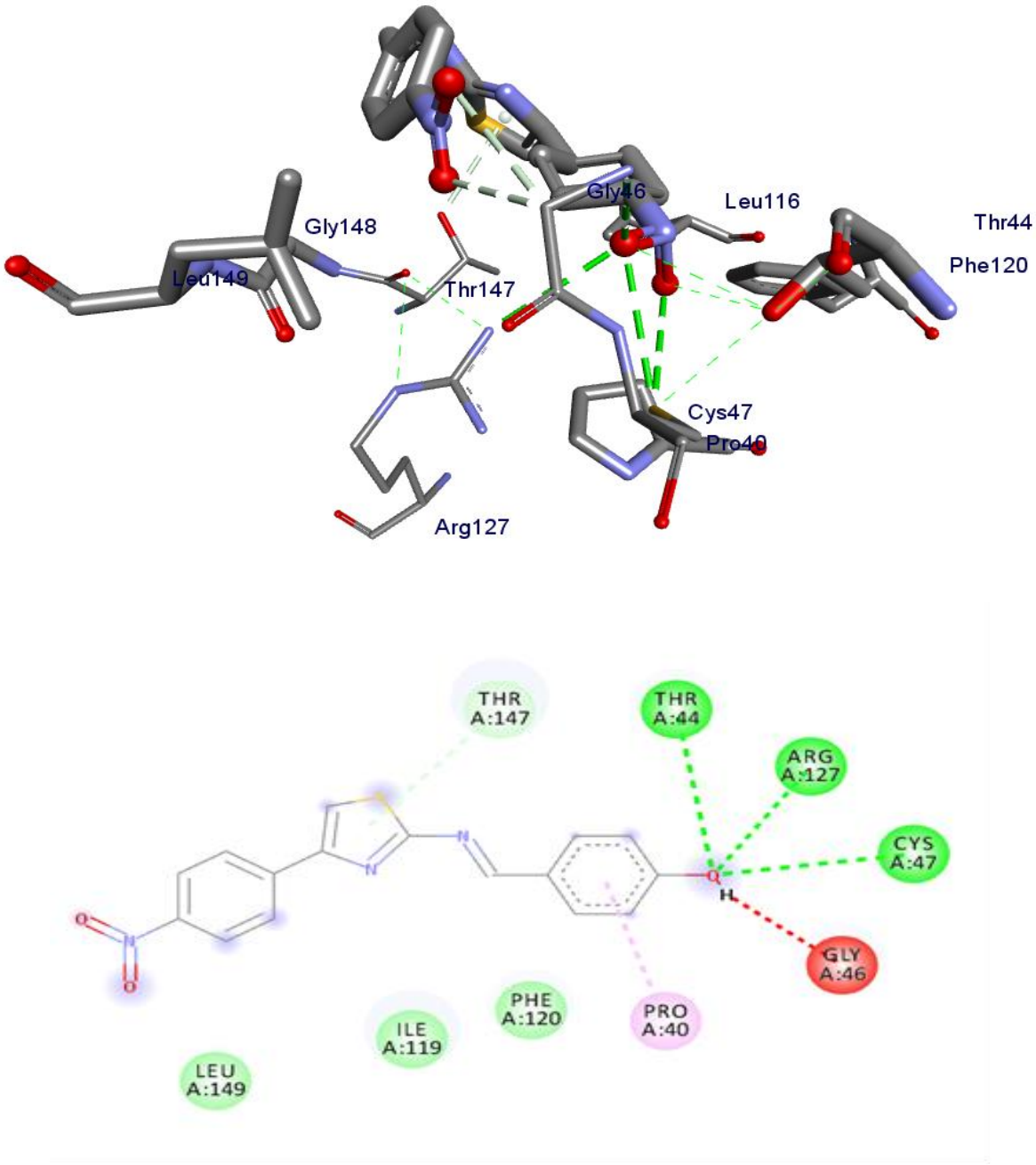

Figure 24: 3D & 2D binding interaction of compound **105** against human peroxiredoxin.

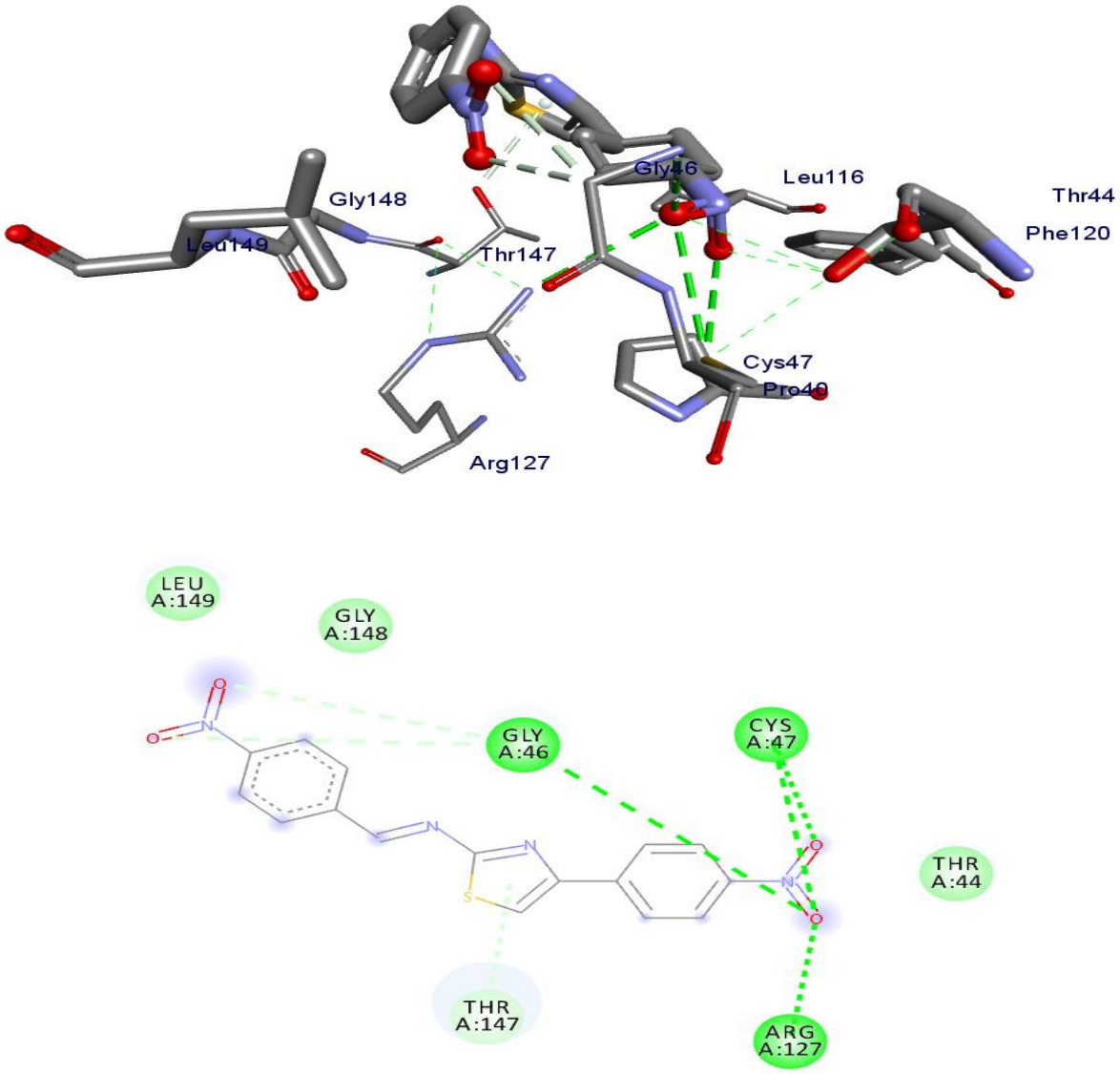

Figure 25: 3D&2D binding interaction of compound **106** against human peroxiredoxin.

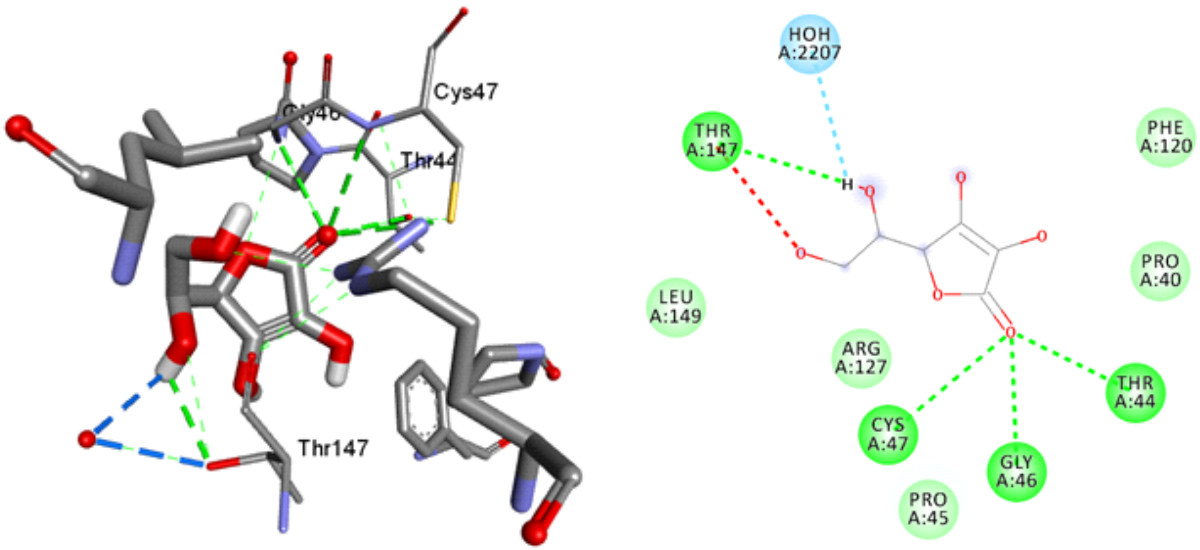

Figure 26: The 2D and 3D binding interactions of Ascorbic acid against human peroxiredoxin 5.

4.4.2 Molecular docking against human topoisomerase II α

Thiazoles have better action as an anticancer agents just as it demonstrates better binding domain and they have less cytotoxicity to normal cell (physiological cell) however alongside that it has site explicit movement to malignant growth cell (Sayed *et al.,* 2019). The human topoisomerase IIα may be a homodimer within the presence of ATPase domain. Topoisomerases split and rejoin DNA strands by forming a covalent connection among the enzyme and the DNA at the site of strand breakage (Murugavel *et al.,* 2019). Topoisomerase II contain targeting drugs are divided into two major class with different of mechanisms of actions as poisons and catalytic inhibitors. Topoisomerase IIα is responsible for maintaining chromosomes in proper topological state and major role in cellular life makes TOPO IIα as perfect anticancer target. In this study, we have explored topoisomerase II α as an effective target for synthesized compound by *in silico* studies. The binding affinities, hydrogen bond and residual interactions of all the synthesized compounds and Vosaroxin are summarized form DNA (PDB ID 3QX3)(Table6). Comparing to Vosaroxin (–6.2 kcal/mol), the synthesized compounds (**101-106**) showed moderate binding affinity and similar residual and DNA interactions profile with amino acid residues Asp-479, Ser-480, Glu-477, Ala-481 and Nucleic acid residues DT-8, DT-9, and DG-10. The molecular docking analysis also showed moderate to higher docking affinities among them, Compounds **105**, **106** and **102** (- 5.9,-5.8 and 5.6 kcal/mol) within the binding pocket of Human topoisomerase II α. compared standard Vosaroxin, anti-cancer drug having binding affinity of -6.2 kcal/mol. Compared to Vosaroxin compounds **105** and **106 s**howed similar hydrogen bond interaction with amino acids Asp-479, Ser-480 and Ala-48 (Figure 31&32). All six compounds showed significant binding affinity with both human topoisomerase IIα. Compounds **105** and **106** formed significant molecular interactions with topoisomerase II in active sites. Thus, signify the *in silico* analysis support that compound **105** is potential promising anticancer candidate shown similar residual interactions and binding affinity with that of references drug(Vosaroxin). This may form a complex with DNA and topoisomerase II, and cause inhibition of the activity of Topoisomerase leading to the inhibition of growth. They could be showing promising anticancer agents against various cancer cell lines. Thus, *in vitro* and *in vivo* experiments are necessary to put forward therapeutic repositioning of those compounds as anticancer agents.

Table 6: Molecular docking value of synthetic compounds against human topoisomerase II α

Ligands	**Affinity (kcal/mol)**	**H-bond**	**DNA**	**Residual interactions**	
				Hydrophobic/Pi-Cation	**Van dar Waals**
101	**-5.4**	--	DC-8, DT-9	Glu-477, Tyr-821	Gly-504, Arg-503, Gly-478, Gly-776, Asp-557
102	**-5.6**	Asp-559, Glu-477	DC-8, DG-7	Asp-557, Tyr-821	Ser-480, Gly-776, His-775, Asp-561, Gly-562
103	**-5.3**	Gly-478	DC-8, DT-9, DG-10	Glu-477, Asp-557, Tyr-821	Ser-480, Asp-479, Arg-503
104	**-5.5**	Gly-504	DC-8, DT-9	Glu-477, Tyr-821	Ser-480, Asp-557, Gly-478, Leu-502, Gly-776
105	**-5.9**	Ser-480, Ala-481, Asp-479, Glu-477	DG-7, DC-8, DT-9, DG-10	Asp-561	Gly-776, His-775, His-774, Asp-559, Gly-478, Gly-504
106	**-5.8**	Ser-480, Asp-479, Ala-481,	DC-8, DT-9, DG-10	--	Gly-478, Arg-503, Gly-504
Vosaroxin	**– 6.2**	Asp-479, Ser-480, Glu-477, Ala-481, Arg-503	DT-8, DT-9, DG-10, DA-12, DG-13	--	Gly-478, Gly-504

Note: DA= Deoxyadenosine, DG= Deoxyguanosine, DT= Deoxythymidine, and DC = Deoxycytosin

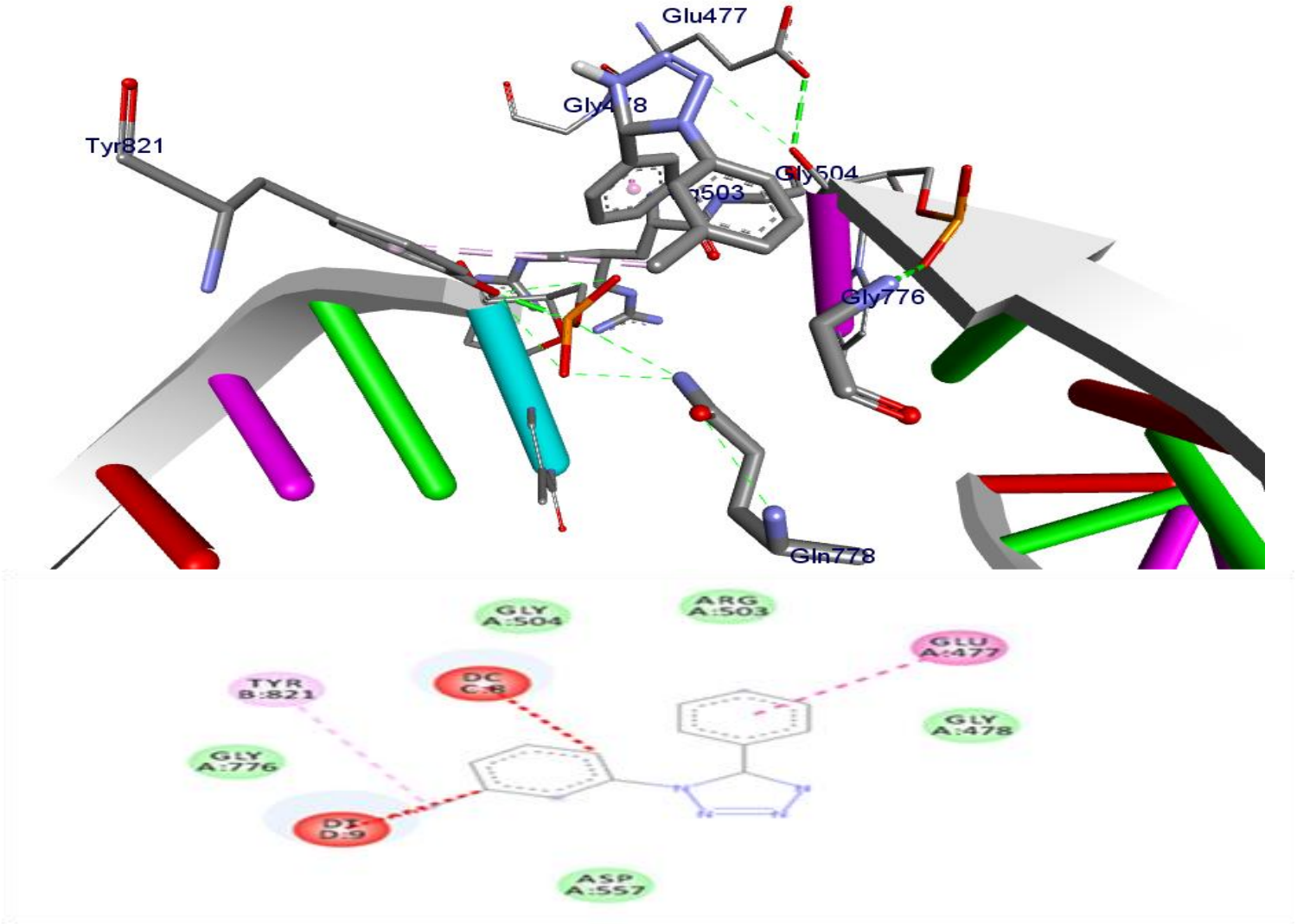

Figure 27: 3D&2D binding interaction of compound **101** against human topoisomerase II α DNA.

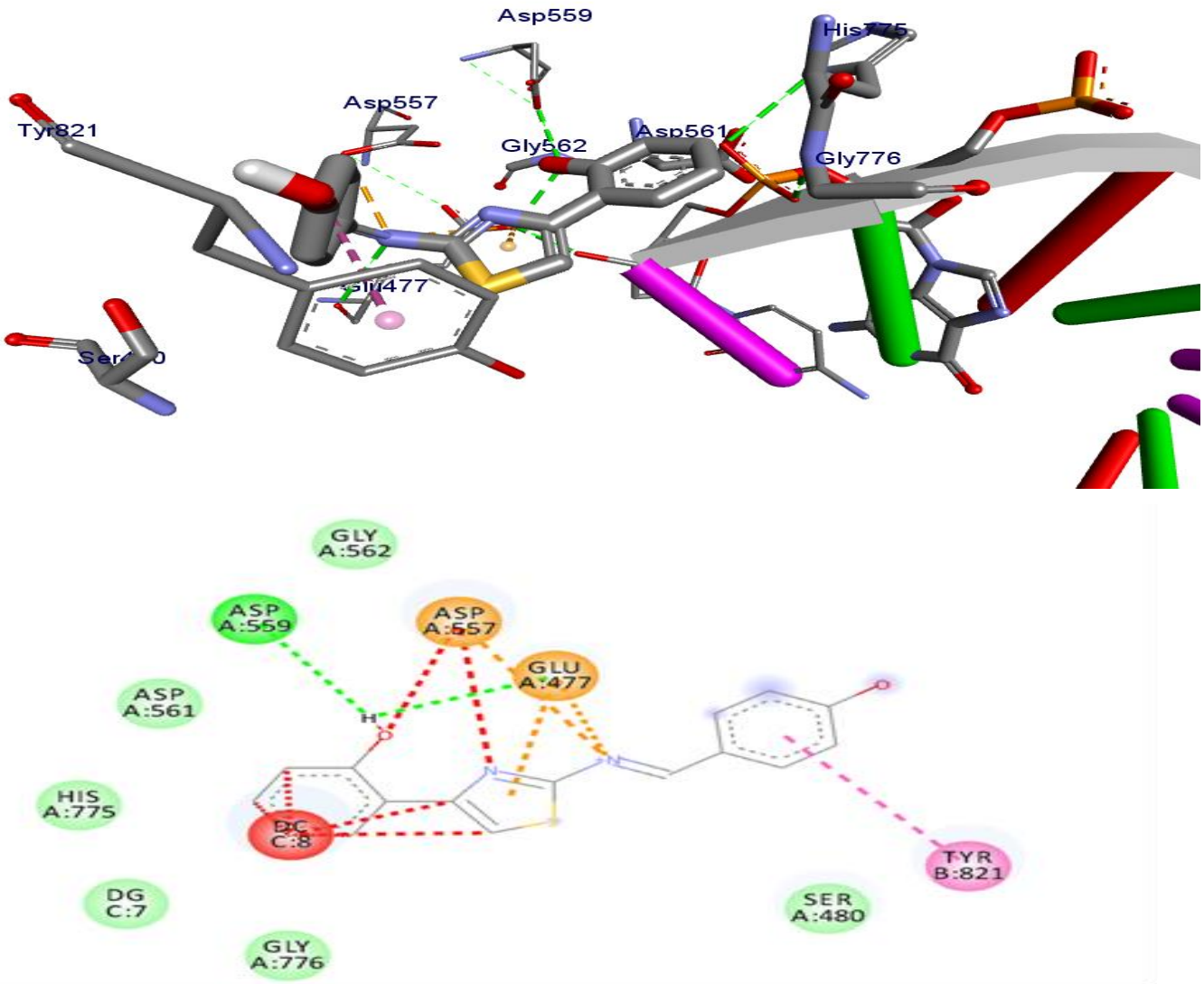

Figure 28:3D & 2D binding interaction of compound **102** against human topoisomerase II α DNA

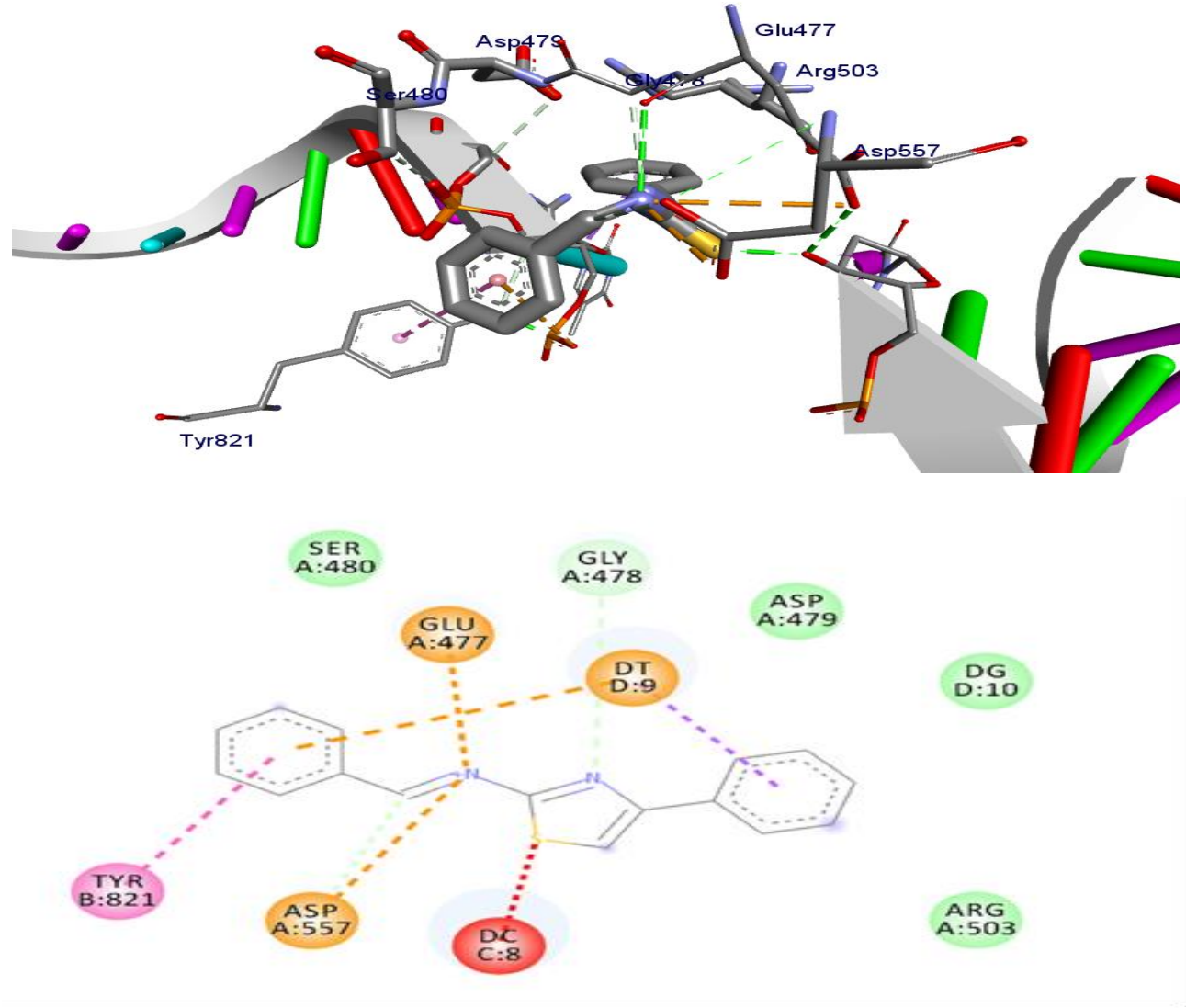

Figure 29: 3D & 2D binding interaction of compound **103** against human topoisomerase II α DNA.

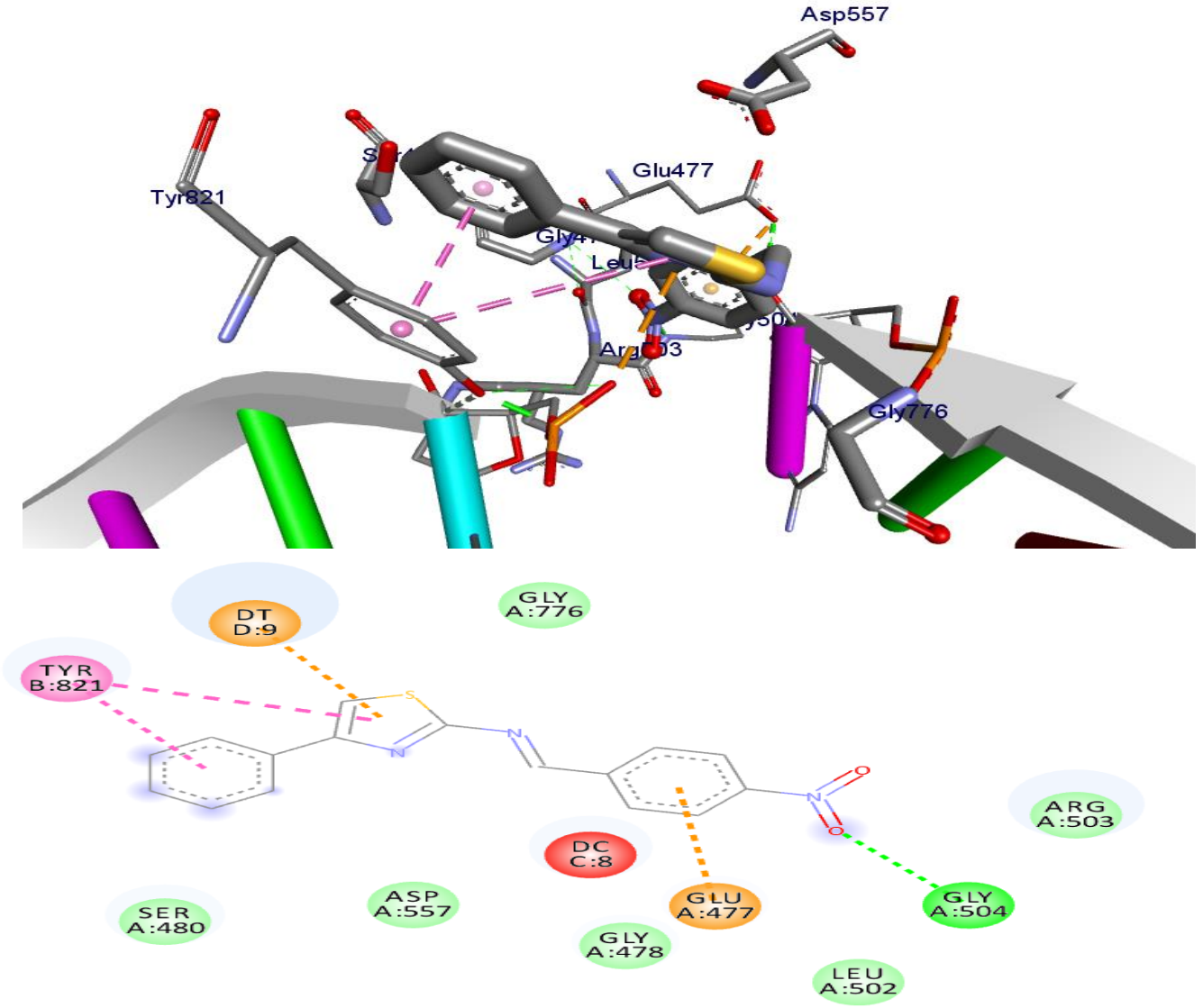

Figure 30: 3D & 2D binding interaction of compound **104** against human topoisomerase II α DNA.

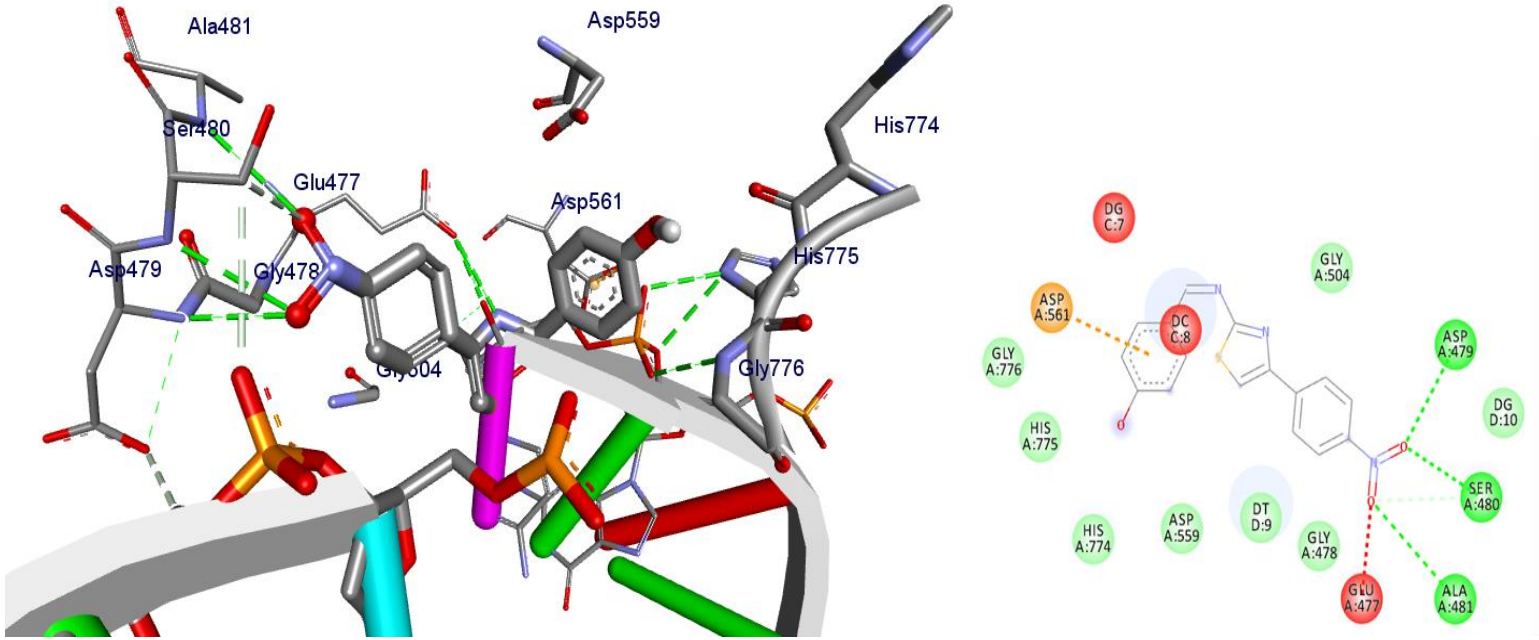

Figure 31: 3D & 2D binding interaction of compound **105** against human topoisomerase II α DNA.

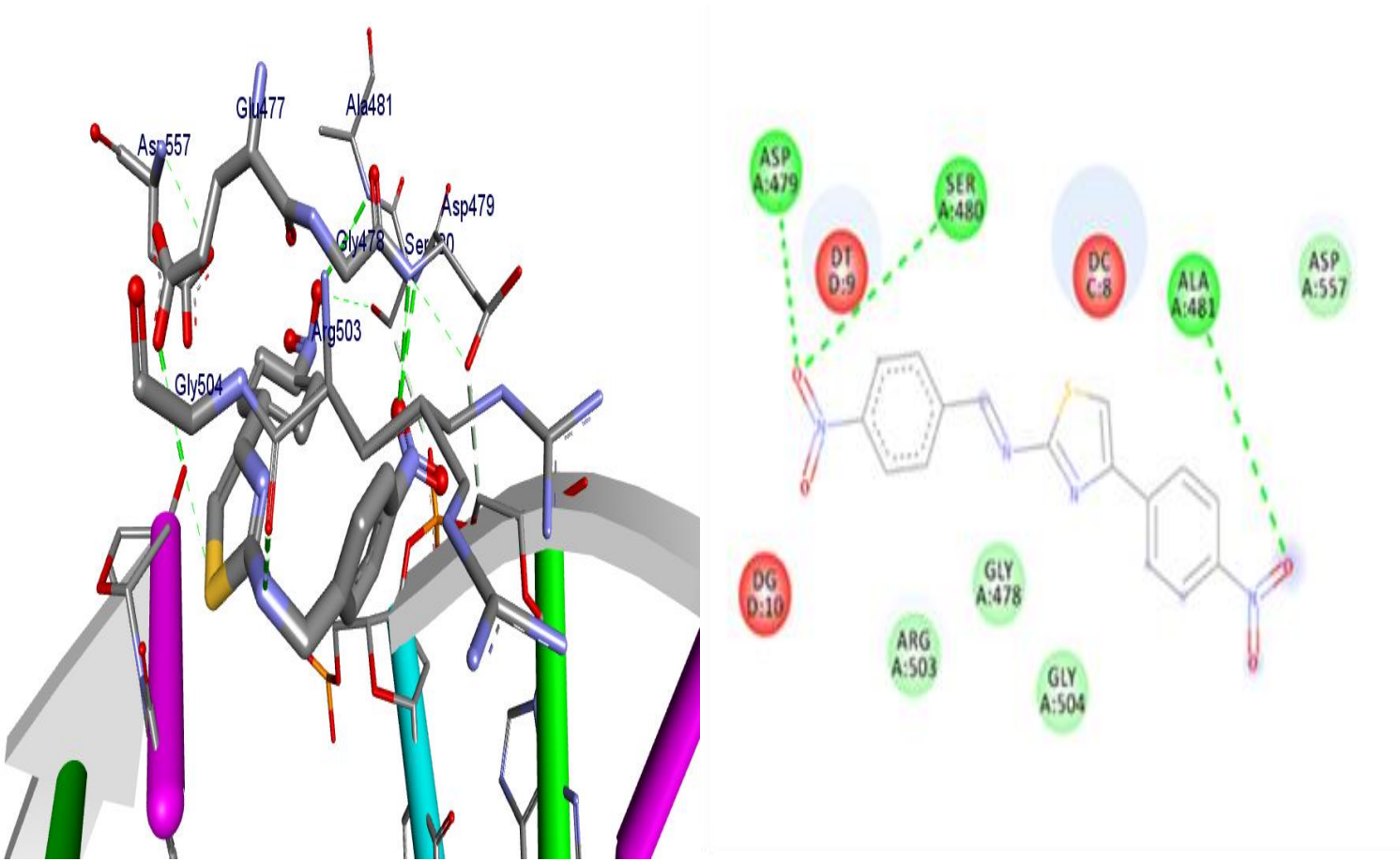

Figure 32: 3D & 2D binding interaction of compound **106** against human topoisomerase II α DNA.

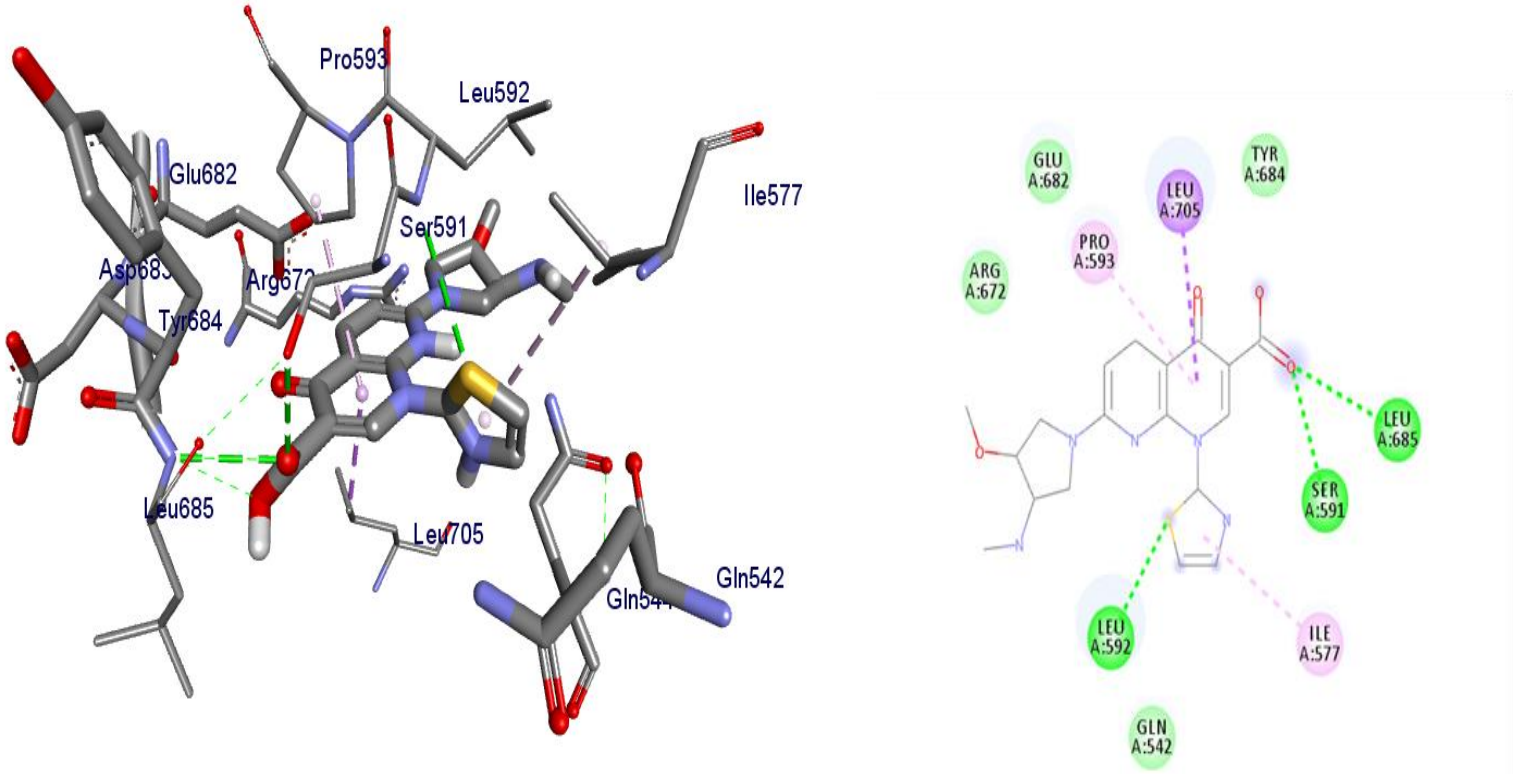

Figure 33: The binding interactions of vosaroxin against human topoisomerase IIα

4.4.3 *In silico* ADMET and drug likeness studies.

The SwissADME predicted results showed that the synthesized compounds (**101-106**) satisfy Lipinski's rule of five with zero violations for their drug like molecular nature (Table 7) (Daina *et al., 2017).* According to the Lipinski's rule of five, the molecular weight of the molecules should be less than 500, the number of hydrogen bond acceptors less than ten, number of hydrogen bond donors less than five and the lipophilicity (iLOGP) values should be less than five (Lipinski *et al.,* 2012). The SwissADME predicted LogP values are in the range from 2.10 to 3.07 assuring optimal lipophilicity of the synthesized compounds. In addition, TPSA of the synthesized molecules were used predict percent absorption descriptor. The predicted TPSA value (in $Å^2$) are in the range from 39.99 to 145.13 inferring very good absorption for compounds (**101-105**) and relatively poor intestinal absorption for compound **106**. It has been suggested that molecules with a TPSA of 140 $Å^2$ and above would be poorly absorbed (< 10 percent fractional absorption), while compounds with a TPSA 60 $Å^2$ would be well absorbed (> 90 per cent)(Salaria *et al.,* 2020). In this work high degree of absorption was predicted for compound other than **106**.

Table 7: Drug-likeness predictions of compounds **101-106**,computed by SwissADME.

S. No.	Formula	Mol. Wt. (g/mol)	NRB	NHA	NHD	TPSA ($A^{°2}$)	LogP (cLogP)	Lipinski's rule of Five Violation
101	$C_{13}H_{11}ClN_4$	258.71	2	2	1	39.99	2.6	0
102	$C_{16}H_{12}N_2O_2S$	296.34	3	4	2	93.95	2.54	0
103	$C_{16}H_{12}N_2S$	264.34	3	2	0	53.49	3.07	0
104	$C_{16}H_{11}N_3O_2S$	309.34	4	4	0	99.31	2.73	0
105	$C_{16}H_{11}N_3O_3S$	325.34	4	5	1	119.54	2.08	0
106	$C_{16}H_{10}N_4O_4S$	354.34	5	6	0	145.13	2.39	0
Amoxicillin	$C_{18}H_{26}ClN_3$	319.87	5	6	4	158.26	1.56	0

Notice: NHD = Number of Hydrogen donor, NHA = Number of Hydrogen acceptor

NRB = Number of rotatable bonds, and TPSA = total polar surface area

The predicted human skin permeability coefficients (logKp) values of the synthesized compounds for their human stratum corneum penetration are found to be in the range of -4.37 to -5.59 cm/s inferring low skin permeability. In this work, a relatively less skin permeant was predicted for compound **102**.

Pharmacokinetically, high GI absorption for **101, 102, 103** and **104**, BBB permeate for **101** and **103**, and none of the synthesized compounds were predicted to as Pg-p substrate Table 8). SwissADME predicted results show that compound **104** can be better active therapeutic agent compared to other synthesized compounds. Besides, the interaction of therapeutic molecules with cytochromes P450 CYP isoforms as substrate of these enzymes has been proposed to screen a therapeutically active molecule. It is reported that the inhibition of CYP isoenzymes is certainly one major cause of pharmacokinetics-related drug-drug interactions (Hollenberg, 2002);(Huang et al., 2008) there by leading to toxic or adverse effects due to the lower clearance and accumulation of the drug or its metabolites (Kirchmair *et al.,* 2015). In this work, except to CYP1A2 isoform, most of the synthesized compounds were substrates of CYP isoforms inferring their good drug like molecular nature.

Table 8:ADME predictions of compounds **101-106**, computed by SwissADME and PreADMET.

S. No.	Chemical Formula	Skin Permeation Value (log Kp) cm/s	GI Absorption	BBB Permeability	Inhibitor Interaction (SwissADME/PreADMET)					
					P-gp substrate	CYP1A2 inhibitor	CYP2C19 inhibitor	CYP2C9 inhibitor	CYP2D6 inhibitor	CYP3A4 inhibitor
101	$C_{13}H_{11}ClN_4$	-4.37	High	Yes	No	Yes	Yes	Yes	No	No
102	$C_{16}H_{12}N_2O_2S$	-5.59	High	No	No	Yes	Yes	Yes	No	No
103	$C_{16}H_{12}N_2S$	-4.66	High	Yes	No	Yes	Yes	Yes	No	No
104	$C_{16}H_{11}N_3O_2S$	-5.29	High	No	No	Yes	Yes	Yes	No	No
105	$C_{16}H_{11}N_3O_3S$	-5.41	High	No	No	Yes	Yes	Yes	No	No
106	$C_{16}H_{10}N_4O_4S$	-5.45	Low	No	No	Yes	Yes	Yes	No	No
Amoxicillin	$C_{18}H_{26}ClN_3$	-9.94	Low	No	No	No	No	No	No	No

Note: GI = Gastro-Intestinal, BBB = Blood Brain Barrier, P-gp = P-glycoprotein, CYP = Cytochrome-

Table 9: Organ toxicity and toxicological end points of synthesized compounds predicted by Pro Tox II

S. No.	Formula	LD_{50} (mg/kg)	Toxicity Class	Organ Toxicity				
				Hepatotoxicity	Carcinogenicity	Immunotoxicity	Mutagenicity	Cytotoxicity
101	$C_{13}H_{11}ClN_4$	700	4	Active	Inactive	Inactive	Active	Inactive
102	$C_{16}H_{12}N_2O_2S$	300	3	Active	Active	Inactive	Active	Inactive
103	$C_{16}H_{12}N_2S$	300	3	Active	Inactive	Inactive	Active	Inactive
104	$C_{16}H_{11}N_3O_2S$	300	3	Active	Active	Inactive	Active	Inactive
105	$C_{16}H_{11}N_3O_3S$	300	3	Active	Active	Inactive	Active	Inactive
106	$C_{16}H_{10}N_4O_4S$	300	3	Active	Active	Inactive	Active	Inactive
Amoxicillin	$C_{18}H_{26}ClN_3$	15000	6	Inactive	Inactive	Inactive	Inactive	Inactive

Absence of toxicity data is one of the life threatening factors for choosing a compound as a therapeutic candidate (Sadeghi *et al.*, 2021). Herein, the organ toxicity (hepatotoxicity) and toxicological end points (carcinogenicity, immunotoxicity, mutagenicity and cytotoxicity) of the six compounds predicted. The Pro Tox II predicted organ toxicity results revealed that all the synthesized compounds show hepatotoxicity organ toxicity and mutagenicity toxicological end point. Besides, all the compounds show no toxicity towards immunotoxicity toxicological end point. Compound **101**, **102**, **104**, **105** and **106** were predicted for their carcinogenicity and cytotoxicity toxicological end points in (Table 9). *In silico* cytoxicity predictions revealed LD_{50} value of class three ($50 \leq LD_{50} \leq 300$) inferring they are toxic if swallowed except compound **101** (class 4, $300 \leq LD_{50} \leq 2000$). Class I: fatal if swallowed ($LD_{50} \leq 5$) Class II: fatal if swallowed ($5 < LD_{50} \leq 50$), Class III: toxic if swallowed ($50 < LD_{50} \leq 300$), Class IV: harmful if swallowed ($300 < LD_{50} \leq 2000$) Class V: may be harmful if swallowed ($2000 < LD_{50} \leq 5000$) Class VI: non-toxic ($LD_{50} > 5000$) (Banerjee *et al.*, 2018).

4.4 Density functional theory and wave function analysis

DFT offers promising applications in the realm of drug design and a number of such applications are currently being employed. Though, the interactions between drug and receptor, drug action mechanism modeling. The energy gap (E_{HOMO}-E_{LUMO}) that is an important stability index helps to characterize the chemical reactivity and kinetic stability of the molecule or compounds (Abu-Melha, 2018). It is a fact that, the smaller the gap that occurs due to the groups that enter into conjugation is more polarized the molecule is and in turn, the molecule is a soft one and easily offer electrons to an acceptor. This in turn affects the biological activity of the molecule. To ascertain the biological activity of the thiazole derivatives, some additional parameters such as the electronegativity (χ), chemical potential (μ), global hardness (η), global softness (S) and global electrophilicity index (w) and others.

The geometries of the synthesized molecules were optimized as described in the method section (3.7.2). The HOMO and LUMO Frontier orbitals were used to analyze the relative reactivity and describe the wave function distribution of the molecules. The HOMO, LUMO, energy gap (ΔE_{L-H}) and quantum chemical descriptors are tabulated in (Table 10). The energy gaps of the synthesized compounds are calculated as 2.731, 0.134, 0.692, 0.455, 0.144 and 0.220 for compounds **101**,**102**, **103**, **104**,**105** and **106** respectively (Table 10). The results revealed that compound **102** showed the least HOMO-LUMO energy gap suggesting high chemical reactivity and considerable intramolecular charge transfer from electron donor (HOMO) to electron acceptor (LUMO) groups. However, except compound **101** all compounds showed small band gap energy ranging from 0.134-0.692 eV inferring good reactivity of molecules. Furthermore, similar electronegativity of the synthesized compounds ranging from 6.052 (for Compound **101**) to 7.379 (for Compound **106**) were calculated. Compound **102** has large electronegativity (7.256 eV), global softness (7.479 eV^{-1}), and global electrophilicity (393.720 eV) compared to other compounds. On the other hand, a relatively large dipole moment values were calculated for compound **105** (14.629 Debye) and compound **106** (10.164 Debye) inferring good antimicrobial activity of the synthesized compounds.

The DFT calculated HOMO-LUMO band gap energy (Figure 35) revealed the role of substituents in the reactivity of the synthesized compounds. The presence of two electron donating hydroxyl groups in compound **102** (Eg = 0.134 eV) increases its relative reactivity to its

structural analog compound **103** (0.692 eV). The substituent difference for compound **103** (no NO_2), **104** (one NO_2) and **106** (two NO_2) was observed in their band gap energy as 0.692 eV, 0.455 eV and 0.22 eV, respectively. In these compounds the wave function distribution for HOMO and LUMO of their orbitals is from uniform (**103**) distribution to the central part of the molecule (**106**) as the number of NO_2 increases.

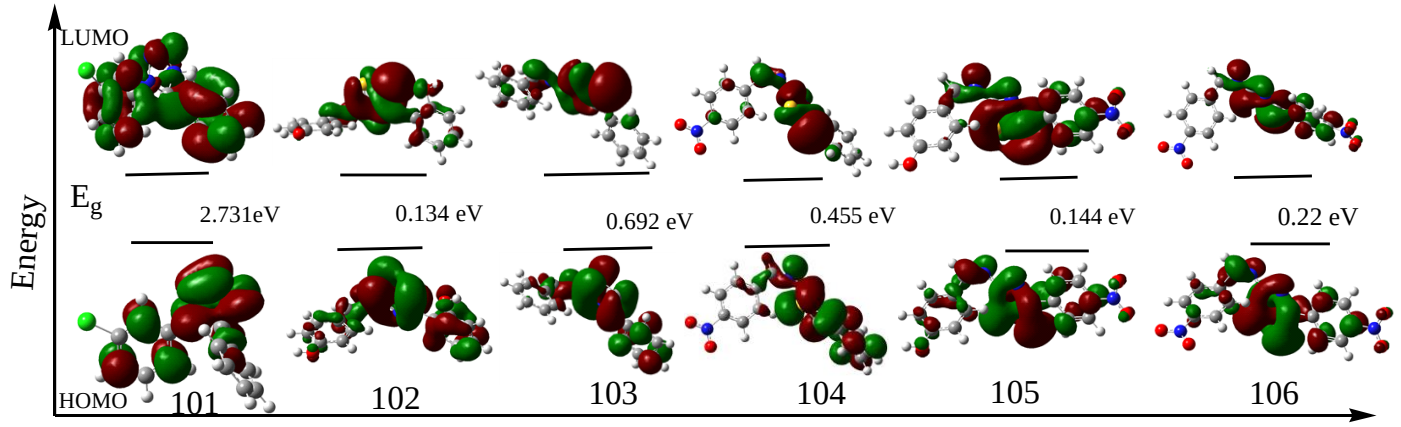

Figure 34: The HOMO-LUMO band gap and wave function distribution of synthesized compounds.

Table 10: Quantum chemical descriptors of the synthesized compounds in (eV)

Cpd	E_{HOMO}	E_{LUMO}	Eg	χ	μ	η	Σ	ω	Nu	Dipole moment (Debye)
101	-7.417	-4.686	2.731	6.052	-6.052	1.366	0.366	13.410	0.075	7.362
102	-7.322	-7.189	0.134	7.256	-7.256	0.067	7.479	393.720	0.003	3.084
103	-7.725	-7.034	0.692	7.379	-7.379	0.346	1.446	78.739	0.013	6.249
104	-7.489	-7.034	0.455	7.261	-7.261	0.228	2.196	115.788	0.009	5.497
105	-7.434	-7.290	0.144	7.362	-7.362	0.072	6.944	376.391	0.003	14.629
106	-7.489	-7.269	0.220	7.379	-7.379	0.110	4.541	247.236	0.004	10.164

.

5 .CONCLUSIONS AND RECOMMENDATIONS

The present work conducted on synthesis of tetrazole and Schiff base derivatives of thiazoles applying conventional and green catalyzed conditions using ZnO NPs as a catalyst. Over all, six compounds were synthesized and fully characterized using spectroscopic methods and also with good to excellent yield (68.3-83.3%). Shorter reaction time was achieved for Nano catalyzed approach compared to glacial acetic acid catalyzed reactions under reflux. The in-*vitro* antibacterial activity of synthetized compounds were also examined against *S. aureus* (ATCC25923), *E. coli* (ATCC25922), *S. pyogenes* (ATCC19615) and *P. aeuroginosa* (ATCC27853) using disk diffusion method. All most all the compounds showed better inhibitory activity against *E. coli*. Compounds **106**, **101** and **105** showed good activities against *E. coli* with mean inhibition zone of 14.4 ± 0.04, $12.5 \pm .04$ and 10.5 ± 0.02 mm diameter at 200 μg/mL compared to Amoxicillin 18 ± 0.01, respectively. Of the synthesized compounds, compound **106** displayed the highest activity with zone of inhibition of 14.4 ± 0.04, 15 ± 0.01, 13 ± 0.02, and 14.45 ± 0.25 at 200 μg/mL against *E. coli*, *S. aureus*, *P. aeruginosa*, and *S. pyogenes*, respectively. Compound **102, 105** and **101** exhibited highest percent inhibition of the DPPH with IC_{50} value of 3.6, 3.65, and 4.91 respectively. The antioxidant activity pattern of synthetized compounds follows **102** > **105** > **101 > 106** > **104**> **103** pattern compared to Ascorbic acid, thus due both side electron donating groups of hydroxyl. The *in vitro* antibacterial activity of compounds **106**, **105**, **101** and antioxidant activity of compounds **102** and **105** suggest the potential use of these compounds as potential drug lead candidates. Molecular docking analysis of the synthesized compounds against DNA gyrase B showed minimum binding energy values ranging from -7.5 to -6 kcal/mol of which best binding affinity was achieved for compounds **106**, **101** and **105** (-7.5, -7.2 and -6.9 kcal/mol, respectively. Compounds **101** and **106** showed better binding affinity compared to standard drug, Amoxicillin. The docking analysis against human peroxidoxin 5 revealed minimum binding energy ranging from - 5.3 to - 5.0 kcal/mol of which compounds **101, 102, 105** and **104** showed better binding affinity (- 5.3, - 5.3, - 5.2 and - 5.1 kcal/mol, respectively) compared to standard drug. *In vitro* antibacterial activity of compounds **106**, **105**, **101** and antioxidant activity of compounds **102, 105** and **101**suggest the potential use of these compounds as potential drug lead candidates, supported by both experimental and computational analysis. Compounds **105** and **106** showed significant molecular interactions with

topoisomerase II at active sites (- 5.8, - 5.9, kcal/mol, respectively) compared to Vosaroxin (- 6.2, kcal/mol). *In silico* cytoxicity predictions revealed LD_{50} value of class three ($50 \leq LD_{50} \leq 300$) inferring they are toxic if swallowed except compound **101** (class 4, $300 \leq LD_{50} \leq 2000$). The DFT and wave function analysis revealed that compound **102** showed the least HOMO-LUMO energy gap suggesting high chemical reactivity and considerable intramolecular charge transfer from electron donor (HOMO) to electron acceptor (LUMO) groups. However, except compound **101**, all compounds showed small band gap energy ranging from 0.134-0.692 eV inferring good reactivity of molecules. The energy gap (E_{HOMO}-E_{LUMO}) that is an important stability index helps to characterize the chemical reactivity and kinetic stability of the molecule or compounds. It is a fact that, the smaller the gap that occurs due to the groups that enter into conjugation is more polarized the molecule is and in turn, the molecule is a soft one and easily offer electrons to an acceptor. This in turn affects the biological activity of the molecule. To ascertain the biological activity of the thiazole derivatives, some additional parameters such as the electronegativity (χ), chemical potential (μ), global hardness (η), global softness (S) and global electrophilicity index (w) and others.

5.1 Recommendations

As result synthesized compound are active in *vitro* and *in silico* studies of against bacteria and they are promisingly novel candidate for drug development. Therefore, further *in vitro* and *in vivo* studies on biological activity such as anti-bacterial and anticancer activity are recommended. Further test using different radical scavenging activity protocols also recommended to.

Research Fund Acknowledgment

This research project is funded by Adama Science and Technology University under the grant number ASTU/SM-R/270/21, Adama, Ethiopia.

6. REFERENCES

Abhale, Y. K., Shinde, A., Deshmukh, K. K., Nawale, L., Sarkar, D., & Mhaske, P. C. (2017). Synthesis, antitubercular and antimicrobial potential of some new thiazole substituted thiosemicarbazide derivatives. *Medicinal Chemistry Research*, 26(10), 2557–2567.

Abu-Melha, S. (2018). Design, synthesis and DFT/DNP modeling study of new 2-amino-5-arylazothiazole derivatives as potential antibacterial agents. *Molecules*, 23(2), 1–11. https://doi.org/10.3390/molecules23020434

Adibi, H., & Nematollahi, D. (2011). Preliminary study of *in-vitro* antimicrobial and antioxidant activities. *Chemical and Pharmaceutical Bulletin*, 59(9), 1149–1152.

Ali, A., Asif, M., Alam, P., Jane Alam, M., & Asif Sherwani, M. (2017). DFT/B3LYP calculations, *in vitro* cytotoxicity and antioxidant activities of steroidal pyrimidines and their interaction with HSA using molecular docking and multispectroscopic techniques. *Bioorganic Chemistry*, 73, 83–99. https://doi.org/10.1016/j.bioorg.2017.06.001

Aliabadi, A., Shamsa, F., Ostad, S. N., Emami, S., Shafiee, A., Davoodi, J., & Foroumadi, A. (2010). Synthesis and biological evaluation of 2-phenylthiazole-4-carboxamide derivatives as anticancer agents. *European Journal of Medicinal Chemistry*, 45(11), 5384–5389.

Althagafi, I., El-Metwaly, N., & Farghaly, T. A. (2019). New series of thiazole derivatives: Synthesis, structural elucidation, antimicrobial activity, molecular modeling and MOE docking. *Molecules*, 24(9). https://doi.org/10.3390/molecules24091741

Amorim, C. R., Pavani, T. F. A., Lopes, A. F. S., Duque, M. D., Mengarda, A. C. A., Silva, M. P., de Moraes, J., & Rando, D. G. G. (2020). Schiff bases of 4-phenyl-2-aminothiazoles as hits to new antischistosomals: Synthesis, *in vitro*, *in vivo* and *in silico* studies. *European Journal of Pharmaceutical Sciences*, 150, 105-371.

Arora, P., Narang, R., Nayak, S. K., Singh, S. K., & Judge, V. (2016). 2,4-disubstituted thiazoles as multitargated bioactive molecules. *Medicinal Chemistry Research*, 25(9), 1717–1743.

Arshad, M., Bhat, A. R., Pokharel, S., & Kim. (2014). Synthesis, characterization and anticancer screening of some novel piperonyl-tetrazole derivatives. *European Journal of Medicinal Chemistry*, 71, 229–236. https://doi.org/10.1016/j.ejmech.2013.11.008

Ayati, A., Emami, S., Asadipour, A., Shafiee, A., & Foroumadi, A. (2015). Recent applications of 1,3-thiazole core structure in the identification of new lead compounds and drug discovery.

European Journal of Medicinal Chemistry, 97(1), 699–718.

Aziz, H., Saeed, A., & Jabeen. (2018). Synthesis , single crystal analysis , biological and docking evaluation of tetrazole derivatives. https://doi.org/10.1016/j.heliyon.2018.e00792

Banerjee, P., Eckert, A. O., Schrey, A. K., & Preissner, R. (2018). ProTox-II: A webserver for the prediction of toxicity of chemicals. *Nucleic Acids Research*, 46(7).

Basyirah, Azemin, A., Mohd Rodi, M. M., & Mohd, K. S. (2018). Chemical composition and antioxidant activity of stingless bee propolis from different extraction methods. *International Journal of Engineering & Technology*, 7(4), 90–95.

Bhatt, U. (2011). Five-membered heterocycles with four heteroatoms: *Modern Heterocyclic Chemistry*, 3, 1401–1430. https://doi.org/10.1002/9783527637737.ch15

Breijyeh, Z., Jubeh, B., & Karaman, R. (2020). Resistance of Gram-negative bacteria to current antibacterial agents and approaches to resolve it. *Molecules*, 25(6), 1340.

Broekema, N. M., Van Tam, T., Monson, T. A., Marshall, S. A., & Warshauer, D. M. (2009). Comparison of cefoxitin and oxacillin disk diffusion methods for detection of mecA-mediated resistance in *staphylococcus aureus* in a large-scale study. *Journal of Clinical Microbiology*, 47(1), 217–219. https://doi.org/10.1128/JCM.01506-08

Buchy, P., Ascioglu, S., Buisson, Y., Datta, S., Nissen, M., Tambyah, P. A., & Vong, S. (2020). Impact of vaccines on antimicrobial resistance. *International Journal of Infectious Diseases*, 90, 188–196. https://doi.org/10.1016/j.ijid.2019.10.005

Bush, K. (2004). Antibacterial drug discovery in the 21st century. *Clinical Microbiology and Infection*, 10(4), 10–17. https://doi.org/10.1111/j.1465-0691.2004.1005.x

Chand, M., Kaushik, R., & chand jain, s. (2018). synthesis and antimicrobial and antioxidant activities of hybrid molecules containing benzotriazole and 1,2,4-triazole. *TurkishJournal of Chemistry*, 42(6), 1663–1677. https://doi.org/10.3906/kim-1803-61

Collin, f., karkare, s., & maxwell, a. (2011). exploiting bacterial dna gyrase as a drug target: current state and perspectives. *Applied Microbiology and Biotechnology*, 92(3), 479–497.

Conn, J. E., Grillet, M. E., Correa, M., & Sallum, M. A. M. (2018). Malaria transmission in South America present status and prospects for elimination. *Towards Malaria Elimination*

Curran, D. P., Hadida, S., & Kim, S. Y. (1999). tris(2-Perfluorohexylethyl)tin azide: A new reagent for preparation of 5-substituted tetrazoles from nitriles with purification by fluorous/organic liquid-liquid extraction. *Tetrahedron Letters*, 55(29), 8997–9006. https://doi.org/10.1016/S0040-

4020(99)00458-5

Daina, A., Michielin, O., & Zoete, V. (2017). SwissADME : a free web tool to evaluate pharmacokinetics , drug- likeness and medicinal chemistry friendliness of small molecules. *Nature Publishing Group, January*, 1–13. https://doi.org/10.1038/srep42717

De Ruyck, J., Brysbaert, G., Blossey, R., & Lensink, M. F. (2016). Molecular docking as a popular tool in drug design, an *in silico* travel. *Advances and Applications in Bioinformatics and Chemistry*, 9(1), 1–11. https://doi.org/10.2147/AABC.S105289

Demko, Z. P., & Sharpless, K. B. (2002). Sharpless amino to tetrazole. *Journal of Organic Letters* 23(40).

Dighe, S. N., Jain, K. S., & Srinivasan, K. V. (2009). A novel synthesis of 1-aryl tetrazoles promoted by employing the synergy of the combined use of DMSO and an ionic liquid as the solvent system at ambient temperature. *Tetrahedron Letters*, 50(45), 6139–6142.

Drwal, M. N., Banerjee, P., Dunkel, M., Wettig, M. R., & Preissner, R. (2014). ProTox: A web server for the *in silico* prediction of rodent oral toxicity. *Nucleic Acids Research*, 42(W1), 3–8. https://doi.org/10.1093/nar/gku401

Elsadek, M. F., Ahmed, B. M., & Farahat, M. F. (2021). An overview on synthetic 2-aminothiazole-based compounds. *Molecule*, 26(5), 1449.

Garofalo, A., Goossens, L., Six, P., Lemoine, Farce, A., & Depreux, P. (2011). Impact of aryloxy-linked quinazolines: A novel series of selective VEGFR-2 receptor tyrosine kinase inhibitors. *Bioorganic and Medicinal Chemistry Letters*, 21(7), 2106–2112.

Geronikaki, A. A., Dearden, J. C., Filimonov, D., Galaeva, I., Garibova, T. L., Gloriozova, T., Krajneva, V., Lagunin, A., Macaev, F. Z., Molodavkin, G., Poroikov, V. V., Pogrebnoi, S. I., Shepeli, F., Voronina, T. A., Tsitlakidou, M., & Vlad, L. (2004). Design of new cognition enhancers: From computer prediction to synthesis and biological evaluation. *Journal of Medicinal Chemistry*, 47(11), 2870–2876. https://doi.org/10.1021/jm031086k

Gharamaleki, J. A., Bolouhari, H. S., Goodarzi, A., Javadi, A., & Notash, B. (2016). A novel Schiff base ligand and its Ni(II) complex: Synthesis and characterization. *Monatshefte Fur Chemie*, 147(12), 2073–2081. https://doi.org/10.1007/s00706-016-1727-5

Halder, M., Islam, M. M., Singh, P., Singha Roy, A., Islam, S. M., & Sen, K. (2018). Sustainable Generation of $Ni(OH)_2$ Nanoparticles for the green synthesis of 5-substituted 1 *H*-tetrazoles: A competent turn on fluorescence sensing of H_2O_2. *Journal of the American Chemical Society*,

3(7), 8169–8180.

Heravi, M. M., & Zadsirjan, V. (2020). Prescribed drugs containing nitrogen heterocycles: an overview. *RSC Advances*, 10(72), 44247–44311. https://doi.org/10.1039/d0ra09198g

Hollenberg, P. F. (2002). Characteristics and common properties of inhibitors, inducers, and activators of CYP enzymes. *Drug Metabolism Reviews*, 34(1–2), 17–35.

Hoti, R., Ismaili, H., Troni, N., Vehapi, I., Pllana, M., & Thaci, V. (2017). Synthesis of some new 4-(benzothiazolylamino)-pyran-2-one derivatives a nd their antibacterial activity. *European Chemical Bulletin*, 6(5), 196. https://doi.org/10.17628/ecb.2017.6.196-200

Huang, S. M., Strong, J. M., Zhang, L., Reynolds, K. S., Nallani, S., Temple, R., Abraham, S., Al Habet, S., Baweja, R. K., Burckart, G. J., Chung, S., Colangelo, P., Frucht, D., Green, M. D., Hepp, P., Karnaukhova, E., Ko, H. S., Lee, J. I., Marroum, P. J., … Lesko, L. J. (2008). New era in drug interaction evaluation: US food and drug Administration update on CYP enzymes, transporters, and the guidance process. *Journal of Clinical Pharmacology*, 48(6), 662–670. https://doi.org/10.1177/0091270007312153

Hussain, Z., Yousif, E., Ahmed, A., & Altaie, A. (2014). Synthesis and characterization of Schiff's bases of sulfamethoxazole. *Organic and Medicinal Chemistry Letters*, 4(1), 1.

Irfan, A., Batool, F., Zahra Naqvi, S. A., Islam, A., Osman, S. M., Nocentini, A., Alissa, S. A., & Supuran, C. T. (2020). Benzothiazole derivatives as anticancer agents. *Journal of Enzyme Inhibition and Medicinal Chemistry*, 35(1), 265–279.

Ishihara, K., Kawashima, M., Matsumoto, T., Shioiri, T., & Matsugi, M. (2018). A Practical synthesis of 5-substituted 1*H*- tetrazoles from aldoximes employing the azide anion from diphenyl phosphorazidate. *Synthesis Letters* 50(6), 1293–1300.

Ishihara, K., Shioiri, T., & Matsugi, M. (2019). Stereospecific synthesis of 1,5-disubstituted tetrazoles from ketoximes via a Beckmann rearrangement facilitated by diphenyl phosphorazidate. *Tetrahedron Letters*, 60(18), 1295–1298.

Ismael, M., Abdel-Mawgoud, A. M. M., Rabia, M. K., & Abdou, A. (2020). Design and synthesis of three Fe(III) mixed-ligand complexes: Exploration of their biological and phenoxazinone synthase-like activities. *Inorganica Chimica Acta*, *505*, 119-443.

Jedhe, G. S., Paul, D., Gonnade, R. G., Santra, M. K., & Hamel. (2013). Correlation of hydrogen-bonding propensity and anticancer profile of tetrazole-tethered combretastatin analogues. *Bioorganic and Medicinal Chemistry Letters*, 23(16), 4680–4684.

Kalkhambkar, R. G., Kulkarni, G. M., Shivkumar, H., & Rao, R. N. (2007). Synthesis of novel triheterocyclic thiazoles as anti-inflammatory and analgesic agents. *European Journal of Medicinal Chemistry*, 42(10), 1272–1276. https://doi.org/10.1016/j.ejmech.2007.01.023

Karaghiosoff, K., Klapo, T. M., & Mayer, P. (2006). Synthesis of aminotetrazoles. *Journal of Chemistry*, 1295–1305.

Karthikeyan, M. S. (2009). Synthesis, analgesic, anti-inflammatory and antimicrobial studies of 2,4-dichloro-5-fluorophenyl containing thiazolotriazoles. *European Journal of Medicinal Chemistry*, 44(2), 827–833. https://doi.org/10.1016/j.ejmech.2008.04.022

Katritzky, A. R., Dennis Hall, C., El-Gendy, B. E. D. M., & Draghici, B. (2010). Tautomerism in drug discovery. *Journal of Computer-Aided Molecular Design*, 24(6–7), 475–484.

Kaushik, N., Kumar, N., Kumar, A., & Singh, U. K. (2018). Synthesis and biological activity of tetrazoles: *Immunology, Endocrine & Metabolic Agents in Medicinal Chemistry*, 18(1), 3–21. https://doi.org/10.2174/1871522218666180525100850

Kerru, N., Gummidi, L., Maddila, S., Gangu, K. K., & Jonnalagadda, S. B. (2020). A review on recent advances in nitrogen-containing molecules and their biological applications. *Molecules*, 25(8). https://doi.org/10.3390/molecules25081909

Khandar, A. A., Hosseini-Yazdi, S. A., & Zarei, S. A. (2005). Synthesis, characterization and X-ray crystal structures of copper(II) and nickel(II) complexes with potentially hexadentate Schiff base ligands. *Inorganica Chimica Acta*, 358(11), 3211–3217.

Kirchmair, J., Göller, A. H., Lang, D., Kunze, J., Testa, B., Wilson, I. D., Glen, R. C., & Schneider, G. (2015). Predicting drug metabolism: Experiment and/or computation *Nature Reviews Drug Discovery*, 14(6), 387–404. https://doi.org/10.1038/nrd4581

Koppireddi, S., Komsani, J. R., Avula, S., Pombala, S., Vasamsetti, S., Kotamraju, S., & Yadla, R. (2013). Novel 2-(2,4-dioxo-1,3-thiazolidin-5-yl)acetamides as antioxidant and/or anti-inflammatory compounds. *European Journal of Medicinal Chemistry*, 66, 305–313.

Kumar, A., Rajput, C. S., & Bhati, S. K. (2007). Synthesis of 3-[4′-(*p*-chlorophenyl)-thiazol-2′-yl]-2-[(substituted azetidinone/thiazolidinone)-aminomethyl]-6-bromoquinazolin-4-ones as anti-inflammatory agent. *Bioorganic and Medicinal Chemistry*, 15(8), 3089–3096.

Kurutas, E. B. (2016). The importance of antioxidants which play the role in cellular response against oxidative/nitrosative stress: *Journal* of *Nutritional Chemistry*, 15(1), 1–22.

Łączkowski, K. Z., Konklewska, N., Biernasiuk, A., Malm, A., Sałat, K., Furgała, A., Dzitko, K.,

Bekier, A., Baranowska-Łączkowska, A., & Paneth, A. (2018). Thiazoles with cyclopropyl fragment as antifungal, anticonvulsant, and anti-toxoplasma gondii agents: synthesis, toxicity evaluation, and molecular docking study. *Medicinal Chemistry Research*, 27(9), 2125–2140. https://doi.org/10.1007/s00044-018-2221-x

Lade, H., & Kim, J. S. (2021). Bacterial targets of antibiotics in methicillin-resistant *staphylococcus aureus*. *Antibiotics*, 10(4). https://doi.org/10.3390/antibiotics10040398

Lakshmi Kantam, M., Shiva Kumar, K. B., & Sridhar, C. (2005). Nanocrystalline ZnO as an efficient heterogeneous catalyst for the synthesis of 5-substituted 1*H*-tetrazoles. *Advanced Synthesis and Catalysis*, 347(9), 1212–1214. https://doi.org/10.1002/adsc.200505011

Lin, X., Li, X., & Lin, X. (2020). A review on applications of computational methods in drug screening and design. *Molecules*, 25(6), 1–17. https://doi.org/10.3390/molecules25061375

Lipinski, C. A., Lombardo, F., Dominy, B. W., & Feeney, P. J. (2012). Experimental and computational approaches to estimate solubility and permeability in drug discovery and development settings. *Advanced Drug Delivery Reviews*, 64(30), 4–17.

Lobo, V., Patil, A., Phatak, A., & Chandra, N. (2010). Free radicals, antioxidants and functional foods: *Pharmacognosy Reviews*, *4*(8), 118–126.

Madni, M., Hameed, S., Ahmed, M. N., Tahir, M. N., Al-Masoudi, N. A., & Pannecouque, C. (2017). Synthesis, crystal structure, anti-HIV, and antiproliferative activity of new pyrazolylthiazole derivatives. *Medicinal Chemistry Research*, 26(10), 2653–2665. https://doi.org/10.1007/s00044-017-1963-1

Malik, M. A., Dar, O. A., Gull, P., Wani, M. Y., & Hashmi, A. A. (2018). Heterocyclic Schiff base transition metal complexes in antimicrobial and anticancer chemotherapy. *MedChemComm*, *9*(3), 409–436. https://doi.org/10.1039/c7md00526a

Marella, A., Verma, G., Shaquiquzzaman, M., Akhter, M., & Alam, M. (2014). Malaria: Hitches and Hopes. *Mini-Reviews in Medicinal Chemistry*, 14(5), 453–470.

Mohammad, H., Mayhoub, A. S., Cushman, M., & Seleem, M. N. (2015). Anti-biofilm activity and synergism of novel thiazole compounds with glycopeptide antibiotics against multidrug-resistant *Staphylococci*. *Journal of Antibiotics*, 68(4), 259–266. https://doi.org/10.1038/ja.2014.142

Mohammadkhani, L., & Heravi, M. M. (2020). Synthesis of N-heterocycles containing 1,5-disubstituted-1*H*-tetrazole via post-Ugi-azide reaction. *Molecular Diversity*, 24(3), 841–853. https://doi.org/10.1007/s11030-019-09972-1

Mohareb, R. M., Ahmed, H. H., Elmegeed, G. A., Abd-Elhalim, M. M., & Shafic, R. W. (2011). Development of new indole-derived neuroprotective agents. *Bioorganic and Medicinal Chemistry*, 19(9), 2966–2974. https://doi.org/10.1016/j.bmc.2011.03.031

Motiwala, H. F., Charaschanya, M., Day, V. W., & Aubé, J. (2016). Remodeling and enhancing Schmidt reaction pathways in hexafluoroisopropanol. *Journal of Organic Chemistry*, 81(4), 1593–1609. https://doi.org/10.1021/acs.joc.5b02764

Mukhia, R., Basistha, B., & Chhetri, D. R. (2018). Variation in antioxidant activity of a rattan species, *plectocomia himalayana griff.* by DPPH assay based on two different methods of methanol extraction. *Research Journal of Pharmacognosy and Phytochemistry*, 10(2), 175. https://doi.org/10.5958/0975-4385.2018.00027.4

Murumkar, P. R., & Chikhale, R. V. (2018). Vicinal diaryl triazoles and tetrazoles. *Vicinal Diaryl Substituted Heterocycles*, 191–219. https://doi.org/10.1016/b978-0-08-102237-5.00006-7

Myznikov, L. V., Hrabalek, A., & Koldobskii, G. I. (2007). Drugs in the tetrazole series. C*hemistry of Heterocyclic Compounds*, 43(1), 1–9. https://doi.org/10.1007/s10593-007-0001-5

Nepali, K., Lee, H. Y., & Liou, J. P. (2019). Nitro-group-containing drugs. *Journal of Medicinal Chemistry*, 62(6), 2851–2893.

Nessim, M. I., Elewa, S. I., & Mohamed, M. G. (2018). Synthesis and study antimicrobial activities of some novel tetrazole derivatives. *Egyptian Journal of Chemistry*, 61(1), 197–206.

Obadahun, J., Agho, O. B., Dike, R. C., Ojeleye, F. S., Akabuogu, E. P., Omotola, M. B., & Jakheng, S. P. E. (2020). Synthesis , characterization and *in -vitro* antimicrobial activities of a Schiff base derived from benzaldehyde with nitroaniline and their cobalt (ii) and nickel (ii) metal complexes. *VII*(Xii), 11–16.

Ommenya, F. K., Nyawade, E. A., Andala, D. M., & Kinyua, J. (2020). Synthesis, characterization and antibacterial activity of Schiff base, 4-chloro-2-{(e)-[(4-fluorophenyl)imino]methyl}phenol metal (ii) complexes. *Journal of Chemistry*.

Palanimurugan, A., & Kulandaisamy, A. (2018). DNA, *in vitro* antimicrobial/anticancer activities and biocidal based statistical analysis of Schiff base metal complexes derived from salicylalidene-4-imino-2,3-dimethyl-1-phenyl-3-pyrazolin-5-one and 2-aminothiazole. *Journal of Organometallic Chemistry*, 861, 263–274. https://doi.org/10.1016/j.jorganchem.2018.02.051

Palimkar, S. S., Siddiqui, S. A., Daniel, T., Lahoti, R. J., & Srinivasan, K. V. (2003). Ionic liquid-promoted regiospecific friedlander annulation: novel synthesis of quinolines and fused

polycyclic quinolines. *Journal of Organic Chemistry*, 68(24), 9371–9378.

Patil, U. B., Kumthekar, K. R., & Nagarkar, J. M. (2012). A novel method for the synthesis of 5-substituted 1*H*-tetrazole from oxime and sodium azide. *Tetrahedron Letters*, 53(29), 3706–3709. https://doi.org/10.1016/j.tetlet.2012.04.093

Pattan, S. R., Kekare, P., Patil, A., Nikalje, A., & Kittur, B. S. (2009). Studies on the synthesis of novel 2,4-thiazolidinedione derivatives with antidiabetic activity. *Iranian Journal of Pharmaceutical Sciences*, 5(4), 225–230.

Petrou, A., Fesatidou, M., & Geronikaki, A. (2021). Thiazole ring a biologically active scaffold. *Molecules*, 26(11), 3166.

Phaniendra, A., Jestadi, D. B., & Periyasamy, L. (2015). Free radicals: properties, sources, targets, and their implication in various diseases. *Indian Journal of Clinical Biochemistry*, 30(1), 11–26. https://doi.org/10.1007/s12291-014-0446-0

Piotto, S., Concilio, S., Sessa, L., Diana, R., Torrens, G., Juan, C., Caruso, U., & Iannelli, P. (2017). Synthesis and antimicrobial studies of new antibacterial azo-compounds active against *staphylococcus aureus* and listeria monocytogenes. *Molecules*, 22(8), 0–9.

Pola, S. (2016). Significance of thiazole-based heterocycles for bioactive systems. Scope of selective heterocycles from prganic and pharmaceutical perspective, 1–10.

Prakash, Karale, N. N., Lawand, A. S., Narang, N., & Patil, R. H. (2014). Synthesis and anti-biofilm activity of thiazole Schiff bases. *Medicinal Chemistry Research*, 23(2), 790–799.

Rajasekaran, A., & Thampi, P. P. (2004). Synthesis and analgesic evaluation of some 5-[*β*-(10-phenothiazinyl) ethyl]-1-(acyl)-1,2,3,4-tetrazoles. *European Journal of Medicinal Chemistry*, 39(3), 273–279. https://doi.org/10.1016/j.ejmech.2003.11.016

Remko, M. (2009). Theoretical study of molecular structure, pKa, lipophilicity, solubility, absorption, and polar surface area of some hypoglycemic agents. *Journal of Molecular Structure:* 897(1–3), 73–82. https://doi.org/10.1016/j.theochem.2008.11.021

Roberts, M. J., Arend, R. C., Samant, R. S., & Buchsbaum, D. J. (2014). Multi-targeted therapy of cancer by niclosamide: A new application for an old drug. *Cancer Letters*, 349(1), 8–14. https://doi.org/10.1016/j.canlet.2014.04.003

Roh, Jaroslav Karabanovich, G. (2017). Development of water-soluble 3,5-dinitrophenyl tetrazole and oxadiazole antitubercular agents. *Bioorganic and Medicinal Chemistry*, 25(20), 5468–5476. https://doi.org/10.1016/j.bmc.2017.08.010

Sadeghi, M., Moradi, M., Madanchi, H., & Johari, B. (2021). *In silico* study of garlic (*Allium sativum L.*)-derived compounds molecular interactions with *α*-glucosidase. *Journal of Pharmacology*, 9(1), 7–14. https://doi.org/10.1007/s40203-020-00072-9

Sakarya, H. C., Görgün, K., & Öğretir, C. (2016). Synthesis and characterization of novel substituted N-benzothiazole-2-yl-acetamides. *Arabian Journal of Chemistry*, *9*, S1314-S1319.

Salaria, D., Rolta, R., Sharma, N., Dev, K., Sourirajan, A., & Kumar, V. (2020). *In silico* and *In vitro* evaluation of the anti-inflammatory and antioxidant potential of *Cymbopogon citratus* from North-western Himalayas. *bioRxiv*.

Salas, E., Ramírez, A., Otero-Bilbao, A., Vázquez, R., Reyes, O., Mendiola, J., Duarte, C. A., Otero-González, A., Gutiérrez, O. A., & Chávez, M. A. (2004). A heterogeneous enzymatic assay for quantification of Plasmepsin II activity and the evaluation of its inhibitors. *Journal of Pharmaceutical and Biomedical Analysis*, 34(4), 833–840.

Shahbazali, E., Hessel, V., Noël, T., & Wang, Q. (2013). Metallic nanoparticles made in flow and their catalytic applications in organic synthesis. *Nanotechnology Reviews*, 3(1), 65–86.

Shaikh, Kamble, R. R., & Somagond, S. M. (2017). Tetrazolylmethyl quinolines: Design, docking studies, synthesis, anticancer and antifungal analyses. *European Journal of Medicinal Chemistry*, 128, 258–273. https://doi.org/10.1016/j.ejmech.2017.01.043

Sharma, P. K., Amin, A., & Kumar, M. (2020). Medicinally important nitrogen sulphur containing heterocycles. *Journal* of *Medicinal Chemistry* 14(1).

Sharma, P. C., Sinhmar, A., Sharma, A., Rajak, H., & Pathak, D. P. (2012). Medicinal significance of benzothiazole scaffold: *Journal of Enzyme Inhibition and Medicinal Chemistry*, 28(2), 240–266. https://doi.org/10.3109/14756366.2012.720572

Sharon, A., Pratap, R., & Tiwari, P. (2005). Synthesis and *in vivo* antihyperglycemic activity of 5-(1*H*-pyrazol-3-yl) methyl-1*H*-tetrazoles. *Bioorganic and Medicinal Chemistry Letters*, 15(8), 2115–2117. https://doi.org/10.1016/j.bmcl.2005.02.060

Shukla, P. K., Verma, A., & Mishra, P. (2017). Significance of nitrogen heterocyclic nuclei in the search of pharmacological active compounds. *New Perspective in Agricultural and Human Health;* 100-126.

Tamoradi, T., Ghorbani-Choghamarani, A., & Ghadermazi, M. (2017). Fe_3O_4-adenine-Zn: A novel, green, and magnetically recoverable catalyst for the synthesis of 5-substituted tetrazoles and oxidation of sulfur containing compounds. *New Journal of Chemistry*, 41(20), 11714–11721.

https://doi.org/10.1039/c7nj02337e

Tsuji, K., & Ishikawa, H. (1994). Synthesis and anti-pseudomonal activity of new 2-isocephems with a dihydroxypyridone moiety at C-7. *Bioorganic and Medicinal Chemistry Letters*, 4(13), 1601–1606. https://doi.org/10.1016/S0960-894X(01)80574-6

Villa, R., Alvarez, E., Porcar, R., Garcia-Verdugo, E., Luis, S. V., & Lozano, P. (2019). Ionic liquids as an enabling tool to integrate reaction and separation processes. *Green Chemistry*, 21(24), 6527-6544.

Wang, M., Wang, L. F., Li, Y. Z., Li, Q. X., Xu, Z. D., & Qu, D. M. (2001). Antitumour activity of transition metal complexes with the thiosemicarbazone derived from 3-acetylumbelliferone. *Transition Metal Chemistry*, 26(3), 307-310.

Vinusha, H. M., Prasad, S. K., Chandan, S., & Begum, M. (2015). Imino-4-methoxyphenol thiazole derived Schiff base ligands: synthesis, spectral characterization and antimicrobial activity. *Journa of Chemical Sciencesl*, 6(3), 1. https://doi.org/10.1023/A:1007159301849

Wang, Xing, J., Xu, Y., Zhou, N., Peng, J., Xiong, Z., Liu, X., Luo, X., Luo, C., Chen, K., Zheng, M., & Jiang, H. (2015). *In silico* ADME/T modelling for rational drug design. *Quarterly Reviews of Biophysics*, 48(4), 488–515. https://doi.org/10.1017/S0033583515000190

Wittenberger, S. J., Park, A., & Wittenberger, S. J. (2009). Recent developments in tetrazole chemistry. *Journal for Organic Synthesis* (22) 37–41.

Zhan, P., Li, Z., Liu, X., & De Clercq, E. (2012). Sulfanyltriazole/tetrazoles: A promising class of HIV-1 NNRTIs. *Jorunal of Medicinal Chemistry*, 9(8), 1014–1023.

LIST OF APPENDIX

Appendix 1:^{1}H NMR (400 MHz, DMSO-d_6) spectrum of compound **101.**

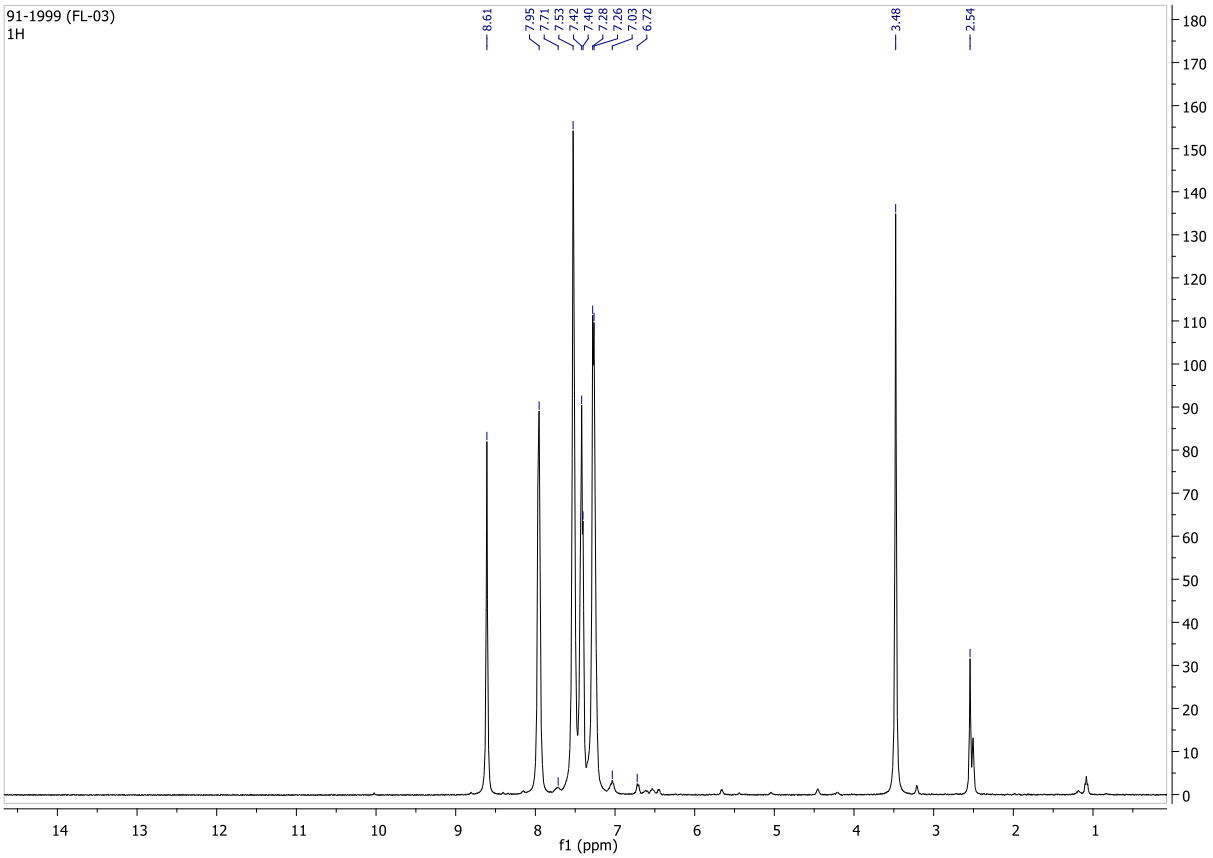

Appendix 2: ^{13}C NMR (100 MHz, DMSO-d_6) spectrum of compound **101**.

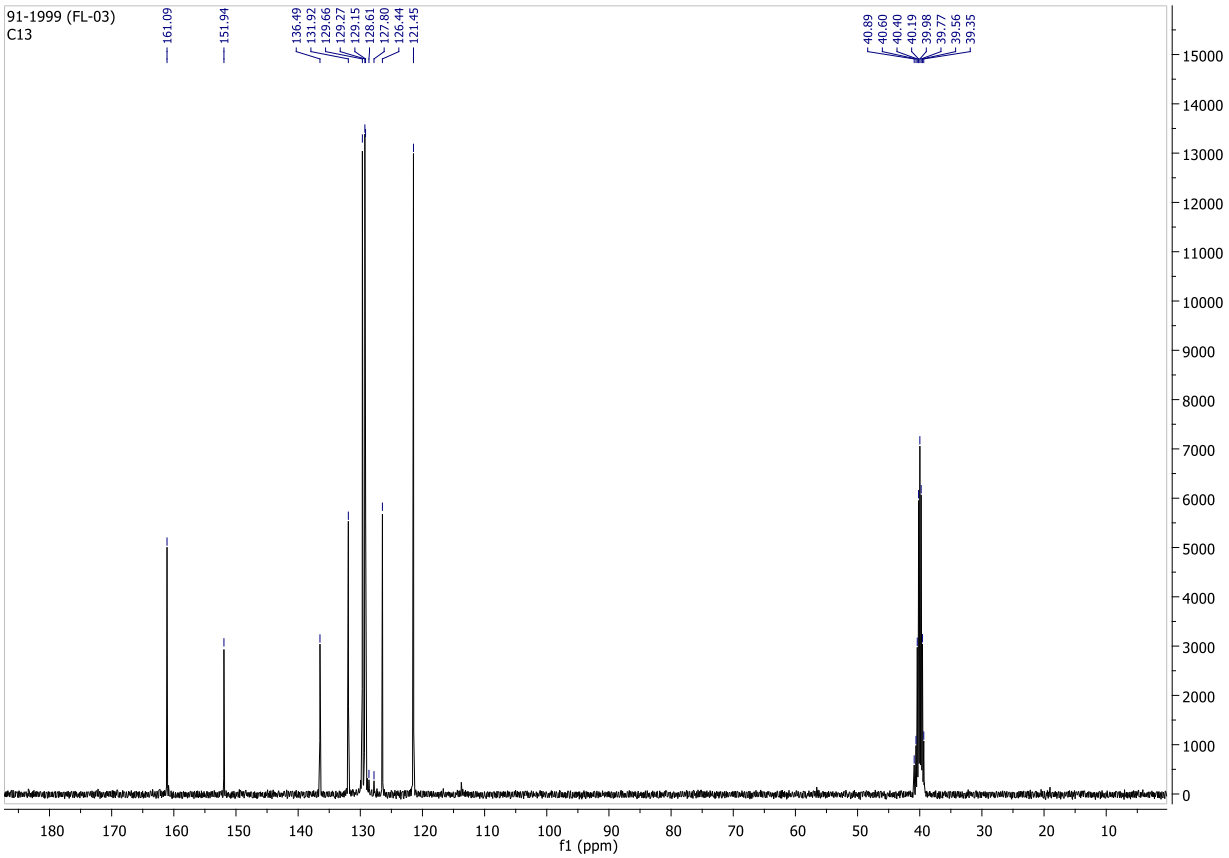

Appendix 3: DEPT-135 (100 MHz, DMSO-d_6) spectrum of compound **101**.

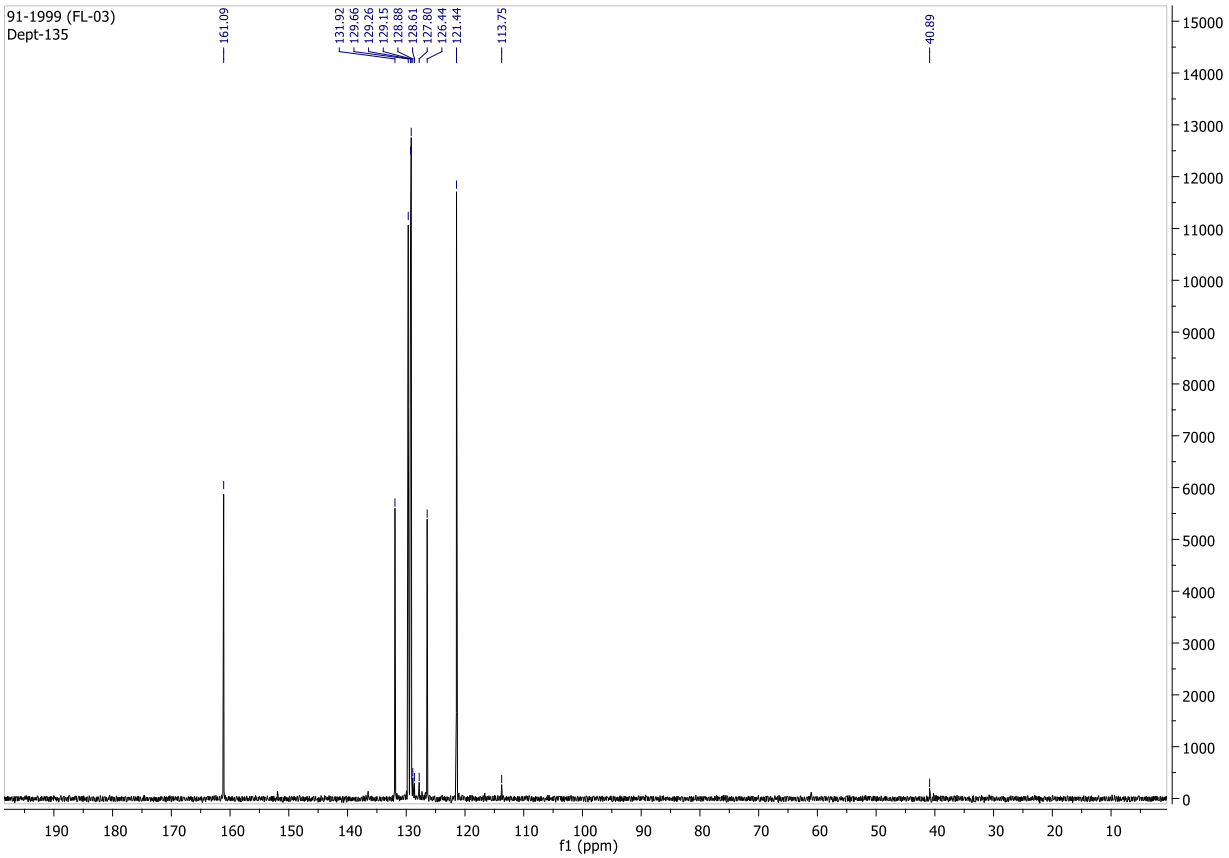

Appendix 4: ^{1}H NMR (400 MHz, DMSO-d_6 and $CDCl_3$) spectrum of compound **102**.

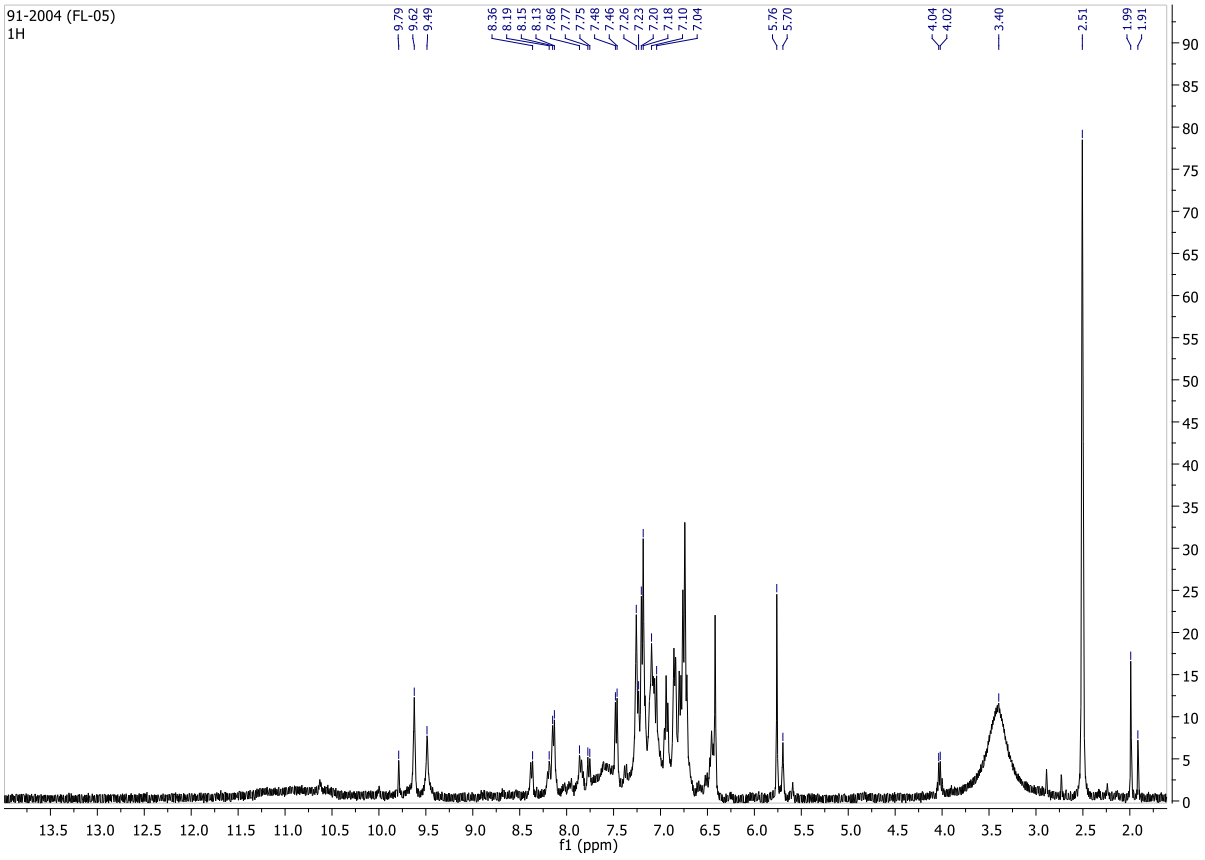

Appendix 5: ^{13}C NMR (100 MHz, DMSO-d_6 and $CDCl_3$) spectrum of compound **102.**

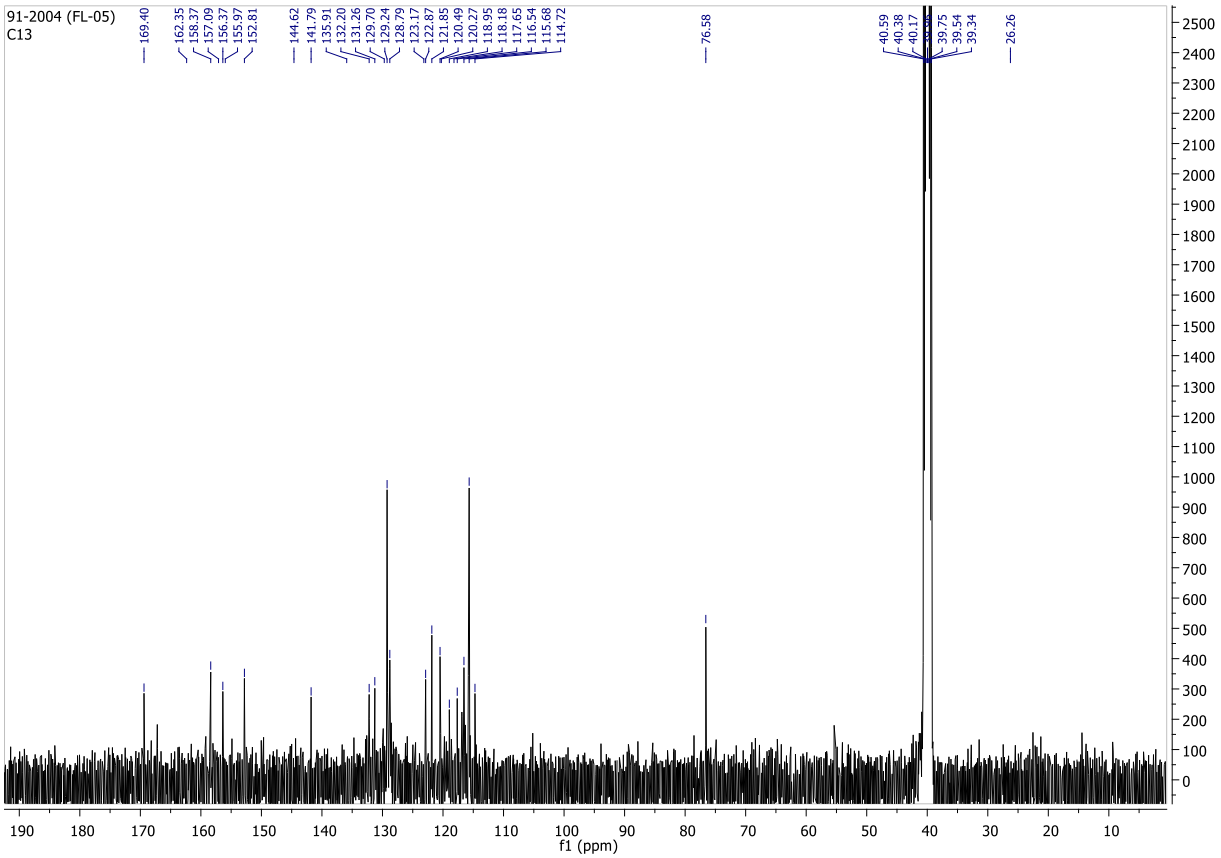

Appendix 6: DEPT-135 (100 MHz, DMSO-d_6 and $CDCl_3$) spectrum of compound **102**.

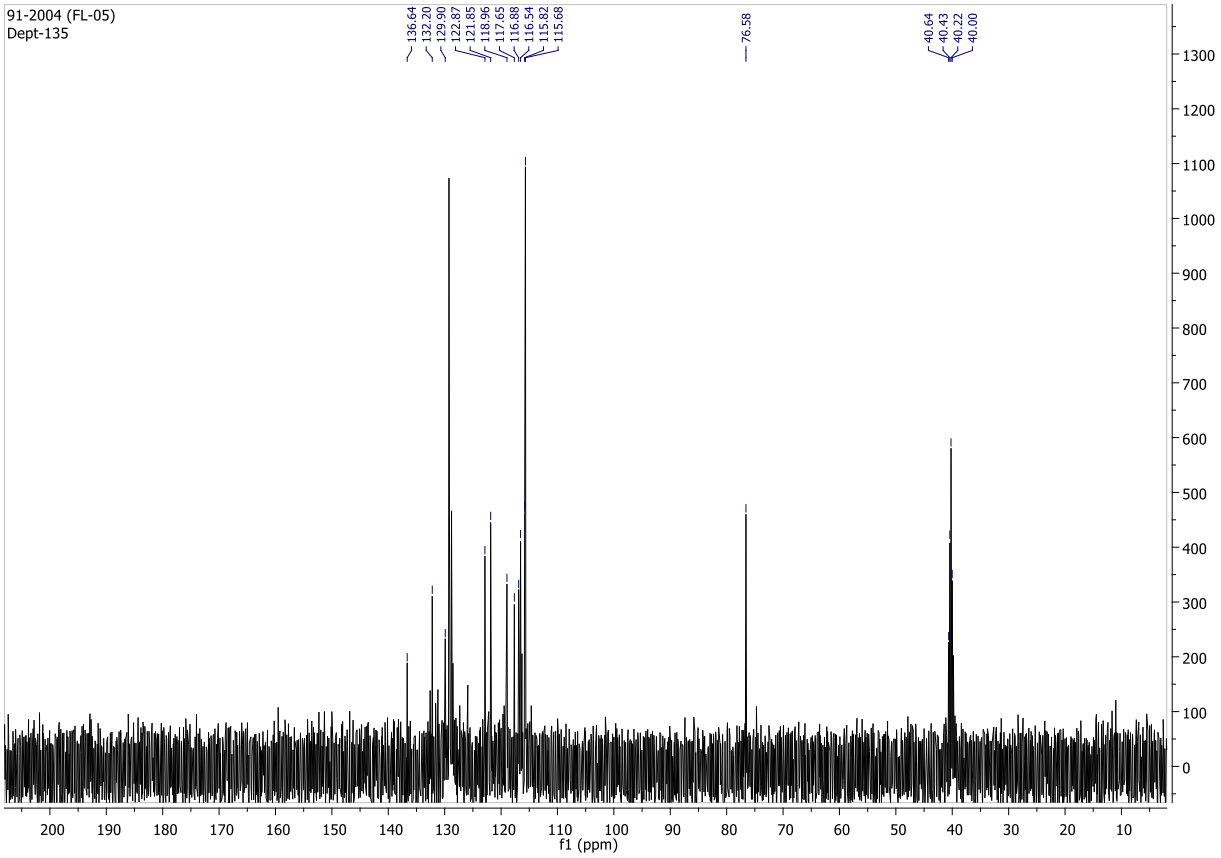

Appendix 7:^{1}H NMR (400 MHz, DMSO-d_6) spectrum of compound **103**.

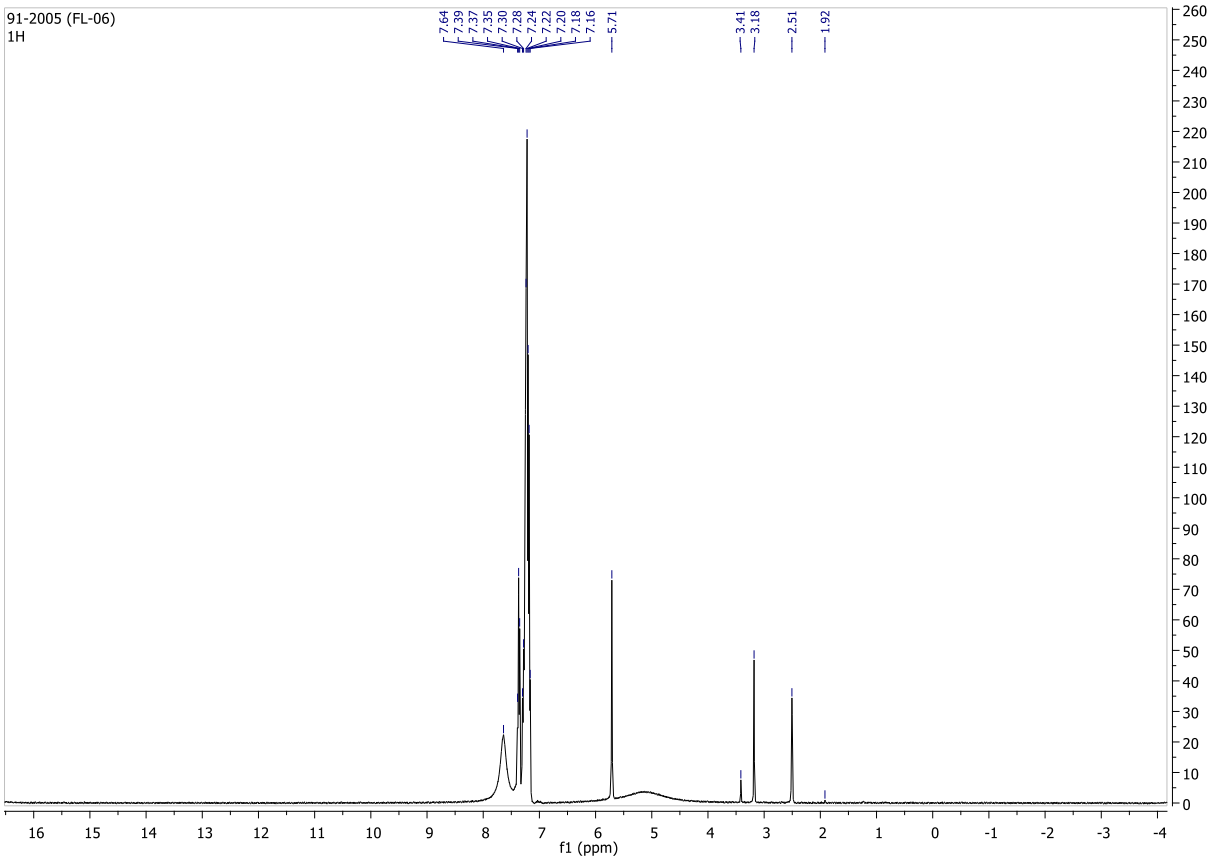

Appendix 8: ^{13}C NMR (100 MHz, DMSO-d_6) spectrum of compound **103**.

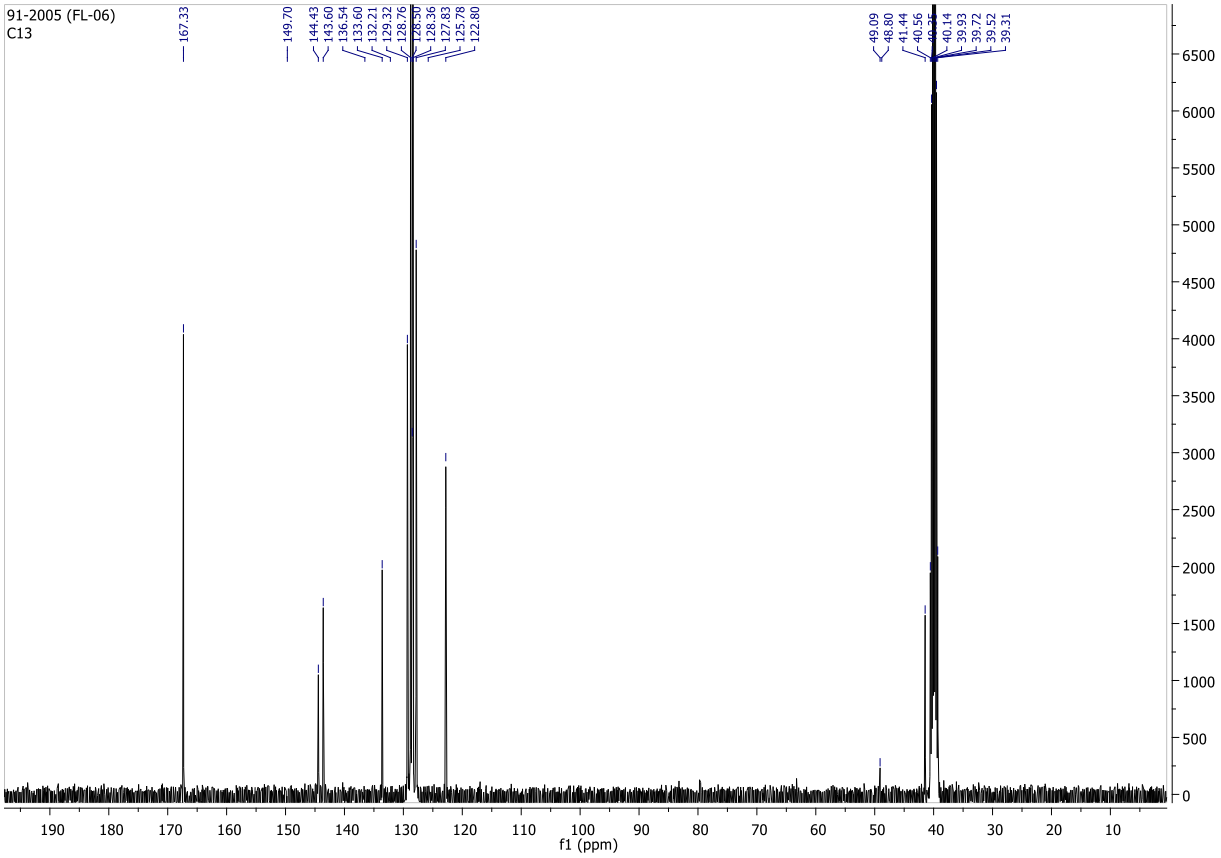

Appendix 9:DEPT-135 (100 MHz, DMSO-d_6) spectrum of compound **103**.

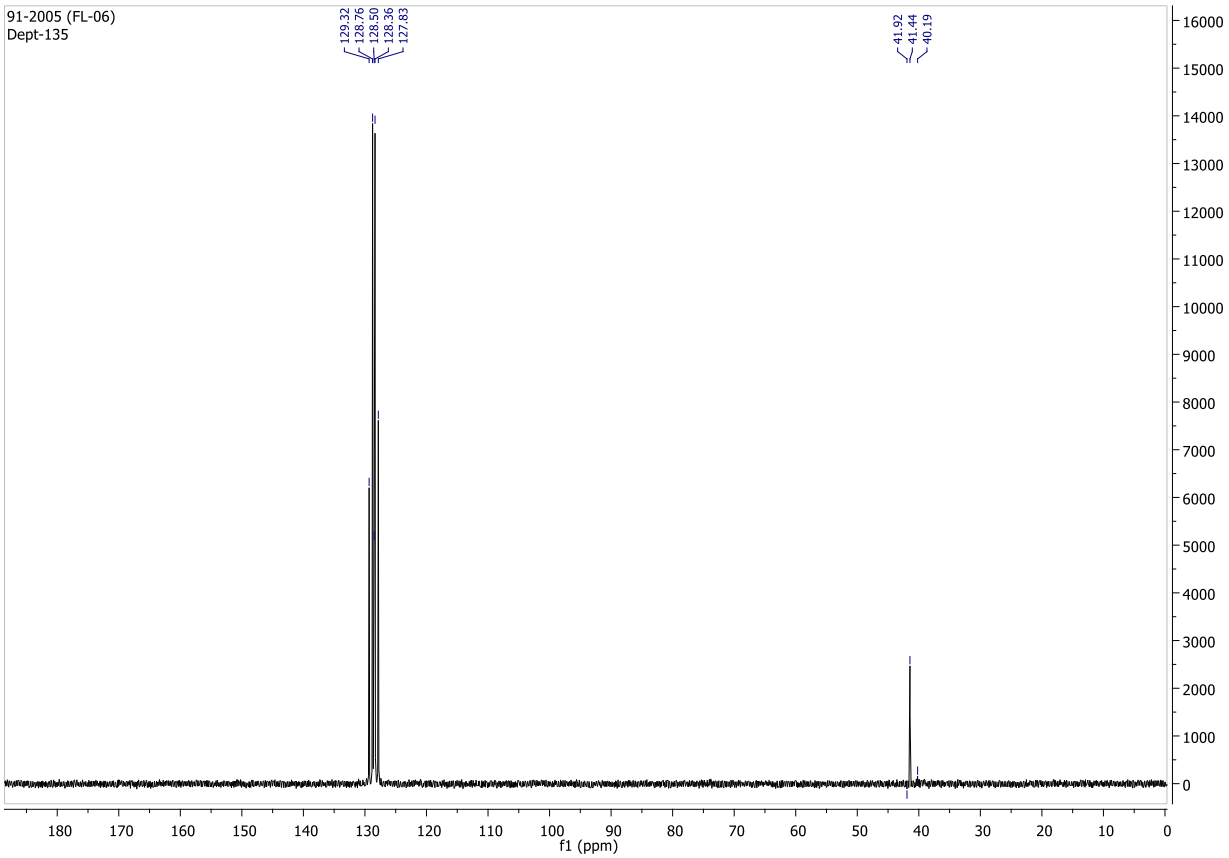

Appendix 10:[1]H NMR (400 MHz, DMSO-d_6) spectrum of compound **104**.

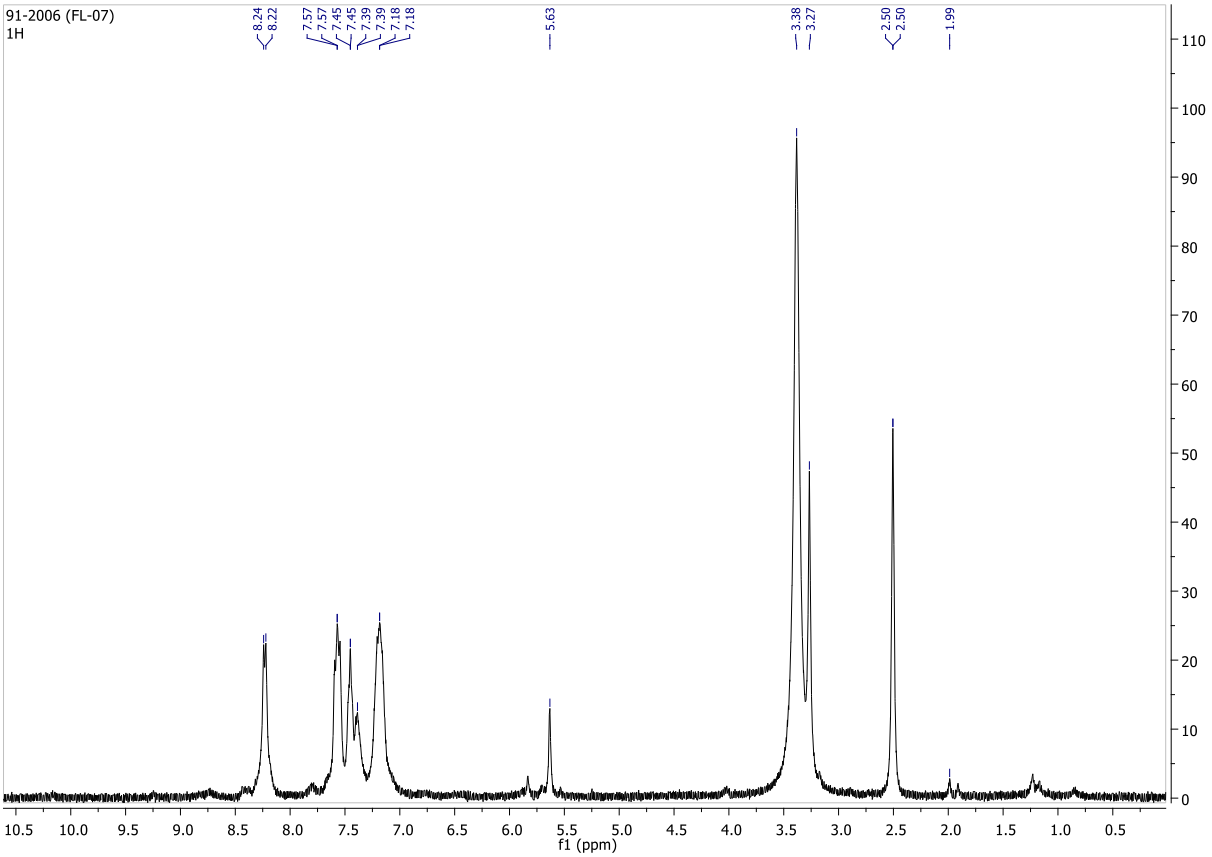

Appendix 11:^{13}C NMR (100 MHz, DMSO-d_6 and $CDCl_3$) spectrum of compound **104**.

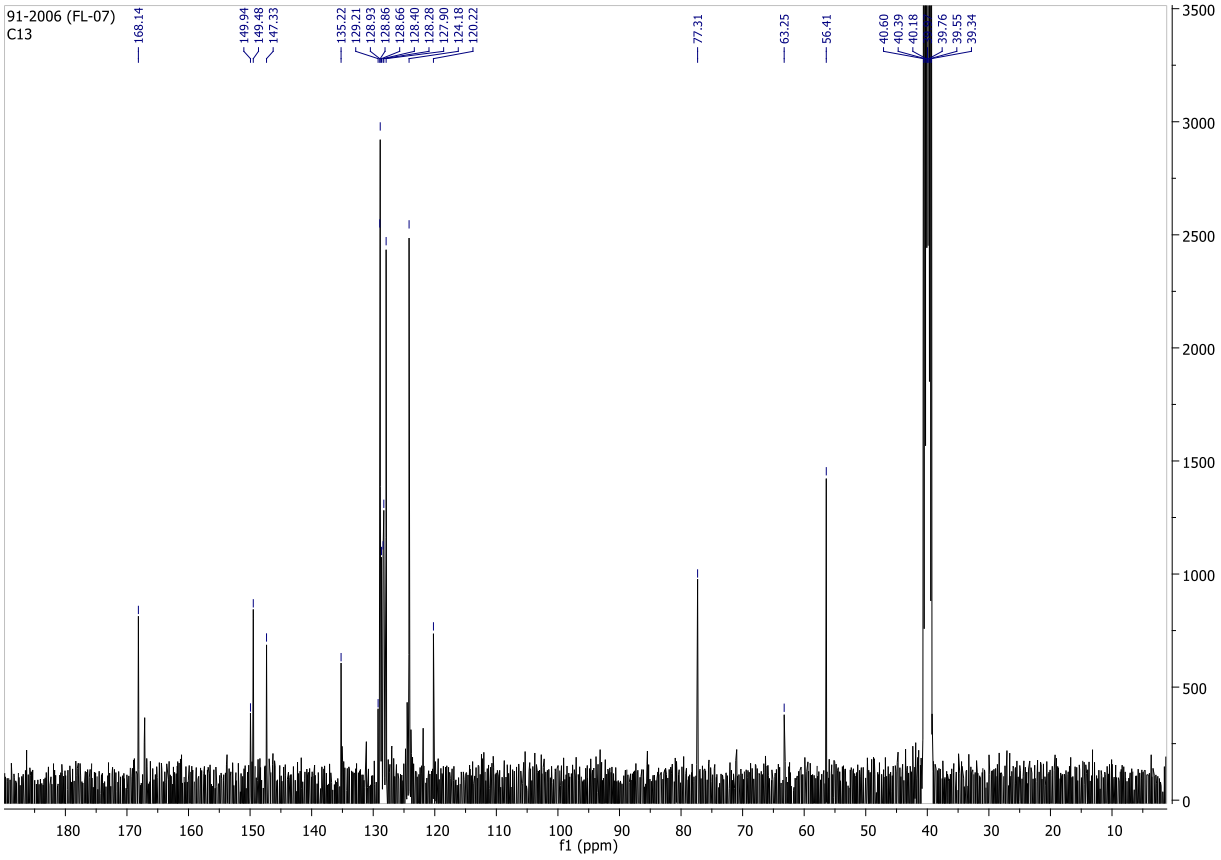

Appendix 12: DEPT-135 (100 MHz, DMSO-d_6 and $CDCl_3$) spectrum of compound **104**.

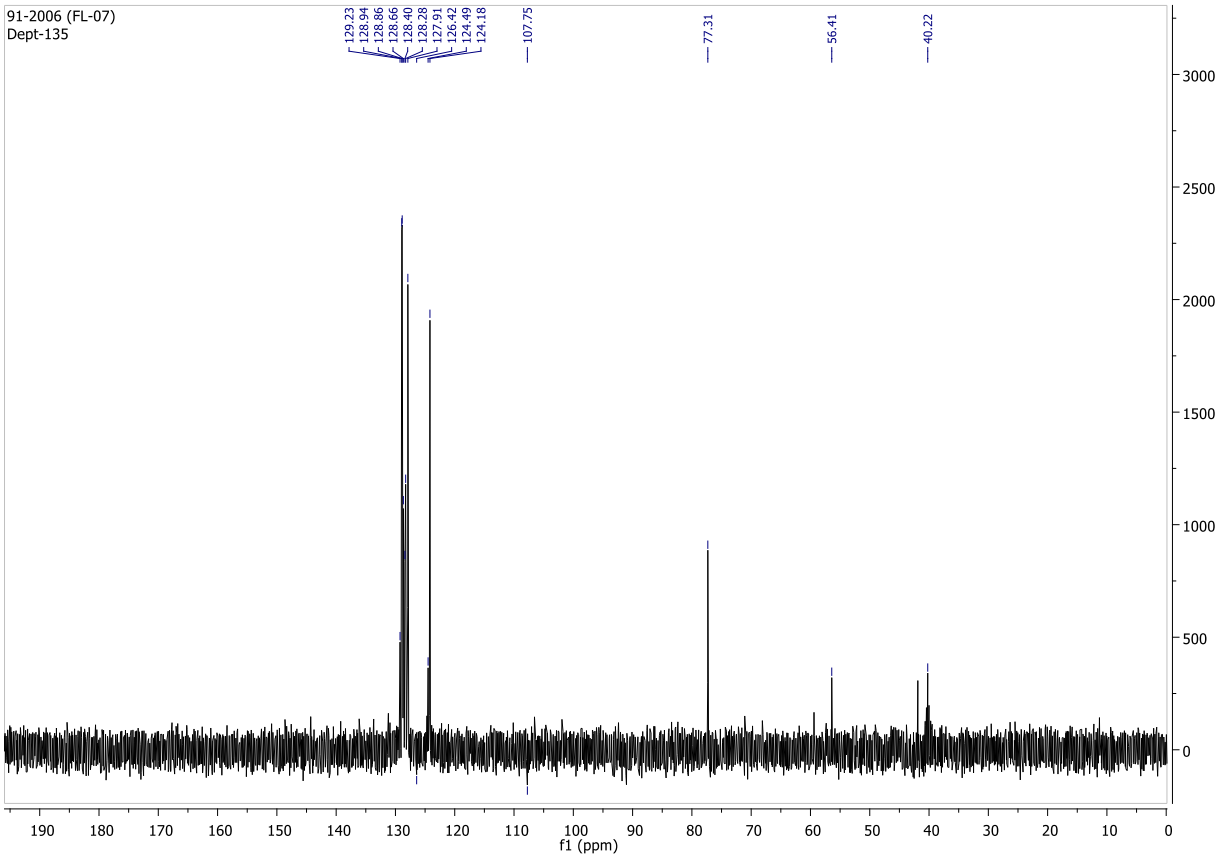

Appendix 13: ^{1}H NMR (400 MHz, DMSO-d_6 and $CDCl_3$) spectrum of compound **105**.

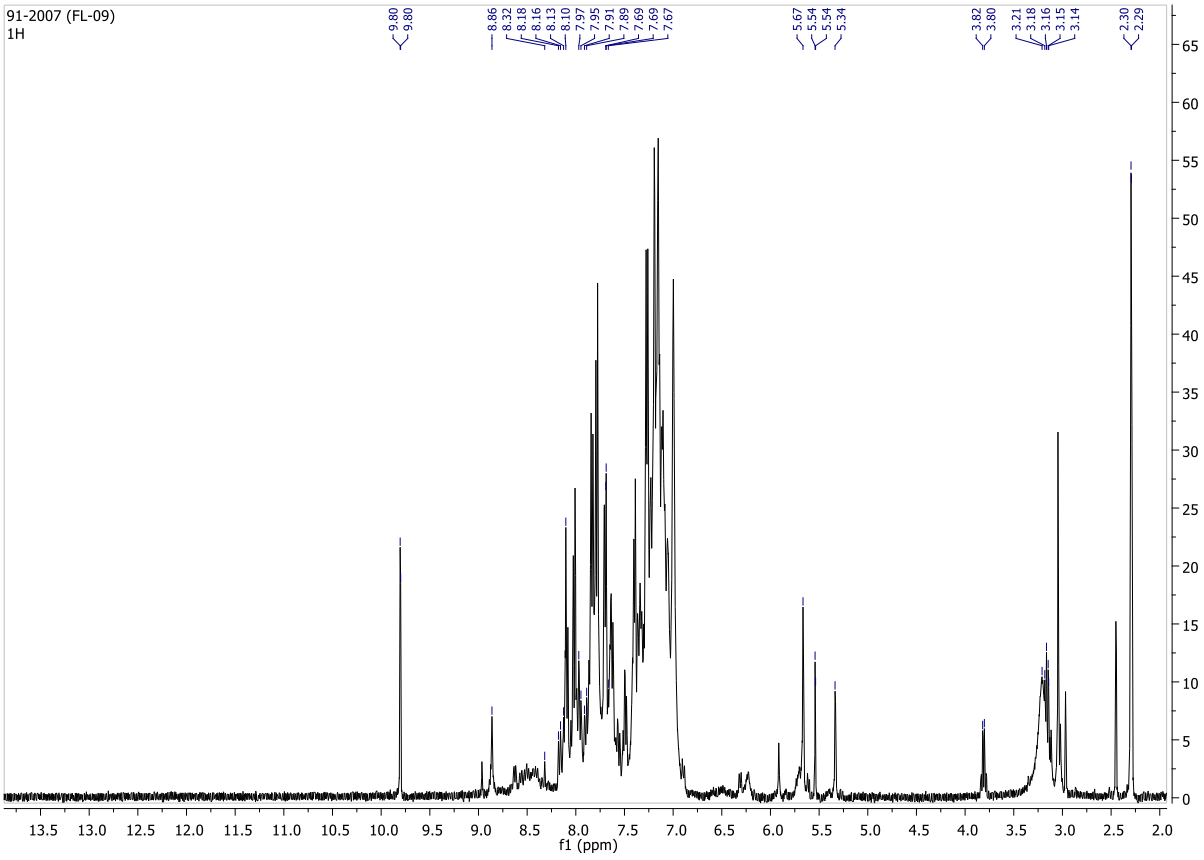

Appendix 14:^{13}C NMR (100 MHz, DMSO-d_6 and $CDCl_3$) spectrum of compound **105**.

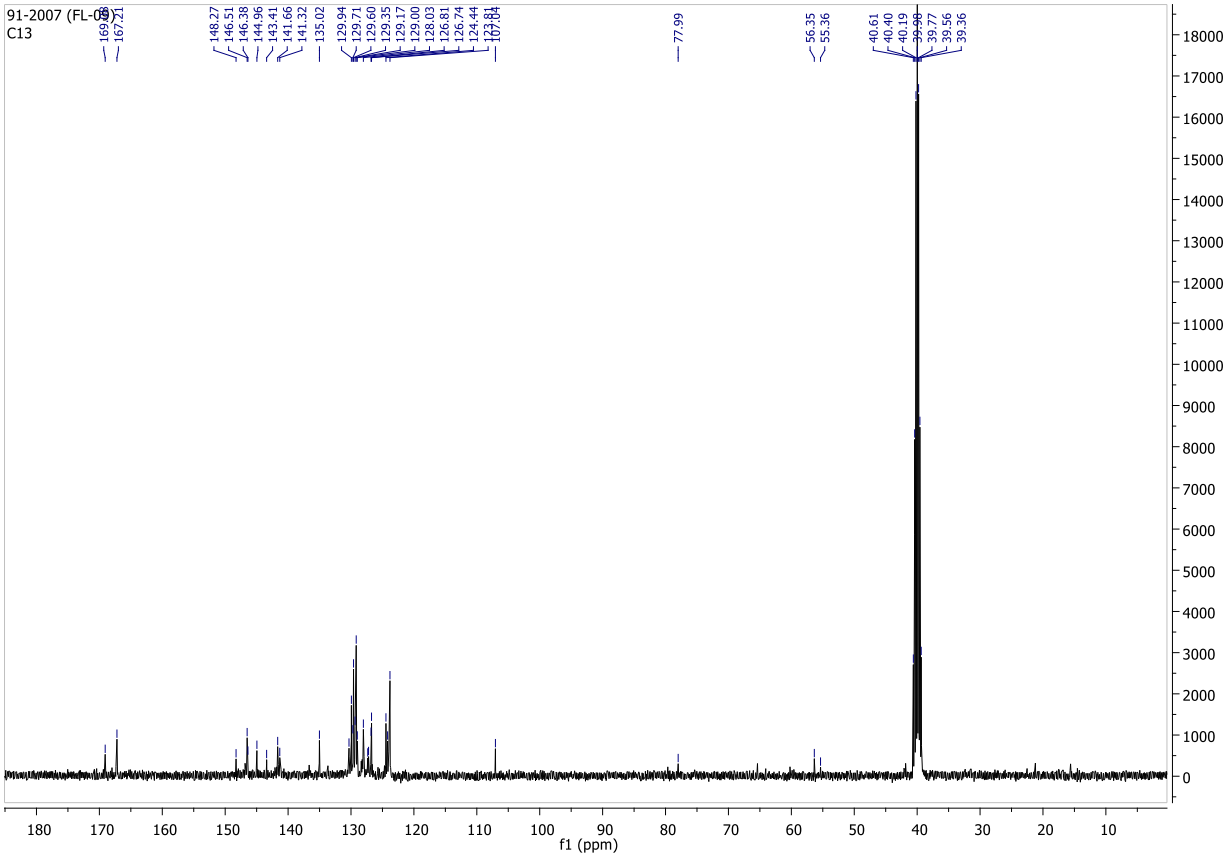

Appendix 15: DEPT-135 (100 MHz, DMSO-d_6 and $CDCl_3$) spectrum of compound **105**.

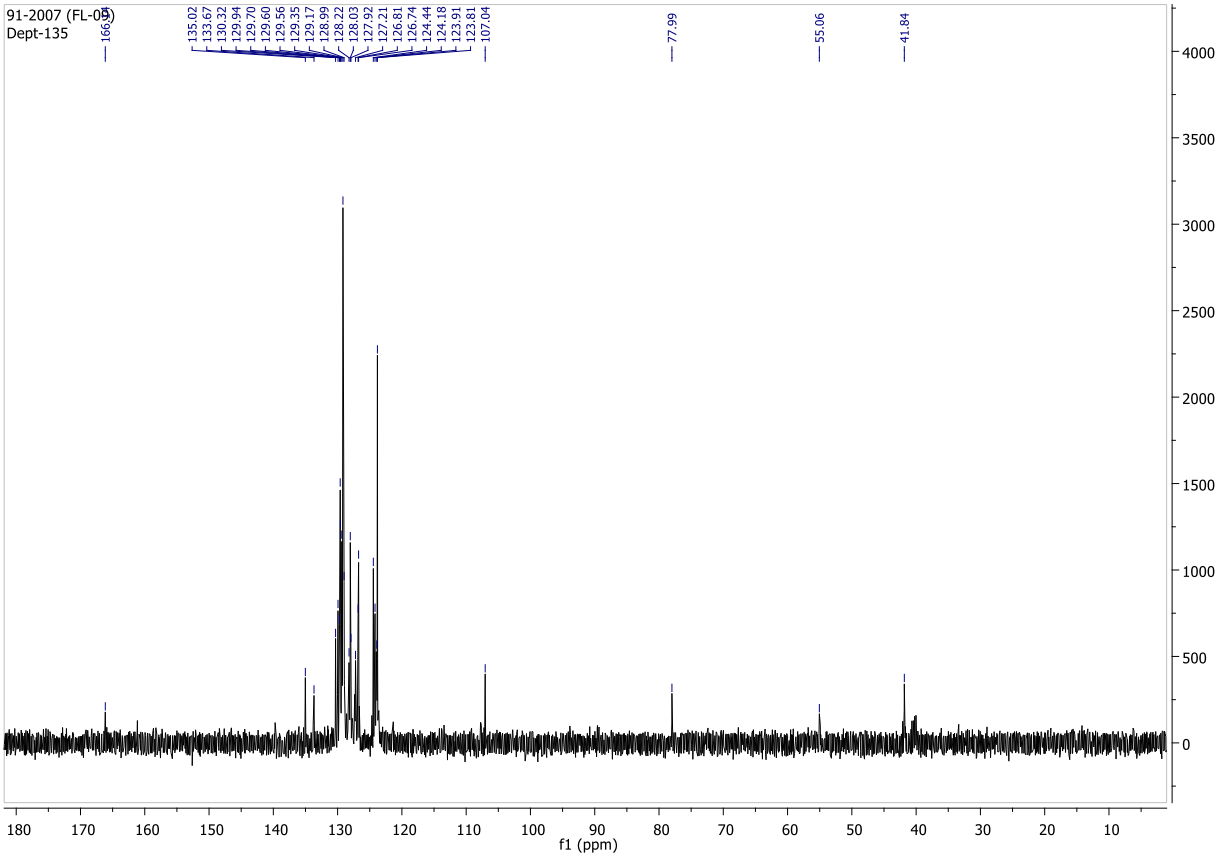

Appendix 16: ^{1}H NMR (400 MHz, DMSO-d_6) spectrum of compound **106**.

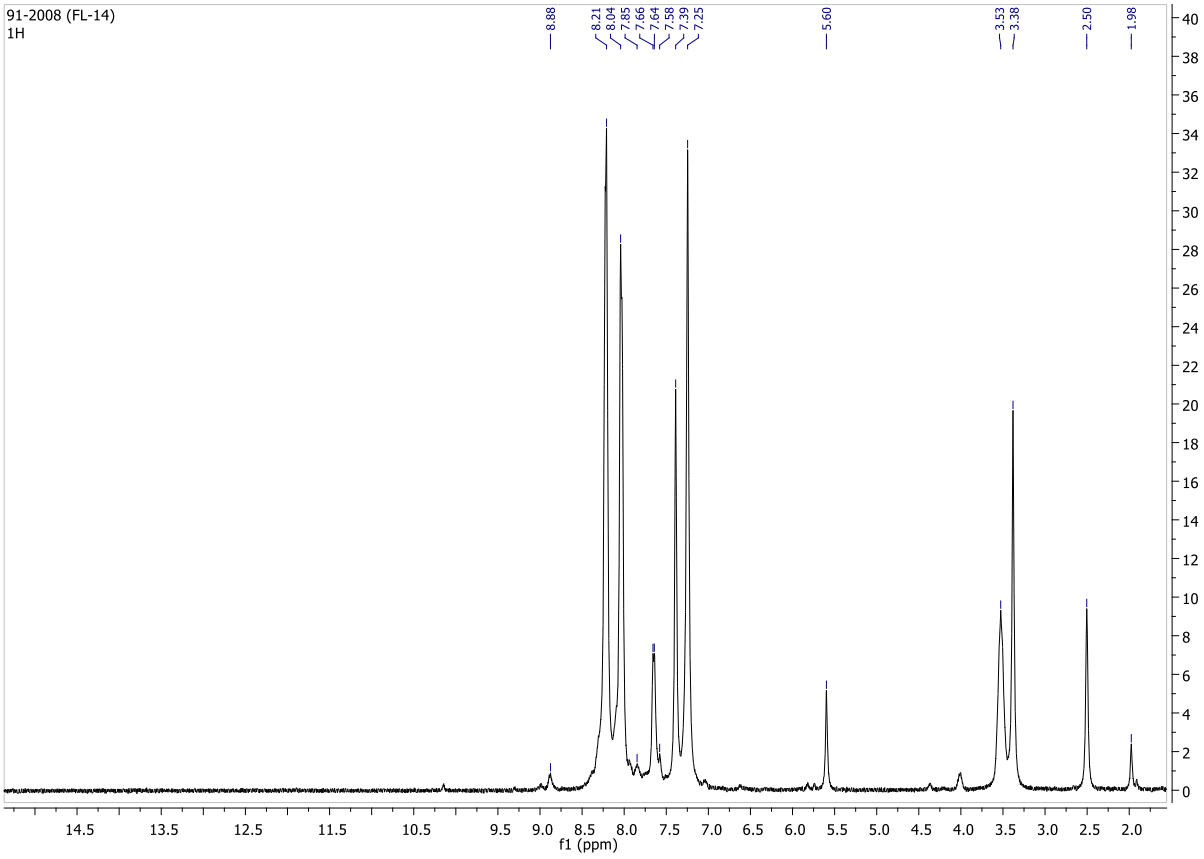

Appendix 17: ^{13}C NMR (100 MHz, DMSO-d_6) spectrum of compound **106**.

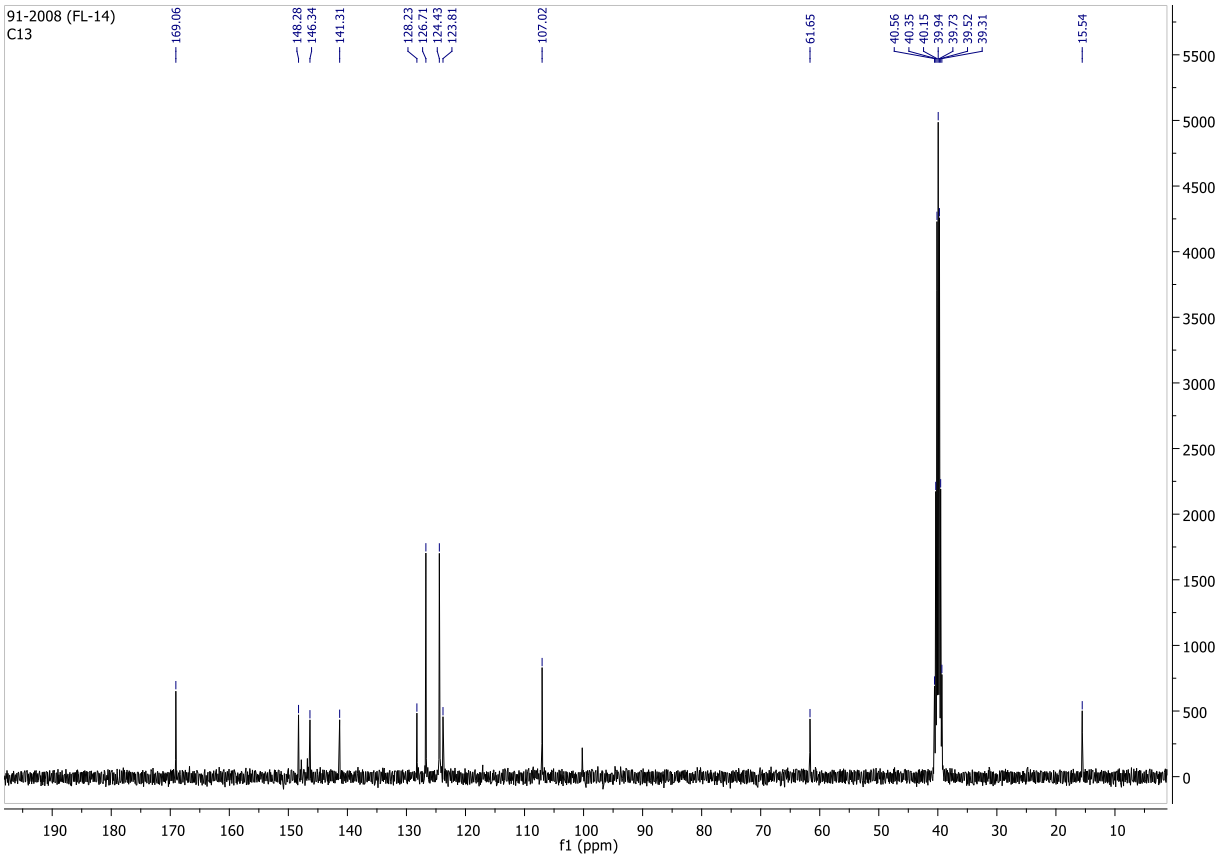
91-2008 (FL-14)
C13
169.06
148.28
146.34
141.31
128.23
126.71
124.43
123.81
107.02
61.65
40.56
40.35
40.15
39.94
39.73
39.52
39.31
15.54
5500
5000
4500
4000
3500
3000
2500
2000
1500
1000
500
0
190
180
170
160
150
140
130
120
110
100
90
80
70
60
50
40
30
20
10
f1 (ppm)

Appendix 18: DEPT-135 (100 MHz, DMSO-d_6) spectrum of compound **106**